UNIVERSITY OF
KWAZULU-NATAL

INYUVESI
YAKWAZULU-NATALI

Solar Thermal Convective Drying Characteristics and Kinetics for Faecal Sludge Treatment

By

Martin Nyanzi Mawejje

218087129

This dissertation is submitted in fulfilment of the requirements for the degree

Master of Science in Engineering (Chemical)

In the School of Engineering, College of Agriculture, Engineering and Science

University of KwaZulu-Natal

Supervisor: Dr. Santiago Septien Stringel

Co-Supervisor: Dr. Jon Pocock

Final Copy

April, 2021

DECLARATION 1 - PLAGIARISM

I, ..., declare that

1. The research reported in this dissertation, except where otherwise indicated, is my original work.
2. This dissertation has not been submitted for examination or degree at any other university.
3. This dissertation does not contain other persons' data, pictures, graphs or other information unless explicitly acknowledged as being sourced from other persons.
4. This thesis does not contain other persons' writing unless explicitly acknowledged as being sourced from other researchers. Where other written sources have been quoted, then:
    1. a) Their words have been re-written, but the general information attributed to them has been referenced
    2. b) Where their exact words have been used, then their writing has been placed in italics and inside quotation marks and referenced.
5. This thesis does not contain text, graphics or tables copied and pasted from the internet, unless explicitly acknowledged, and the source being detailed in the thesis and in the references sections.

Candidate: Martin Nyanzi Mawejje

Signature: Date: 12/04/2021

This Dissertation is submitted for examination with our approval as the candidate's supervisors

Supervisor: Santiago Septien Stringel, PhD

Signature: ..... Date: 12/04/2021

Co-supervisors: Jonathan Pocock, PhD

Signature: ..... Date: 12th April 2021

DECLARATION 2 - PUBLICATIONS AND PRESENTATION

The following paper that has a link with this dissertation is in the process of being written;

- Mawejje M.N., Pocock J., Buckley C.A., Septien S.S. Solar thermal convective drying kinetics and characteristics for faecal sludge

Oral presentations of the work in this dissertation was presented at the following conferences;

1. The 6th South Africa UNESCO Engineering Conference, 26-27 September 2019, North-West University, Mafikeng Campus
2. The 6th South African Young Water Professionals Biennial Conference, 20-23 October 2019, Durban International Conference Centre
3. UKZN College of Agriculture, Engineering and Science Postgraduate Research and Innovation Symposium, 17 October 2019, Westville Campus

Invitations/ confirmations of presentation at these conferences are shown in appendix A

ACKNOWLEDGEMENT

The study and completion of this dissertation has been possible due to a variety of assistance and support that was received. I feel greatly indebted to my supervisors, Dr Santiago Septien Stringel and Dr Jon Pocock, for all the ever-useful thoughts, guidance and recommendations throughout the undertaking of this research study. It has been enriching working closely with you, and I have enjoyed the opportunity to watch and learn from your knowledge and experience.

I am very grateful to the WASH Research and Development Centre, University of KwaZulu-Natal as an institution for the opportunity and conducive atmosphere it offered me to complete this work. Many thanks to its wonderfully competent and industrious staff notably Prof Chris Buckley for his wise leadership and guidance, Kerry Philip and the admin team for all the logistical support, Merlien Reddy and her laboratory team for the support in all laboratory work, Christy, Couben and Ridwan for their immense support in building/fabricating the experimental set-up.

My heartfelt thanks go to fellow post graduate research students Tracy, Nkosi, Tanaka, Savanna, Jimson, Sisekelo, Danica, Arun and Principal from whom I often obtained guidance and motivation. To my housemates Dani, Chris, Max, Noree, Shelby, Santi, Eva, Prince, Leticia, Regina, Simone, Arun and Anthony, it was fun staying with each one of you and the light moments refreshed my mind.

I do thank my dear mother and family for the love and never-ending support, you encouraged and inspired me to achieve, to grow, to learn, and to never give up. You gave me ground to walk on when things were tough, and you helped to shine light into the dark places

Saving the best for last, I genuinely thank the Almighty God for giving me the strength to accomplish this excellent task and making me victor at the end of the long struggle.

ABSTRACT

One-third of the global world population faces a challenge of ensuring safe, adequate, effective and sustainable sanitation. The most significant percentage of this population relies on on-site sanitation systems which necessitate proper Faecal Sludge Management (FSM). Treatment of faecal sludge (FS) is a crucial step during the faecal sludge management process. It enables suitable disposal of the waste without risks for the population and the environment, and with the possibility of resource recovery in the ultimate goal. Drying enables removal of moisture from the sludge, thereby reducing its mass and volume. Solar energy a free resource could supplement heat for drying purposes and reduce the operating costs.

This research experimentally investigated and characterized the solar drying process for faecal sludge from ventilated improved pit latrines (VIPs), and urine diversion toilets (UDs) within a laboratory-scale solar thermal convection drying rig. The drying parameters investigated included air stream temperature (ambient, 40°C, 80°C), air velocity (0, 0.5, 1m/s), and solar irradiation (sunny and overcast weather). Drying time significantly reduced with increased air temperature, increased air velocity and increased solar irradiance. Moisture reduction was significantly higher in VIP sludge as compared to UD sludge. Drying initially occurred in the constant rate period followed by a falling rate period observed at a later stage of drying. Page model seemed to be the most appropriate empirical model to describe the drying curves for faecal sludge, followed by Henderson and Pabis model.

Some physical properties for the dried faecal sludge were investigated. Shrinkage ranged between 20% and 70% and it was directly proportional to the moisture content of the dried samples. Density of dried sludge samples ranged between 1678 kg/m^3 at 2.09 g/g db moisture content to 1222 kg/m^3 at 0.66g/g db moisture content. Water activity for all dried samples was in the range 0.9374 to 0.9810, which indicated moisture in the dried sludge was predominantly slightly bound. Visual observation of the dried samples indicated the presence of a crust layer and cracking on the surface of the dried sludge. Cracking was more pronounced with samples dried at higher air temperature conditions. There was not observed any relationship between the formation of crust and drying conditions, however crust formation was more significant in UD sludge as compared to VIP sludge. Qualitative observations also indicated reduction in shininess (reflectivity) of the sludge surface and fading of the sludge smell as drying progressed.

The solar thermal convection drying system was characterized in terms of heat and mass transfer parameters. The hydraulic regime of flow of convective airstream was turbulent for both experiments at 0.5m/s and 1m/s air velocity. Convective mass transfer coefficients ranged from 7.47×10^{-3} to 9.49×10^{-3} m/s at 0.5 m/s air velocity and 1.04×10^{-2} to 1.34×10^{-2} at 1m/s air velocity. Convective heat transfer coefficients significantly increased when air velocity was increased i.e. from roughly 8 W/m^2.K at 0.5m/s to 11.5 W/m^2.K at 1m/s. The moisture diffusivity D_{eff} varied in the range of 4.56×10^{-9} to 1.52×10^{-8} m^2/s and increased by increasing drying temperature and velocity. The activation energy was greater at 0.5 m/s air velocity (25.82 KJ/mol) as compared to 1 m/s air velocity (8.97 KJ/mol). The obtained Arrhenius constant values for were 1.67×10^{-4} m^2/s at 0.5 m/s and 4.91×10^{-7} m^2/s at 1 m/s. The power and efficiency of the drying system was determined from the energy transferred to the drying chamber from the solar radiation and convective air stream heating. There was notable reduction of the contribution of solar irradiation to the power input during overcast weather as compared to sunny weather. Efficiency was in the range 13.5% to 36.6% and increased with increasing air flow temperature and velocity.

TABLE OF CONTENTS

LIST OF FIGURES

LIST OF TABLES

LIST OF ABBREVIATIONS

COD	Carbon Oxygen Demand
FS	Faecal Sludge
FSM	Faecal Sludge Management
PRG	Pollution Research Group
SOP	Standard Operating Procedure
TS	Total Solids
TVS	Total Volatile Solid
UD	Urine Diversion
UKZN	University of KwaZulu-Natal
VIP	Ventilated Improved Pit
FSTP	Faecal Sludge Treatment Plant

NOMENCLATURE

D	mass diffusivity	[m^2/s]
DR	drying rate	[$g/min.m^2$]
H	absolute humidity	[kg/m^3]
K	thermal conductivity	[$W/m.K^{-1}$]
l	thickness	[m]
m	mass	[g]
MR	moisture ratio	[-]
Pr	Prandtl number	[-]
Q	volumetric flowrate	[m^3/s]
r	radius	[mm]
Re	Reynold's number	[-]
Sc	Schmidt's number	[-]
Sh	Sherwood's number	[-]
T	temperature	[°C]
t	time	[min]
u	velocity	[m/s]
V	volume	[m^3]
μ	dynamic viscosity	[kg/ms^{-1}]
v	kinematic viscosity	[m^2/s]
d	density	[kg/m^3]
A	surface area	[m^2]
M	moisture content	[g /g]
D_{eff}	moisture diffusivity	[m^2/s]
R	correlation coefficient	[-]
B	slope of the straight line	[-]
R_g	perfect gas constant	[$J.mol^{-1}.K^{-1}$]
L	linear diameter of sample	[m]
E_a	activation energy	[$KJ.mol^{-1}.K^{-1}$]
P	power	[W]

SUBSCRIPTS NOMENCLATURE

d	dry sample
e	equilibrium
o	initial sample
cal	calculated value
exp	experimental value
wb	wet basis
db	dry basis

1 INTRODUCTION

The purpose of this chapter is to highlight briefly the global sanitation situation, the challenge facing urban sanitation in low and middle-income countries. This section also serves as a preface to the subject and relevance for the study. Within this section are also the specific study objectives, scope and intended outcomes.

1.1 Background and Rationale

Although having access to water and sanitation is regarded as a necessity to living life in dignity, research has shown that more than a third of the global population, that is 2.4 billion people globally have inadequate access to safe sanitation. The world is off-track to meet the Sustainable Development Goal 6 (SDG 6) of clean water and sanitation although there is considerable progress. The trend in sanitation coverage differs depending on the presence of geographic, economic and socio-cultural inequalities, which have led to the uneven distribution of sanitation facilities. The vast majority of those without access to proper sanitation are the more unfortunate people living in rural areas, ethnic minorities and other marginalized groups, as well as women and children. Some of the major causes highlighted for this situation are aspects relating to leadership, inadequate financing, unmotivated human resource, poor community participation and inadequate appropriate sanitation technological options (WHO/UNICEF, 2017).

In urban regions of most developing countries, the faecal sludge disposal practices are problematic. On a daily basis, all over the world, large volumes of faecal sludge from on-site sanitation systems, i.e. from septic tanks, aqua privies and non-sewered household and public toilets is disposed of untreated (Strande et al., 2018). This sludge is discharged onto open urban spaces and into water catchments, estuaries and the sea, leading to water pollution, eye and nose nuisance and related health impacts. On-site sanitation systems are the most widely used form of faecal sludge disposal for the biggest percentage of urban dwellers in Africa and Asia and a considerable proportion in Latin America (Ingallinella et al., 2002). Safe management of faecal sludge, therefore, remains a significant area of concern, especially for urban and peri-urban areas. Challenges faced range from a shortage of appropriate on-site sanitation facilities, high volumes involved making collection, haulage and treatment difficult and/or costly. Given these immense problems, a combination of technical, economic and institutional/organisational measures are needed to enhance safe faecal sludge management practices (Akumuntu et al., 2017).

The treatment of faecal sludge is one of the critical steps in proper faecal sludge management (Ingallinella et al., 2002). It enables suitable disposal of the waste without risks for the population and the environment, and with the possibility of resource recovery as the ultimate goal (Singh et al., 2017). Faecal sludge can be re-used in different ways, as pointed out by Diener et al. (2014) such as fertilizer, soil conditioner, biofuel, animal protein and building material.

Drying represents a critical process in the treatment of faecal sludge. It enables the removal of moisture from the faecal sludge and also kills the pathogen content found in the faecal sludge (Chen et al., 2006). The removal of moisture leads to the decrease of mass and volume of the material (Léonard et al., 2004), reducing costs related to transportation and storage. The deactivation of pathogens leads to a product safer to handle. Drying can be the final treatment

before re-use or a pre-treatment step before further processing of faecal sludge (Shanahan et al., 2010).

Faecal sludge drying comes with high operational costs, mainly due to the heat energy required. Solar drying could supplement heat for drying purposes and thereby reduce operating costs. This is because solar drying involves the use of energy from the sun which is free and abundant, especially in significant parts of the developing world (Aman et al., 2015).

According to Chen et al. (2006), determination of the appropriate drying process and its operating conditions requires an understanding of the drying kinetics. Also, faecal sludge undergoes several simultaneous physical changes when subjected to solar drying and other heat treatments (Cai et al., 2016). Thus, in the design and optimization of the solar drying process, an understanding of the drying kinetics and structural changes in sludge under different conditions is necessary. Several studies have been published on sewage sludge drying, limited studies in literature could be traced related to solar drying processes for faecal sludge under controlled conditions. This study was therefore undertaken to investigate the solar drying kinetics and behaviour of faecal sludge from various sources as a function of different parameters as the weather conditions, air temperature, and air velocity so as to aid subsequent design, construction and operation of faecal sludge solar dryers.

1.2 Problem statement

Ideally, all faecal sludge generated from on-site sanitation systems is supposed to be safely managed, i.e. treated and re-used either on-site or offsite. This is, however, not the case especially for low and middle-income countries that are faced with limited resources and increasing urbanization. This often results from the establishment of unplanned settlements which increases pressure on the few existing sanitation facilities/treatment options. This leads to an increase in volumes of unsafely managed faecal sludge. A 2016 field-based research by Pollution Research Group (PRG) and McGill University was conducted in Durban, South Africa to visualize the excreta disposal situation in the area (figure 1-1). This study (PRG, 2016) showed that 26% of excreta was unsafely managed, 15% of which was from on-site sanitation systems and was neither contained nor treated. Existing sludge treatment methods are either inadequate, unsustainable or costly, for example, the drying beds, which are a conventional sludge dehydration technique requiring large land space and takes a long period to reach the desired moisture content values. There are research and pilot studies documented regarding incorporating external energy sources like thermal energy in the sludge drying processes. However, the operation is expensive because the high energy costs. Use of solar energy which is a free resource, could potentially lower the energy requirements and subsequent costs (Kurt et al., 2015). To date, there is hardly any documented research to guide and support the application of solar energy in drying processes of faecal sludge.

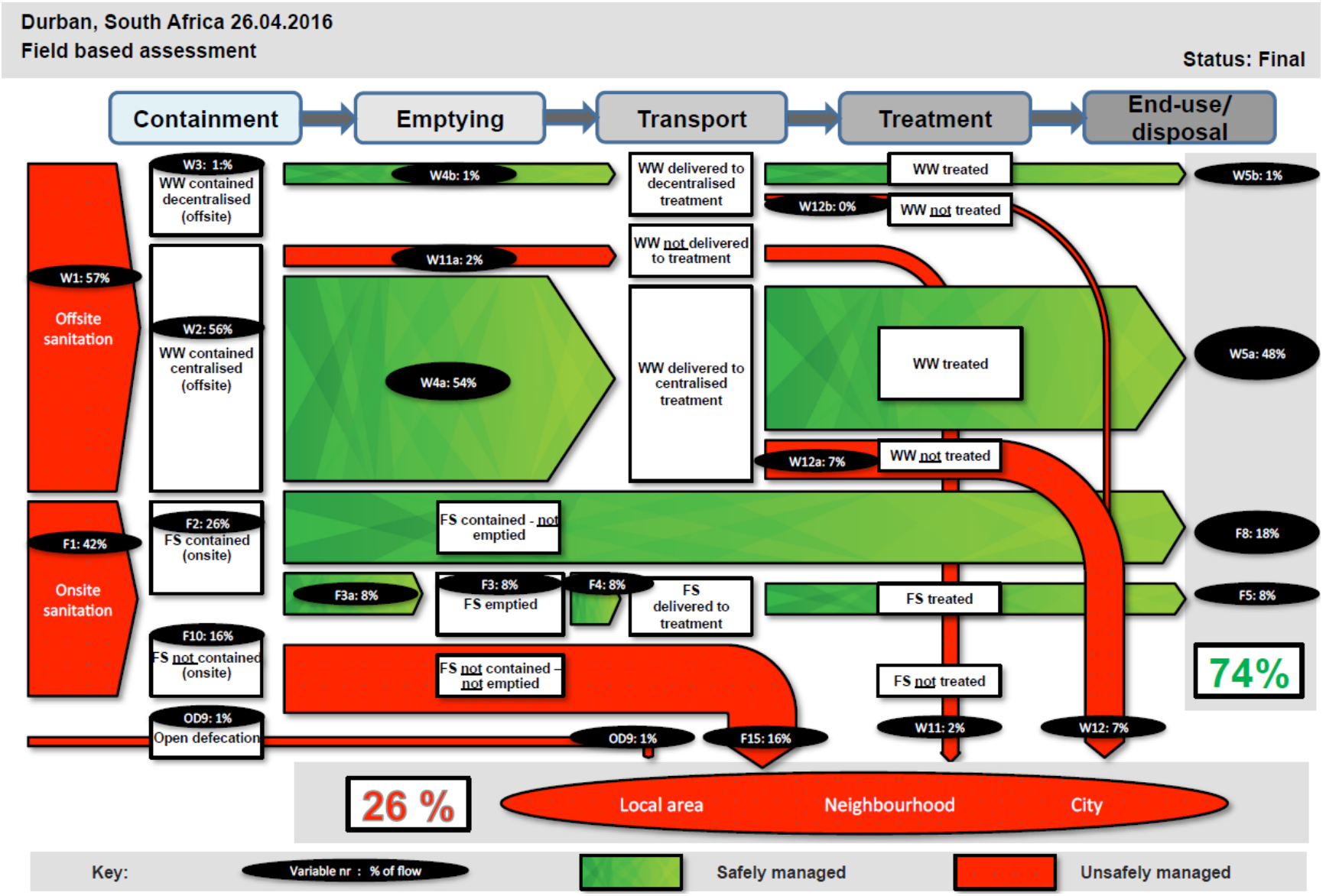

Figure 1-1: Shit Flow Diagram (SFD) for Durban, South Africa (adopted from PRG (2016))

1.3 Aim of the study

Drying kinetics and behaviour of faecal sludge within a solar thermal convective system are not well understood or documented. The aim of this work was, therefore, to investigate the solar thermal convection drying processes for faecal sludge. The fundamental aspects were related to analyses of the drying kinetics for varying operating conditions, i.e. air temperature, velocity, and weather conditions (sunny or overcast) as well as a study of the physicochemical changes during the solar drying process. The other aspect was as an evaluation of the performance of the solar drying rig system.

1.4 Specific objectives of the study

The following objectives were formulated so as to achieve the aim of the research study;

1. To investigate the drying kinetics as a function of different parameters, and select the best mathematical model for the drying curves. This involved a study of;
    a. Effect of the weather conditions on drying processes;
    b. Effect of the air temperature on drying processes;
    c. Effect of the air velocity on drying processes;
    d. Internal temperature evolution in faecal sludge during drying;
    e. Differences of drying between the VIP and UD sludge.

2. To examine the physical and morphological properties of the dried faecal sludge in terms of:
    a. Shrinkage, density and water activity of dried sludge as a function of moisture content;
    b. Qualitative observations of the material to identify characteristics as cracking, crust formation, odour and reflectivity.

3. To characterize the solar thermal convection drying system and evaluate its performance through a study of;
    a. Flow pattern, convective heat and mass transfer coefficients;
    b. Effective moisture diffusivities and activation energy;
    c. Power and efficiency at the varying experimental conditions.

1.5 Study scope

The study entailed 5 months solar drying experiments within a laboratory-scale solar thermal convective drying rig. The drying setup was located at the rooftop of the chemical engineering building, at Howard College Campus, University of KwaZulu-Natal. This experimental setup and equipment had been used in a previous research (Mugauri, 2019). However, unlike in the previous investigation, the setup was modified to allow for variation of convection air velocity.

Faecal sludge from both urine diversion (UD) and ventilated improved pit (VIP) latrines were involved. The sludge was collected from a black soldier fly faecal sludge treatment plant located in Isipingo, eThekwini municipality, South Africa. The samples consisted of faecal sludge from various random VIP and UD toilets within the municipality and can be considered representative of faecal sludge from within this area. Experiments were carried out during both sunny and overcast weather conditions and the experimental setup was in open place with no shading at any moment of the day.

This research study, material and experimental methods were ethically approved. An ethical clearance approval letter from the UKZN Biomedical Research Ethics Committee is shown in appendix B.

1.6 Research significance

This work characterised solar thermal convection drying that is a currently unexploited area in both research and practice fields. The data from this investigation is expected to aid further researchers in the design of appropriate in-situ and offsite faecal sludge solar dryers. Furthermore, this is expected to inform sanitation practitioners of the potential value add that comes with incorporating solar energy in faecal sludge management, particularly for drying purposes.

1.7 Dissertation outline

This dissertation consists of five major sections as briefly described below;

INTRODUCTION

This section includes the background, problem, justification and purpose for this study. Main objectives, study scope and expected outcomes are also presented.

LITERATURE REVIEW

This section contains a narrative review of existing academic-oriented knowledge relevant for this study. There are three basic parts: an introduction of the basic drying principles and theory; description of faecal sludge drying aspects, i.e. the purpose and challenges, existing sludge drying practices and the transformation of the material along the process; description of solar energy as an usable energy resource and the existing solar drying practices for sludge. The literature review was mainly from published scientific journal articles/papers and books.

MATERIALS AND METHODS

This section describes the material (faecal sludge samples) as well as the experimental set-up and methods employed in the study. It also outlines the data analysis methods used to meet the study objectives.

RESULTS AND DISCUSSIONS

The experimental results are presented in this section and discussed. The main trends deduced from the experimental results are highlighted and analysed with comparison to results in the existing literature.

CONCLUSIONS AND RECOMMENDATIONS

This section is a summary of the findings from the experimental results obtained and their implication in the sanitation field. The limitations of this study are also presented, and possible future research areas that could complete this study are suggested.

2 LITERATURE REVIEW

This chapter discusses the available literature related in some extent to faecal sludge solar drying. It is based on published and grey literature that is related to moisture in faecal sludge, reasons and existing ways for moisture removal from sludge as well as the opportunities for the use of solar energy resource for drying the sludge.

2.1 Drying Principles and Theory

This section discusses the generalities of the drying process and the science behind the removal of moisture from solids. The basic concepts and definitions related to drying are presented. Factors that could affect the drying processes, internal and external material properties of the product to dry, and the various ways of presenting drying data are showcased.

2.1.1 Concept of drying

Drying is defined as a process of moisture removal from a wet product. This wet product can be in solid, semi-solid or liquid form. Drying results from evaporation of the moisture from the wet product. Evaporation happens when liquid molecules escape from the wet product and turn into a vapour. Drying is necessary for one or several of the following reasons: preservation and storage, reduction in the cost of transportation, achieving the desired product quality and the need for easy-to-handle solids,

Drying can be achieved through different ways such as: natural evaporation, thermal drying and freeze drying. Freeze drying involves freezing a wet product, lowering pressure and removing the moisture by sublimation of the formed ice. Freeze drying is applied for removal of moisture in both liquids and solids. Thermal drying involves supply of heat to the wet product causing the vaporization of moisture within the wet product and its evaporation to the atmosphere. Thermal drying is the most commonly applied form for drying wet solid materials, Natural drying occurs when materials are dried through evaporation without heat, i.e. laying on the natural drying potential of the air.

The drying of wet solids involves the escape of moisture in form of vapour from the the solid surface to the surrounding atmospheric air. This therefore leads to the increase of the humidity at the surrounding air in relation to the drying solid surface. For moisture to evaporate from the solid, its vapour pressure must be higher than the partial vapour pressure of the moisture in the gas that is in contact with the wet solid. The moisture removal capacity of the air increases by increasing the temperature and decreasing the air humidity.

2.1.1.1 Moisture in solids

Wet solid products could be categorised into two basic groups in accordance with their drying behaviour:

1. Granular/crystalline solids: these solids hold moisture in open pores between particles and are usually inorganic materials. The nature of solids is generally unaffected by moisture removal; therefore, the drying conditions may not influence the properties and appearance of the dried product.

2. Fibrous, amorphous and gel-like materials – these are mainly organic materials and tend to dissolve the moisture or trap it in fibers, flocs or fine pores. Such materials are affected by the removal of moisture and often reduce in volume upon drying and swell when wet. Drying in the later stages tends to be slower.

Wet solids could also be categorized according to their physical, chemical, structural and biochemical properties. These properties may significantly affect the drying process. Despite this variability, Raghavan (1990) states that, in practice, the basic parameters to consider are the forms of moisture existence in the wet solid. The form of moisture existence is defined as a function of the type of bonding with the material. The types of moisture present in a solid are broadly bound moisture and unbound moisture. These are diagrammatically presented in Figure 2-1 (Pskovski and Mujumdar, 2010)

- Bound moisture is that which is held to the solid matrix. Bound moisture exerts a vapour pressure which is less than the vapour pressure of a pure liquid at a given temperature. Moisture can be bounded biologically, chemically or physically
- Unbound moisture: this exerts an equilibrium vapour pressure which is equal to that of the pure liquid at the same temperature. This type of moisture can be removed relatively easier in a solid in comparison to bound moisture.
- Free moisture: this is the moisture contained in a wet product in excess of the equilibrium moisture content at given air temperature and humidity. Free moisture can be either bounded and / or unbounded. Equilibrium moisture content is detailed in section 2.1.2.2.

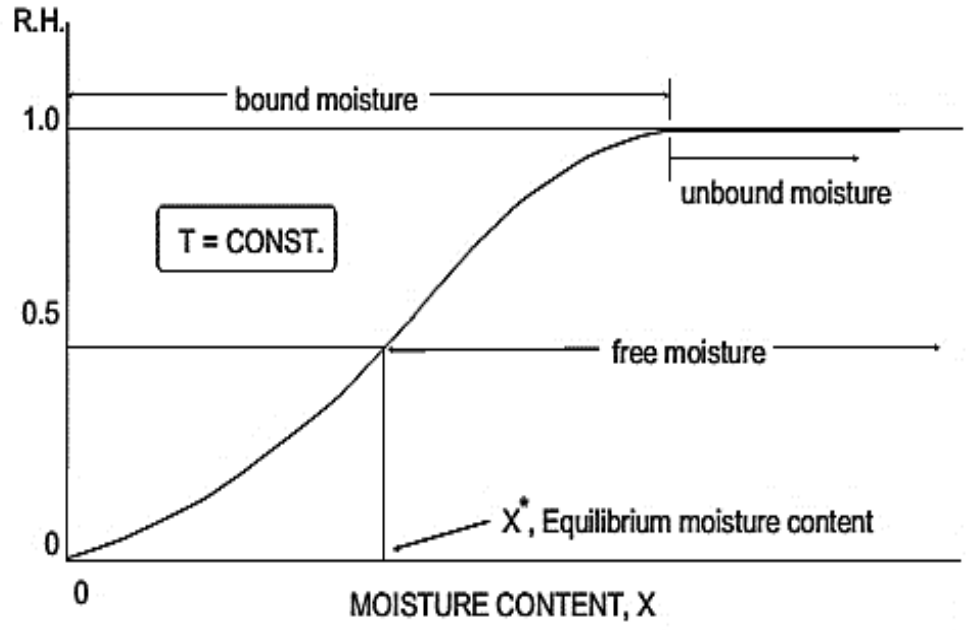

Figure 2-1: Different kinds of moisture within a wet solid product (Pskovski and Mujumdar, 2010)

2.1.1.2 Methods of drying

Drying methods are categorized according to the mechanism of how heat is transmitted to the wet material and how the evaporated moisture is evaporated. Drying methods that expose the wet product to a hot gas stream are known as direct or adiabatic. Drying methods that involve supply of heat by conduction or radiation are called indirect or non- adiabatic. The most conventional drying categories are the following (Pskovski and Mujumdar, 2010);

- Convective drying (direct drying): This method involves the supply of heat to a wet material by convection from a heated air stream and the evaporated moisture is taken away in the air stream. Convective drying is the most common despite the relatively low thermal efficiency, which is due to the lack of a cost-effective method to recover

the latent heat of vaporization from the exhaust (Castro et al., 2018).

- Contact drying (indirect drying): This method involves supply of heat to a wet product through contact with another material (conductor) which is at a higher temperature. Method of heat transmission to the wet product is therefore by conduction.

- Radiative drying (indirect drying): Heat is transmitted to the wet material by infrared, microwave or radio dielectric frequency radiation. This type of heating arises from the oscillation of dipolar molecules (as water) in the wet product after exposure to microwave or radio dielectric radiation. Infrared radiation has relatively low penetration within the wet product and then heats mostly the surface of the wet solid. Microwave and radio dielectric frequency waves can penetrate deeper within the solid. Microwave heating is applied in the food processing field for example, for drying, pasteurization, cooking and preservation of food materials (Chandrasekaran et al., 2013).

- Solar drying: This involves use of solar energy from the sun radiation. Solar energy can be in direct form were the wet product is exposed to direct sun light, or indirect form whereby an air stream preheated by solar radiation is passed over the wet product. Detailed discussions about solar drying are presented in section 2.3.

2.1.2 Drying terminologies

Relevant definitions encountered in the study drying are presented below.

2.1.2.1 Moisture content

Moisture content refers to the quantity of water/moisture in a wet product. The quantity of moisture within a wet product can be measured either on a volumetric or gravimetric basis. Volumetric basis involves measurement of the moisture by volume while gravimetric basis involves measurement by mass/weight.

Moisture content can be presented in form of a wet basis or a dry basis. The moisture content in a wet basis is presented in terms of the weight of moisture present in a product per unit weight of the undried material as shown in equation 2-1. The moisture content on a dry basis is presented in terms of the weight of moisture present in the product per unit weight of dry matter in the product as shown in equation 2-2.

$$M_{wb} = \left[\frac{(m_t - m_d)}{m_0}\right] * 100 \qquad (2-1)$$

The moisture content on the dry matter basis M_{db} was also calculated using equation 3-2.

$$M_{db} = \left[\frac{(m_t - m_d)}{m_d}\right] \qquad (2-2)$$

Where m_t represents mass (g) of the sample at a given time *t*, m_d is the total solids mass in the sample and m_o is the initial mass of the sample before drying.

The moisture content in the wet basis is normally computed for practical applications. The moisture content in dry basis has mostly been applied for research. This is because the weight change associated with each percentage point of moisture reduction on the dry basis is constant. For wet basis, the amount of moisture involved in a moisture content reduction of one percentage point changes as drying progresses because of the weight of water and total weight change (Ekechukwu, 1995). The ratio of the moisture content in a wet product at a given stage

of drying process to the initial moisture content before drying is known as the moisture ratio. Moisture ratio, MR is computed as in equation 2-3 below.

$$MR = \frac{M_t - M_e}{M_0 - M_e} = \frac{M_t}{M_0} \qquad (2-3)$$

Where M_t, M_0 and M_e are moisture content at any time (g water/g dry matter), initial moisture content (g water/g dry matter) and equilibrium moisture content (g water/g dry matter) respectively.

2.1.2.2 Equilibrium moisture content

A wet solid has a defined water vapour pressure at a specific temperature and moisture content. This is what defines whether the wet solid at that given temperature absorbs or desorbs moisture if exposed to air. The equilibrium moisture content of a wet product is defined as the moisture content of the material after it has been exposed to a particular environment for an indefinitely long period of time (Raghavan, 1990). At equilibrium moisture content, vapour pressure exerted by the moisture held within the product is equal to the vapour pressure of the immediately surrounding air. This is known as the equilibrium condition; that is, the rate of moisture desorption by the material to its immediate surrounding is the same as the rate of moisture adsorption from the surrounding environment. Relative humidity of the immediately surrounding air at the equilibrium condition (which is also in equilibrium with its environment) is referred to as the equilibrium relative humidity. In the case the surrounding air is replaced continuously by air of low relative humidity, a vapour deficit is created, and the product will continue to desorb moisture to the air.

The relationship between equilibrium moisture content and relative humidity at constant temperature is graphically displayed by sigmoid curves known as moisture equilibrium isotherms (Figure 2-2)

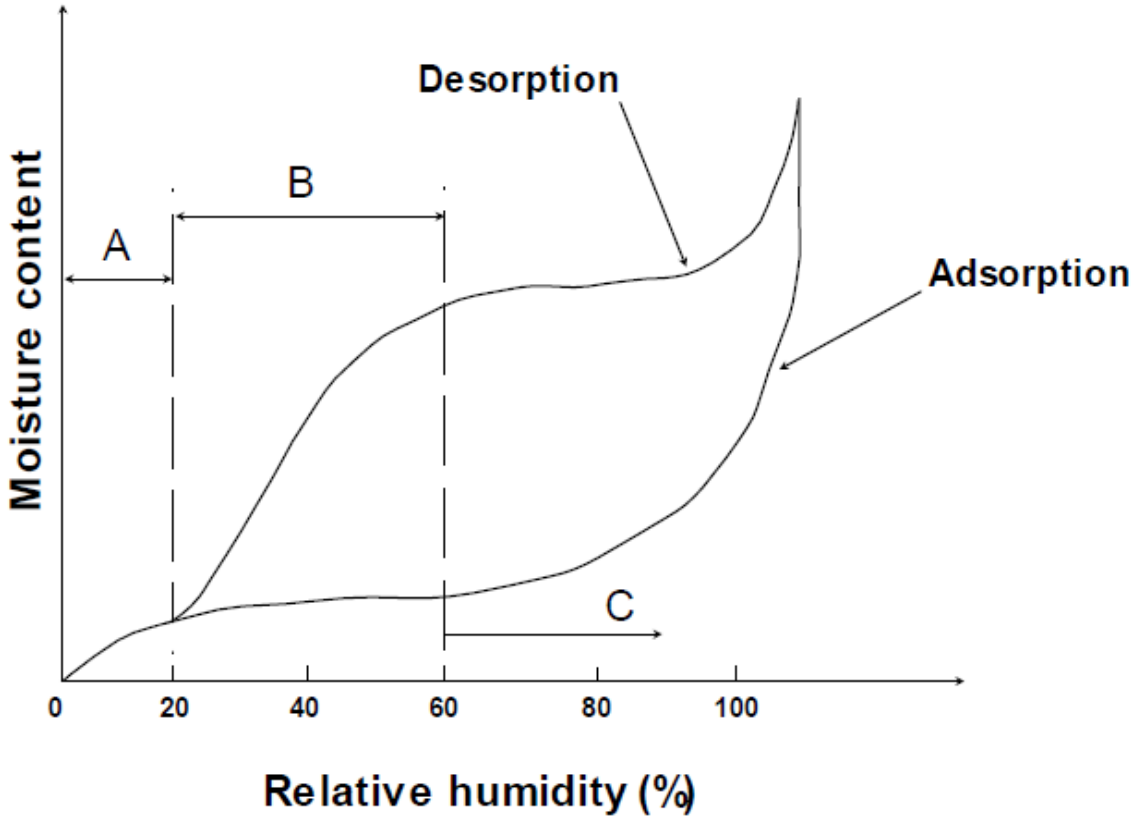

Figure 2-2: Sorption isotherms (Pskovski and Mujumdar, 2010)

Region A is corresponding to the hydration monolayer. In this region water molecules are bonded to the wet material by very strong interactions. Region B is corresponding to the linear part of the sorption isotherm. Water is adsorbed as multilayers of molecules of hydrogen-bonded to the monolayer, or entrapped in the wet product by Van der Waals forces, capillarity, etc. Region C corresponds to that of the free or solvent water. In region C, water molecules are much less strongly bound than in regions A and B. The isotherms in figure 2-2 denote the equilibrium in terms of moisture between the air and the solid. The process of bonding the water molecules to the wet product surface is called adsorption. Removal of the water molecules from the solid surface is called desorption. Adsorption isotherm is obtained by plotting the amount of bonded water molecules to the adsorbent (wet solid) surface as a function of the partial pressure or concentration of the vapor water (relative humidity) in the air. The desorption isotherm is a plot of the amount of water molecules released from the wet solid as a function of the relative humidity of the air.

2.1.2.3 Water activity

Water activity (a_w) is defined as the ratio of partial vapour pressure of water in a substance to the standard state partial vapour pressure of pure water measured at the sample temperature. The standard state vapour pressure refers to the saturation vapour pressure. The sole determination of moisture content is not sufficient to explain nature of moisture within a wet substance or even predict its shelf life. Water activity is another type of analysis within a wet substance alongside moisture content. Water activity is a good indicator of the amount of free water in a wet product and the extensiveness of one or another of the biological/degradation reactions that might take place during storage of wet solid products (Mathlouthi, 2001). Water

activity values can vary in the range of zero to one. Water activity equal to one means unbound moisture, whereas water activity below one indicates bound moisture. The boundedness of moisture increases as water activity is reduced. Water activity values close to one do indicate high likelihood of degradation within the product whereas values close to zero indicate less/no likelihood for degradation during storage of wet product. An increase in a_w is usually related to an increase in water content but in a non-linear fashion. Water molecules migrate from areas of high a_w to areas of low a_w (Slade and Levine, 1991).

2.1.2.4 Heat of drying

Heat of drying refers to energy that must be absorbed by the wet product to cause vaporization of moisture from the product, without a rise in temperature of the product. The calorific energy required for vaporization is absorbed from the surrounding from a hot airflow, hot surface or radiative heating. Heat of drying for convective drying depends on the nature of product, the level of moisture boundedness and temperature. Heat of drying increases as the moisture content of the product decreases. This is because the remaining moisture is more bounded to the solid product as drying progresses, so more energy will be required to evaporate it.

2.1.2.5 Drying rate

Drying rate refers to the mass of water removed from a wet product per unit time per unit mass of dry matter or the mass of water removed per unit time per unit area during the drying process. The drying rate depends on the contact area between the drying medium and the material; the temperature and the humidity of the drying air; the speed and direction of the drying air; retention time, and the method of contacting the sludge with the heating source.
This drying rate is determined as the difference between two consecutive moisture contents (in dry basis) in a given drying time interval, as shown in equation 2-4.

$$DR = \frac{\Delta M_t}{\Delta t * A} = \frac{M_t - M_{t+\Delta t}}{\Delta t * A} \qquad (2-4)$$

Where A represents the area of drying the sample in m^2.

In the drying of wet products, it is necessary to determine the size of dryer required, the various operating conditions like air temperature and velocity as well as the time needed to perform the amount of drying required (Castro and Coelho Pinheiro, 2015). All this requires drying rate data.

2.1.3 Factors affecting drying

The rate at which drying occurs depends on the power supplied by the heating source, type of moisture and the conditions influencing the transfer rates, such as the characteristics of the solid (geometry, size, porosity) and the external conditions (air temperature, velocity and humidity).

2.1.3.1 Temperature

For different applications, for example drying of food products, and wastewater sludge, the temperature is a parameter of significance, as it influences the drying rate. From a heat transfer viewpoint, the greater the temperature difference between the drying air and the wet product, the greater the heat transfer rate occurs between the drying air and wet product. Higher temperatures also imply higher input of heat for moisture vaporisation (Mewa et al., 2018). However, high temperatures may result in deterioration of product quality, change of chemical structure and charring. Singh (1994) came to the conclusion that most properties that are important in drying, that is thermal conductivity, mass diffusivity, and latent heat of vaporization greatly depend on temperature.

2.1.3.2 Relative humidity

Another relevant operating parameter is the amount of moisture present in the drying air as compared to the total amount of moisture that the air can hold at a particular temperature. This parameter is known as the relative humidity. The relative humidity influences the external mass transfer, and also, the drying rate (Sigge et al., 1998). In other words, the increase of air relative humidity decreases the moisture concentration transfer potential between the surface of the material and the drying air, resulting in a reduced external mass transfer rate. Higher drying rate occurs at minimum humidity of drying air. At a given temperature, any increase in humidity reduces the capacity of air for holding additional water vapour (section 2.1.2.2). Therefore, relative humidity directly affects the final dryness of the solids. A dynamic equilibrium exists between the moisture in the solids and the vapour in the air. When a wet hygroscopic product is left in contact with moist air for long periods of time, its moisture content will reach equilibrium moisture content and this increases as relative humidity increases.

The relationship between relative humidity and the various properties of moist air at a constant pressure is best described using a psychrometric chart (figure 2-3). This is a series of graphs that describes physical and dynamic properties of air vapour mixtures at a given pressure. Figure 2-3 presents a psychrometric chat relating the dry bulb temperature (air temperature as indicated by a thermometer) and wet bulb (saturation) temperature and humidity ratio to the relative humidity (Callahan et al., 2019). Humidity ratio refers to the dry basis moisture content of air i.e. weight of water vapour per unit weight of dry air. From the psychrometric chart (figure 2-3), the relative humidity of the air vapour mixture can be determined at a given temperature and humidity ratio. Given that at thermodynamic equilibrium, the water activity in the solid and the relative humidity are equal, we can determine the moisture content from the sorption isotherms. Relative humidity of the air vapour mixture decreases with increase in dry bulb temperature. Relative humidity of the air vapour mixture also increases with increase in the humidity ratio of the wet product.

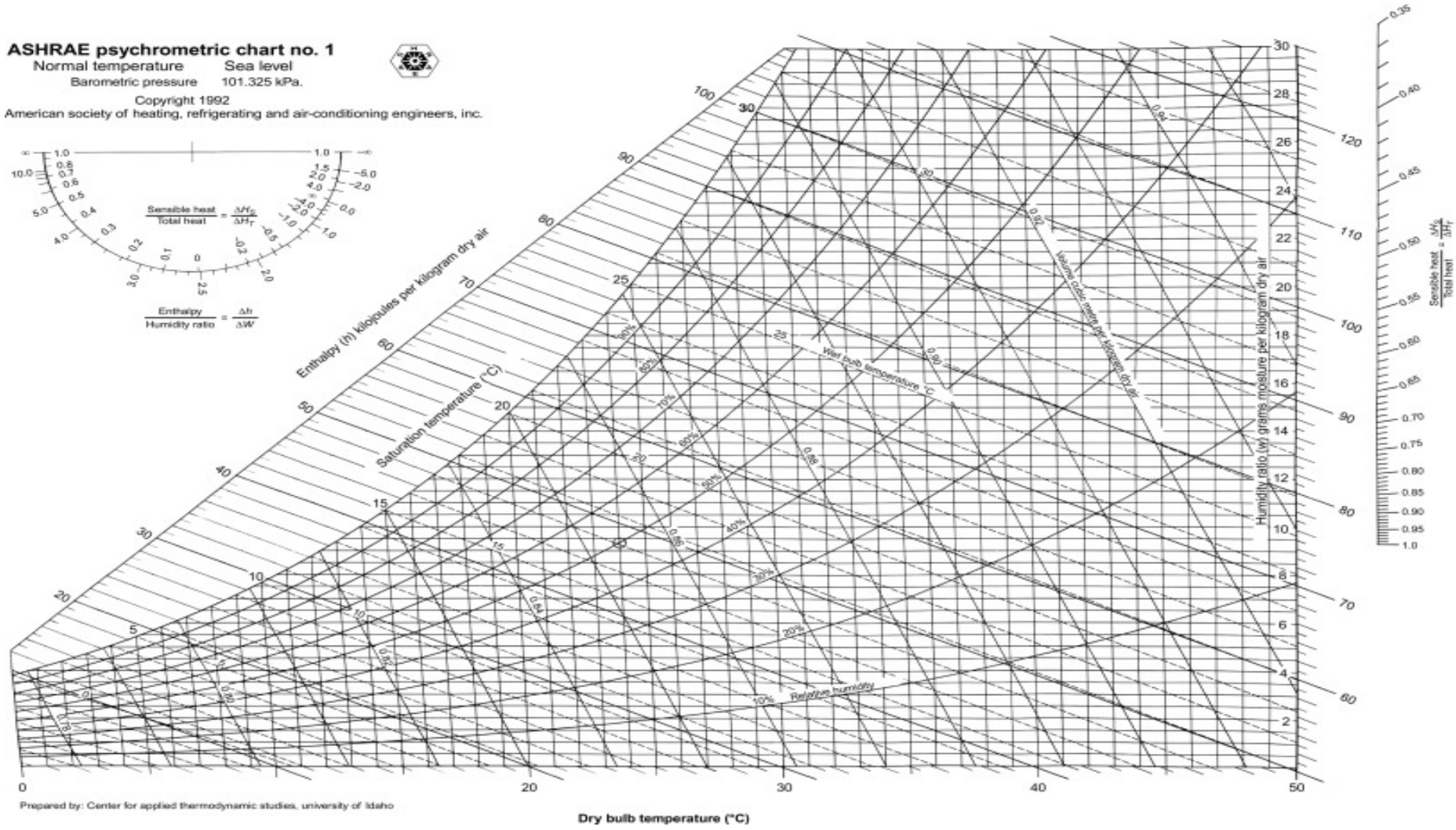

Figure 2-3: ASHRAE psychrometric chart 1 normal temperature—sea level, 0–50°Cdb (Callahan et al., 2019)

2.1.3.3 Air velocity

Air velocity during drying affects the drying rate through its influence on the external heat and mass transfer. Increase in velocity of air provides potential of reduction of the boundary layer of the air with the solid and consequently enhancing the convective heat and mass transfer. Increase of air velocity therefore allows for the removal of more moisture from the material surface at the given instance. Iguaz et al. (2003) reported that the effect of air velocity is more significant for low-temperature drying.

2.1.3.4 Size and surface area of the material

The surface area of the material available for heat and mass transfer affects the drying rate. A larger surface area causes greater moisture reduction rate from the total surface area and this lowers the drying times. Material size is also an influencing parameter, the decrease of the material size decreases the distance for the moisture to diffuse from the core of the wet product to the surface, leading to faster drying rate and thus shorter drying times.

2.1.4 Phenomena during thermal drying

Thermal drying is the form for drying most commonly used for wet solid products. Thermal drying involves supply of heat to the wet product. The heat supplied leads to vaporization of moisture within the material. This subsequent causes evaporation of moisture as vapour from the product

Thermal drying, therefore, is associated with simultaneous heat and mass transfer. Depending on the material, moisture transfer from within the material to the surface (due to moisture gradient) is done as liquid or vapour formm, while as only vapour, from the surface to the environment (Pskovski and Mujumdar, 2010).

2.1.4.1 Heat and mass transfer during drying

Energy transfer (mostly as heat) from the surrounding environment is used to heat the wet product for drying. Heat transfer occurs through radiation, convection, and / or conduction to increase the temperature of the wet solids and to evaporate the water. Typically, there are two heat transfer resistances: the transfer resistance between the surface of the material and the environment; the transfer resistance within the material.

Mass transfer of internal moisture to the surface of the solid is achieved by moisture migration from the interior of the solid out to the surface, from where it leaves the material. The internal movement of moisture within the solid to the surface is a function of the morphological characteristics of the solid (porosity, tortuosity, pore size), temperature and moisture concentration (Xu et al., 2020).

When a wet product is subjected to convective drying, heat and mass transfer processes occur simultaneously within the product being dried and in the boundary layer of the product. These processes are depicted in Figure 2-4. The rate at which drying occurs is governed by the rate at which these transfer processes proceed (Lu et al., 2008).

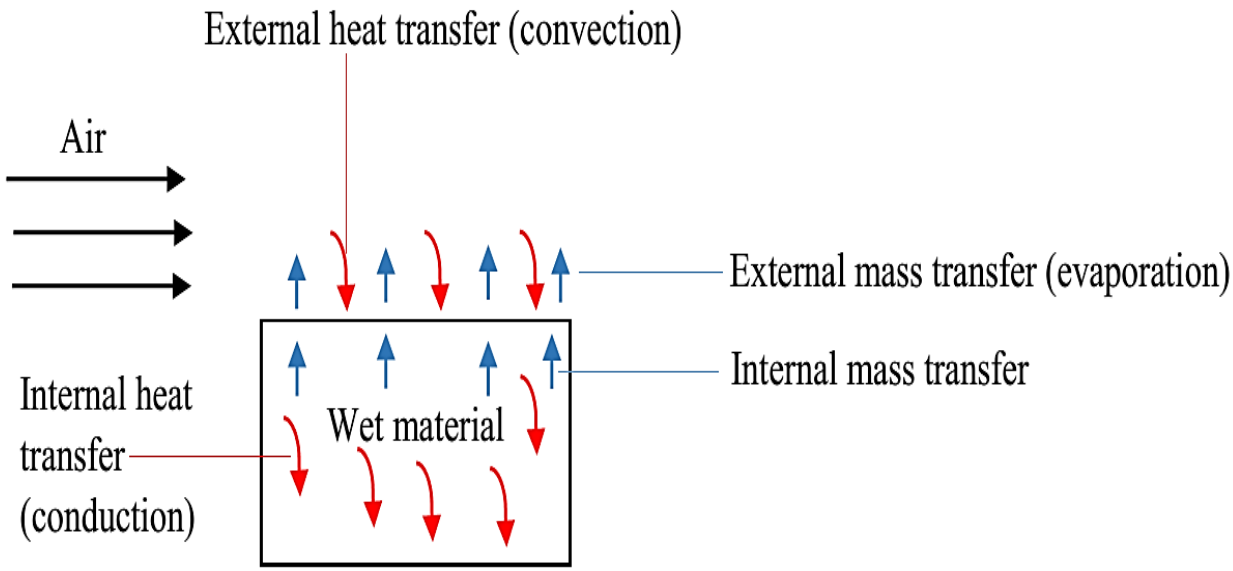

Figure 2-4: Heat and mass transfer during convective drying

2.1.4.2 Mechanisms for moisture migration

The moisture transfer from a wet product must overcome two resistances; the movement of the internal moisture, which is a function of the moisture content and the internal structure of the solid; and the movement of water vapour from the material surface, which is dependent on external conditions

The removal of moisture from the surface of the material by convection depends on the external conditions of air temperature, air humidity, airflow, the external surface area of the solid, and pressure.

Movement of moisture within the solid may be affected by one or several of the following mass transfer mechanisms (Xu et al., 2008):

- Liquid diffusion when the temperature of the wet product is below the boiling point of the liquid. It is regarded that the rate at which moisture is transferred is proportional to the change in moisture concentration of the material subjected to drying.
- Vapour diffusion when the liquid vaporizes within the material. This usually occurs during the final stages of drying. This is perceived as the main mechanism by which moisture is transferred in its vapour state. It occurs in materials which have pores with size greater than 10^{-7} m.
- Capillary moisture movement when a number of capillaries of different radii exist within a material forming interconnected channels. Capillary pressure gradient causes the redistribution of moisture by capillary suction from the large capillaries to the small ones.
- Hydrostatic pressure differences when internal vaporization rates exceed the rate at which the vapour moves through the solid structure to the peripheral and to the surrounding. This creates a build-up of pressure within the solid thereby causing a flow in the internal channels from the porous solid.

2.1.5 Drying kinetics

Every product has representative drying characteristics at given drying operating conditions. Drying kinetics describe the evolution of moisture concentration with time and are helpful for the determination of drying rates. Drying kinetics are experimentally determined by measuring the change in mass of a sample per given period of time during drying. There are three experimental methods for this (Kemp et al., 2001):

- Periodic sampling or weighing: The whole or part of the drying sample is extracted at regular intervals during drying, and its moisture content is measured. This method is time-consuming and usually a few points on the moisture content versus time graph can be determined.

- Continuous weighing: The drying sample is linked to a thermo-balance, and its weight is recorded continuously. Using this method, a big number of points on the moisture content versus time graph can be determined. However, slight variations in mass during drying can be recorded as a result of random noise, e.g., by perturbations of the sample caused by the prevailing wind or air stream.

- Intermittent weighing: The drying sample is linked to a mass balance. At intervals, the supply of air flow around the sample is stopped or diverted. This enables determination of an accurate weight reading after the system has stabilized. This method does not affect the overall drying kinetics unless the drying times are very short.

2.1.5.1 Presentation of drying data

Raw drying data is usually in terms of mass readings at given intervals of drying time. This data can be represented in various different ways which include the following;

1. Drying curves: These are determined directly from data of weight/mass loss as a function of time data. Moisture content is plotted versus drying time.
2. Drying rate curves: Drying rate graphs are the derivative of the drying curves, and they depict the drying rate versus drying time.
3. Krischer curves: These curves are derived from the combination of the drying curves and drying rate curves. Krischer graphs show the drying rate versus the moisture content.

The typical drying curves of a wet product being dried at constant conditions are shown in Figure 2-5.

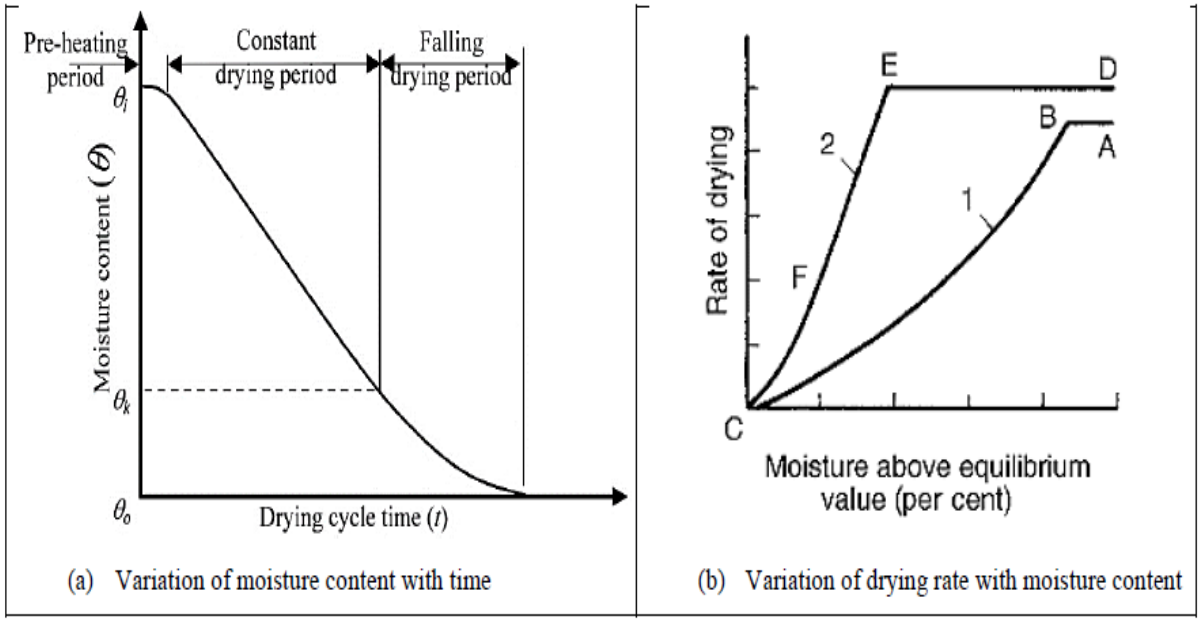

Figure 2-5: Typical drying curves obtained during the drying of a wet product (Makununika, 2017)

Figure 2-5(a) depicts the typical evolution of the moisture content with time for a wet product undergoing convective drying. Figure 2-5(b) shows the Krischer curves that correspond to the plot of drying rate versus moisture content. There are 3 major drying phases; the pre-heating period (stabilization period), the constant rate drying phase and the falling rate drying phase. In figure 2-5(b), one can clearly see these typical drying phases. The first drying curve (ABC) depicts two clearly-defined segments. Segment AB represents a constant drying rate period, and BC represents the region where there is a gradual decline fall of the drying rate as the moisture content decreases. The second curve (DEFC) illustrates three different stages that may occur during drying. Segment DE represents the constant rate period, the same period represented by AB. Segments EF and FC represent the falling rate periods in which EF is known as the first falling rate period, and subsequently, FC is referred to as the second falling rate period. Generally, the two can be distinguished apart because the first falling rate period is a straight line, whereas the second falling rate period is curved. Points B and E represent the transition from the constant rate period to the falling rate period. The moisture content at which this transition occurs is known as the critical moisture content.

- Constant rate period: During the constant rate period, the entire surface of the drying product is saturated in moisture which continuously evaporates and is replaced immediately by moisture from inside the product. Indeed, the internal moisture transfers to the surface and the evaporation at the surface are in equilibrium; therefore, the moisture at the surface will be evaporated in a steady mode. The temperature of the material during this drying phase is constant, and it approximates to the wet-bulb temperature value. The length of the constant rate period is dependent on the difference between the moistness on the surface of the sludge and the amount of unbounded moisture within the sludge. Constant rate period is completely dependent on the rates of external heat and mass transfer. This is because a film of free moisture is always present at the evaporating surface (Wu et al., 2017). Thus, the heat transferred to the material is utilized for the latent heat necessary to evaporate the water at the surface.

- First falling-rate period: After the critical moisture content, the surface of drying product ceases to be completely saturated in moisture. The temperature of the sludge will begin to increase from the wet-bulb temperature to the temperature of heating. Moisture from the surface of the material evaporates at a faster rate than it can be replaced from inside the particle. The speed of drying will decrease until a balanced hydration is accomplished (when moisture from the surface evaporates at the same rate as it is replaced from the inside of the particle). When these conditions are reached, the drying rate greatly depends on the internal mass transfer.

- Second falling-rate period: At the end of the first falling rate period, it could be assumed that the surface is completely dry and that the evaporation front within the drying product has been created and moves towards the center of the drying product. Drying in this phase is not influenced by the external drying conditions, and moisture migration may be as a result of any of the mechanisms of internal moisture migration (in particular gas diffusion).

NB. Not all material exhibit all the drying phases mentioned.

2.1.5.2 Effective diffusivity

The effective diffusivity is a term that describes diffusion/movement of moisture through the pore structure of the drying material. Effective diffusivity particularly applies to porous materials and treats the material (solid and pores) as one pseudo-homogenous medium. The effective diffusivity (D_{eff}) parameter lumps up all the different internal moisture transfer phenomena described in section 2.1.4.2. A complete drying profile is made up of 3 major phases; the first (stabilization) phase, a constant-rate period, and a falling-rate period (section 2.1.5.5). In many applications, the longest stage is the third period (Dincer and Dost, 2007). The mechanism of moisture migration within a hygroscopic product during the third stage (falling-rate period) could be represented by the diffusion Fick's second law. The one-dimensional diffusion is a good approximation for most practical systems (Koukouch et al., 2017). Thus, the unsteady state diffusion of moisture by Fick's second law can be expressed as in equation 2-1;

$$\frac{\partial M}{\partial t} = \nabla * \left(D_{eff} \nabla \mathrm{M}\right) = D_{eff} \nabla^2 \mathrm{M} \qquad (2-1)$$

Where M represents moisture content of the product (g/g db), t represents the drying time (s) and D_{eff} is the effective moisture diffusivity (m^2/s). D_{eff} varies with temperature and moisture content of the product and is affected by the shrinkage of the product.
Analytical solutions for Fick's second law are available in the literature and are dependent upon the geometry of the solid (Koukouch et al., 2017).

2.1.5.3 Drying models

Drying models can be necessary to predict drying kinetics of wet materials under varying operating conditions. Modelling is necessary for the design, operation and optimization of drying systems (Castro et al., 2018). There exist various drying models in literature. These models are used to generate drying curves to estimate the drying time of several products under varying conditions.

Drying of wet products is modelled as a thin or deep bed layer. Thin-layer drying is the drying process where the entire drying sample is fully exposed to the drying air at constant drying conditions, that is at a constant temperature, air velocity and relative humidity. Akpinar and

Toraman (2015) defined thin layer drying as to dry as one layer of sample particles or slices. It is assumed that the temperature distribution within a thin-layer product is uniform. This makes the use of lumped parameter models appropriate for thin-layer drying (as for example the effective diffusivity).

Thin-layer drying models are categorized into three, that is theoretical, semi-theoretical and empirical models. The theoretical models consist of simultaneous heat and mass transfer equations. The semi- theoretical models are based on more simplified theoretical equations, such as Fick's second law using the effective diffusivity approach (section 2.1.4.3), but they are only valid within the drying conditions of temperature, relative humidity, airflow velocity and the range of moisture content for which they have been developed. The empirical models define a direct relationship between drying time and average moisture content. Empirical models do not consider the fundamentals of the drying process and their parameters have no physical meaning. Empirical models have an advantage of being easy to apply in drying simulations, however they do not give a clear accurate view of the important processes occurring during drying although they may describe accurately the drying curve for the conditions of the experiments (Castro et al., 2018).

Thin layer empirical drying models describe the drying phenomena in a unified way regardless of the controlling drying conditions. Thin layer empirical models have been used to determine drying times of food products and to predict drying curves. In the formulation of thin-layer drying models, the moisture content of the material at any time, at constant relative humidity and temperature conditions is measured and correlated to the drying parameters. The prediction of the drying rate of a specified food product subject to various conditions of drying is essential for the design of drying systems (Prakash et al., 2016).

Several empirical thin layer drying models are reported in literature. These equations are expressed in terms of the moisture ratio (MR) and the model constants. Table 2-1 shows the most widely used models (Ertekin and Firat, 2017).

Table 2-1: Thin layer empirical drying curves models (Ertekin and Firat, 2017)

Model name	**Model**
Newton	$MR = \exp(-kt)$
Page	$MR = \exp(-kt^n)$
Henderson and Pabis	$MR = \text{a}\exp(-kt)$
Logarithmic	$MR = \text{a}\exp(-kt) + c$
Two-term	$MR = a\exp(k_0 t) + b\exp(k_1 t)$
Two-term exponential	$MR = a\exp(-kt) + (1-a)\exp(-kat)$
Wang and Singh	$MR = 1 + at + bt^2$
Approximation of diffusion	$MR = a\exp(-kt) + (1-a)\exp(-kbt)$
Modified Henderson and Pabis	$MR = \text{a}\exp(-kt) + b\exp(-gt) + c\exp(-ht)$
Midilli	$MR = \text{a}\exp(-kt^n) + bt$

To determine the accuracy of the prediction from the models to the experimental data, several statistical indicators are used. For the validation of these models, the coefficient of determination R^2 is the primary criteria for determining the more accurate equation to describe the drying curves. Other than the R^2, there are many other statistical parameters for example, reduced chi-square (χ^2), mean bias error (*MBE*), root mean square error *RMSE* and t-test which are used to evaluate the fitting of a model to the experimental data. Statistical models $RMSE$, R^2 and X^2 are computed, as shown below in equations 2-5, 2-6 and 2-7 respectively:

$$RMSE = \sqrt{\frac{\sum_{i=1}^{N}\left(MR_{exp,i} - MR_{pre,i}\right)^2}{N}} \qquad (2-5)$$

$$R^2 = \sqrt{\frac{\sum_{i}^{N}\left(MR_{exp,i} - \overline{MR}_{exp}\right)^2}{\sum_{i=1}^{N}\left(MR_{pre,i} - \overline{MR}_{exp}\right)^2}} \qquad (2-6)$$

$$X^2 = \frac{\sum_{1}^{N}\left(MR_{exp,i} - MR_{cal,i}\right)^2}{N-n} \qquad (2-7)$$

Where $MR_{exp,i}$ is the moisture ratio determined by experimental observation, $MR_{pre,i}$ is the moisture ratio as predicted by the model, $\overline{MR}_{exp}$ is the average moisture ratio through the experimental period, N is the number of points and n is the number of model constants.

The highest values of R^2 and lowest values of χ^2, *RMSE*, *MSE* and t-values determine the best fit (Castro et al., 2018, Prakash et al., 2016). The equations from these parameters are displayed in the Material and Methods chapter, section 3.4.4.

2.2 Faecal sludge drying

This section relates to the drying of faecal sludge. The reasons to dry and the behaviour of faecal sludge during drying as well as existing practices are presented.

2.2.1 Description, characteristics and sources of faecal sludge

Faecal sludge is defined as the excreta of variable consistency collected from on-site sanitation systems, such as latrines, non-sewered public toilets, septic tanks and aqua privies. Faecal sludge is a term used to describe undigested or partially digested slurry or solid that results from the storage or treatment of black water or excreta. Solids or settled content that comes from pit latrines and septic tanks is referred to as faecal sludge (Schoebitz et al., 2014). Faecal sludge can either be raw or partially digested and this depends on the type of on-site sanitation facility and how it is used (Strande et al., 2018). According to Ingallinella et al. (2002), faecal sludge consists of settleable solids and other non-faecal materials with varying concentrations. The characteristics of faecal sludge vary widely from different geographical locations. Characteristics of faecal sludge are affected by the duration of its storage, the extent of groundwater or surface water intrusion in septic tanks or pits, performance of septic tanks, and technique for sludge emptying, pattern and user habits.

2.2.1.1 Characteristics of faecal sludge

Faecal sludge is characterized according to its physical, biological and chemical properties. Physical parameters that can be considered for the characterization of faecal include; texture, density, porosity, thermal properties, consistency, qualitative properties such as odour and colour, among other. Chemical parameters for faecal sludge characterization include; solids concentration, nutrients, biochemical oxygen demand (BOD), chemical oxygen demand (COD), and metals content, among other. Biological parameters for faecal sludge characterization are commonly pathogens content. Most of these parameters are similar to those applied in domestic wastewater analysis, however, it needs to be noted that the characteristics of domestic wastewater and faecal sludge are very different. Table 2-2 presents selected characteristics for faecal sludge from on-site facilities as reported in literature (Niwagaba et al., 2014, Radford and Sugden, 2014)

Table 2-2: Characteristics of faecal sludge from on-site sanitation facilities

Parameter	**Value/description**
Moisture content (g/g db)	1.5 - 4
Odour	unpleasant/foul
Colour	blackish/dark brown
Density (kg/m3)	1100
pH	6.55 - 9.34
Total Solids, TS (mg/L)	30,000 - 50,000
Chemical Oxygen Demand, COD (mg/L)	20,000 – 50,000
Nitrates (mg N/L)	0.2 - 21
Faecal coliforms (cfu/100ml)	1×10^{-5}
Helminths eggs (Numbers/L)	20,000 – 60,000

2.2.1.2 Sources of faecal sludge

On-site sanitation system are the major source for faecal sludge. Such systems are where the excreta is contained in the area of the household or institution from which it is generated. For safe on-site sanitation system such as in ventilated improved pit latrines (VIP) and urine diversion (UD) toilets, the excreta are contained safely, in a well-designed, well-constructed and well-maintained pit or tank, without giving off unpleasant odours (Taweesan et al., 2015). The main feature of an on-site sanitation system is a pit or vault from where faeces and urine are collected. Other material in the pit or vault may include cleansing material and all other household waste that may be disposed of by the users. Processes such as water infiltration into the pit (example: through rain) and out of the pit (example: soil percolation), biological degradation and pathogen deactivation may also occur within the pit or vault.

To qualify as a VIP (figure 2-6), the latrine should provide hygienic separation of faecal waste from contact with humans, have a vent pipe fitted with a fly-screen to minimise odour and flies, be built on a firm slab that will resist collapse of the superstructure, and should provide privacy and dignity for the user.

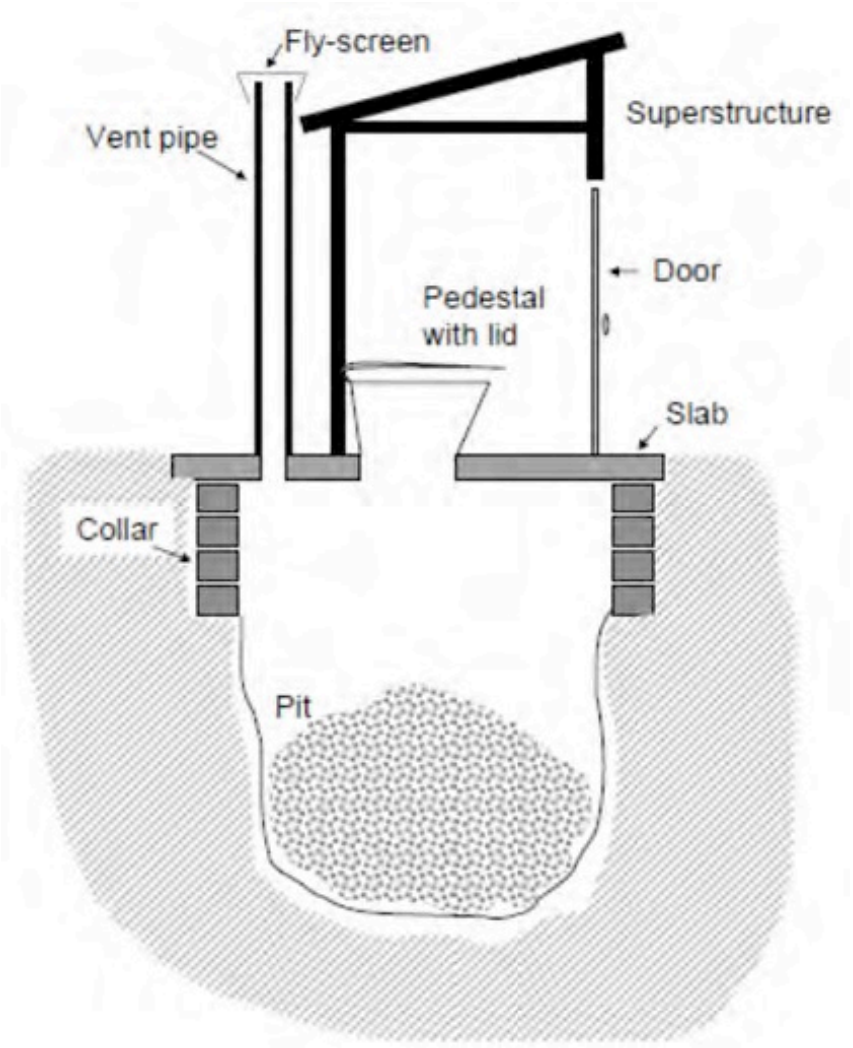

Figure 2-6: Schematic representation of VIP latrine (adopted from Bhagwan et al. (2008))

The appropriate design of the UD toilet system (figure 2-7) consists a double vault dry toilet with a urine diversion to a soak-away located near the unit. A pedestal which is located above one of the vaults into which faeces, anal cleansing material and a cover material (e.g. soil) are dropped. (Bhagwan et al., 2008).

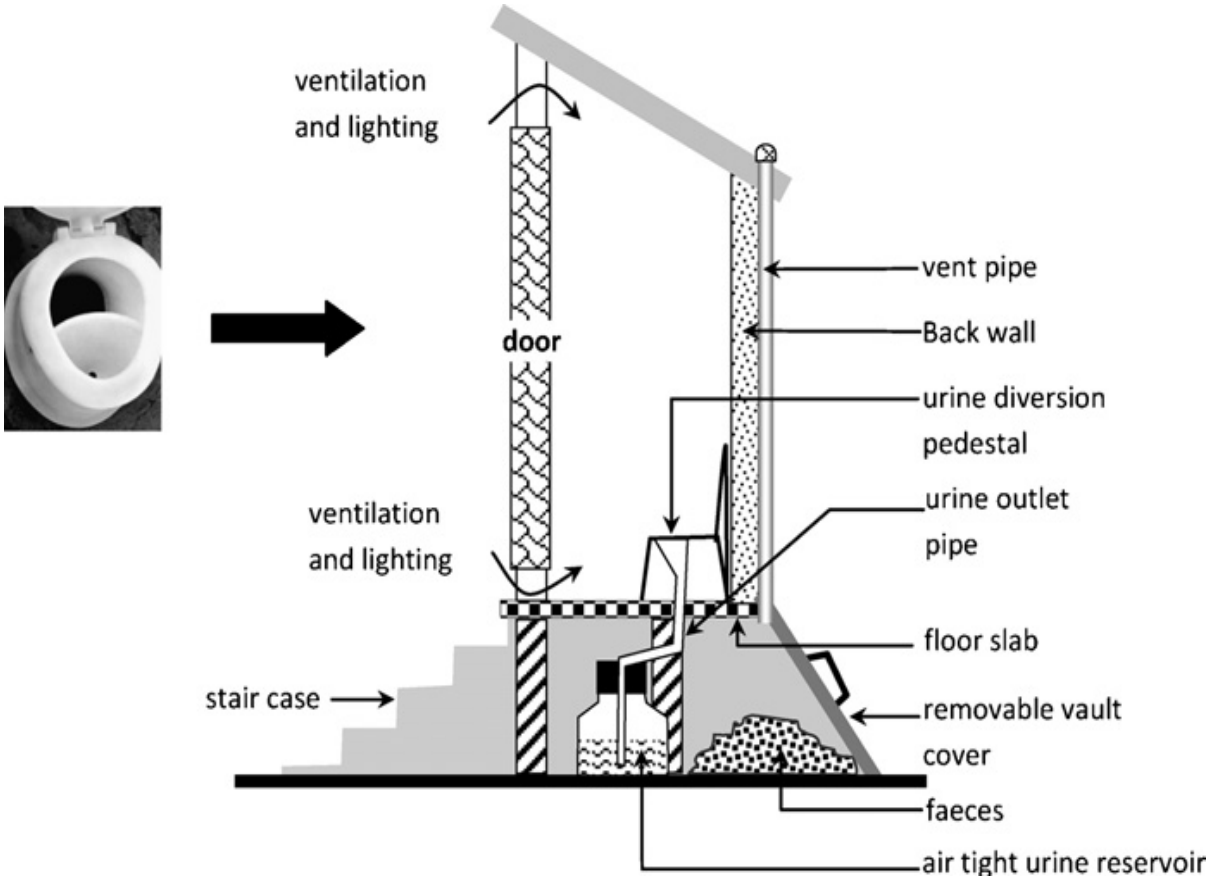

Figure 2-7: Schematic representation of a UD toilet (adopted from Karak and Bhattacharyya (2011))

2.2.2 Motivation for drying faecal sludge

Feacal sludge is a mixture of organic and inorganic matter and its composition greatly depends on its origin. Faecal sludge is mainly comprised of moisture (i.e. water) in proportions which are dependent on the type of on-site sanitation technology. Typically, 60-80% of faecal sludge volume is water (Niwagaba et al., 2014). This water makes faecal sludge heavy, bulky and expensive to transport, and discharging this polluted water to the environment has significant negative health impacts. The use of faecal sludge in its raw form also represents a health hazard due to its high pathogen content.

Drying is a methods for moisture removal from the faecal sludge through evaporation. This significantly reduces the volume of the sludge and thus easing its handling and transportation. The primary goal for faecal sludge drying is therefore the removal of moisture through evaporation and thereby reduce the sludge volumes for easy handling.

Drying also has potential to neutralise the pathogen content in the faecal sludge into a safe level. This is possible by killing the pathogenic organisms present in the sludge, by the effect of moisture reduction and increasing temperatures. The development of most bacteria is inhibited below a water activity of 0.91 (Chen et al., 2006), including pathogens such as Escherichia Coli, Salmonella, Shigella and Vibrio Cholera. This means that most of the pathogenic bacteria in the faecal sludge can be deactivated if drying achieves a moisture content corresponding to a water activity lower than 0.91. Drying of faecal sludge is also necessary prior to resource recovery for applications such as composting, or combustion as a fuel.

2.2.3 Moisture in Faecal sludge

Moisture in faecal sludge can be available in unbound or bound forms just like other hygroscopic products (section 2.1.1.1). These forms of moisture are important for the understanding of the drying mechanisms because the unbound water can be removed with less difficulty than bound water. The majority of water in undried faecal sludge is unbound water (sometimes known as bulk water). Unbound water can be separated from the solid structure easily through gravity. Unbound water is not adsorbed, bound, or influenced by capillary forces. From Figure 2-8 (Chen et al., 2006), bound water can be in form of interstitial, surface, and intracellular. Interstitial water (also known as capillary water) is in sludge pore spaces, bound to the solid structure through capillary forces. The surface water (sometimes known as colloidal water) is bound to the sludge solid structure and microorganisms by adsorption and adhesion. The intracellular water is contained within microorganisms and can only be removed by drying mechanisms that result in the breakdown of sludge cellular structure, thus releasing the moisture. When water is bound to faecal sludge, it is much more difficult to remove through drying and requires more energy for its removal.

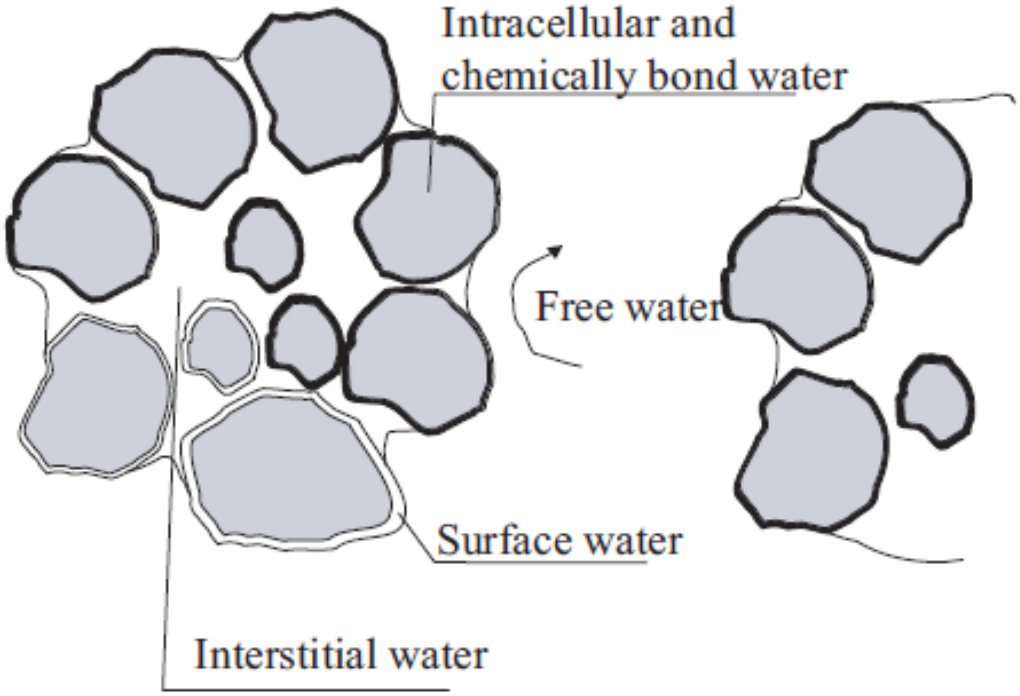

Figure 2-8: Different types of moisture in the faecal sludge (adopted from Chen et al. (2006))

2.2.4 Behaviour of faecal sludge during drying

The drying of faecal sludge can potentially result in changes of the structural properties of the material. This is as a result of the induced mechanical stresses and a re-arrangement of the dry bone structure as moisture is removed from the sludge. The changes in faecal sludge structure have to be taken into consideration for a full comprehension of drying process, because this has a direct effect on the heat and mass transfer properties during drying.

The major physical changes undergone by sludge during drying include; change of phase, shrinkage, cracking and crust formation (Leonard et al., 2004, Cai et al., 2016).

Change of phase during drying occurs from a liquid slurry to a solid-state. LOWE (1995) described how the changes in phase occur in sludge as it moves through a thin film dryer. This is illustrated in figure 2-9 and categorized into three stages; the wet sludge zone, where the sludge is free-flowing; the sticky zone, where the sludge is pasty; the granular zone, where the sludge is a crumbly solid.

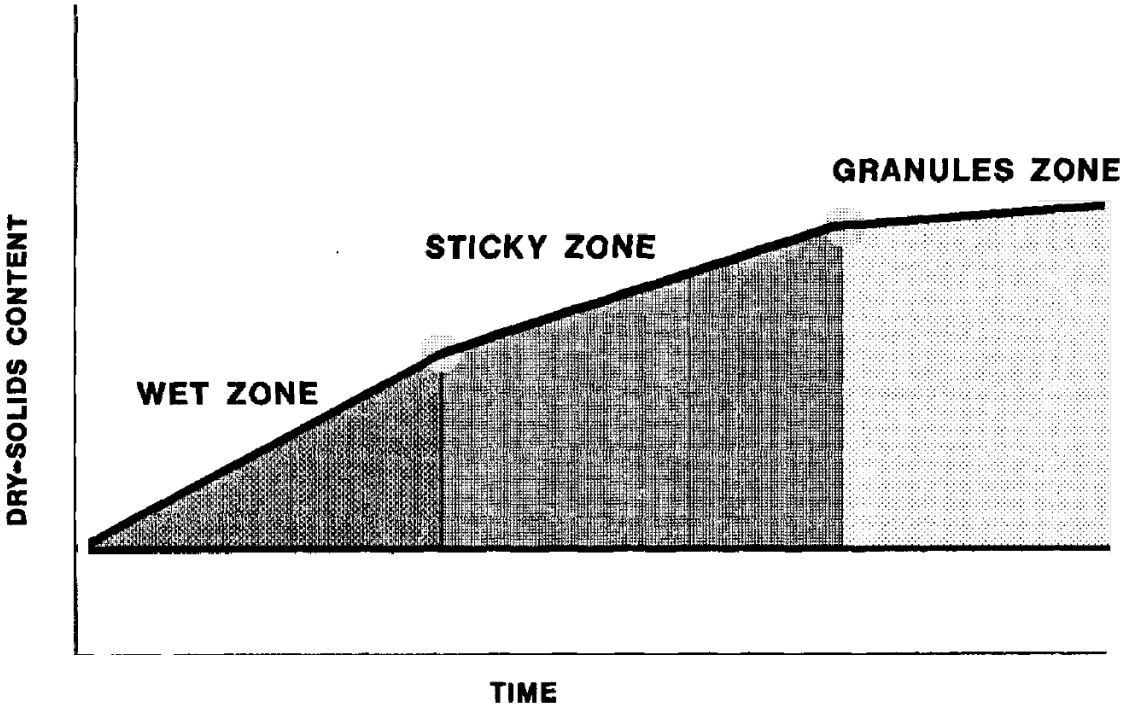

Figure 2-9: Changes in phase of sludge during drying in a thin film dryer (LOWE, 1995)

Shrinkage results from the collapse of the sludge dry bone structure as moisture is removed from within its pores. Formation of crust layer may result from an internal moisture transfer limitation as compared to the external sludge surface drying. This causes hardening or formation of a skin layer on the top of the drying sludge (Léonard et al., 2004). Cracking of the sludge is usually observed on the top surface and arises from the internal stresses within the sludge structures as moisture is removed.

2.3 Solar thermal drying

Within this section, the solar energy resource is introduced, and the possible opportunities related to the incorporation of solar energy resource in the drying process are discussed. The existing solar drying techniques, particularly for faecal sludge, are presented.

2.3.1 Solar energy

Solar energy refers the radiant light and heat from the sun collected and used to provide electricity, heating, cooling in homes, businesses or industries. It is sustainable and environmentally friendly resource of energy that does not require the burning of fossil fuels (except for its installation). Solar energy, therefore, leads to low greenhouse air emissions. Solar energy is also considered renewable because the energy is produced from the sun does not deplete any natural resources, and will be always available (Kannan and Vakeesan, 2016). However, although solar energy is a free source, its conversion into usable energy requires equipment and an initial investment (Kabir et al., 2018).

The whole of Africa and, in particular, the region of Southern African have sunshine all year round. Annually, the 24-hour global solar irradiation is about 220 W/m^2 on average for South Africa, compared with roughly 150 W/m^2 for parts of the USA and about 100 W/m^2 for Europe and the United Kingdom. This makes solar energy resource in South Africa as one of the highest in the world. Most areas in South Africa average more than 2 500 hours of sunshine per year, and average solar-radiation levels range between 4.5 and 6.5 kWh/m^2 in one day (Mulaudzi et al., 2012).

There are different ways through which solar energy can be used such as: photovoltaic systems which convert solar energy into electrical energy via inorganic or organic semiconductor materials; thermal systems which convert solar energy into thermal energy using solar irradiance absorbents and concentrator devices; photosynthetic, photochemical, thermal and thermochemical processes which convert solar energy into fuels for chemical energy storage.

2.3.1.1 Solar radiation

Solar radiation from the sun reaches the earth surface after it passes through the atmosphere surrounding the earth. Therefore, radiation is received at the earth surface in an attenuated form because it is subjected to mechanisms of adsorption and scattering as it passes through the atmosphere. According to Badescu (2014) for any given location on the earth's surface, the terms 'clear sky' and 'cloudy sky' are used to often classify the types of the sky. A clear sky is described as one with no clouds and relatively low turbidity while a cloudy sky implies a sky covered with some clouds or a sky that is totally overcast. A clear sky is characterized by an atmosphere in which there are very little adsorption and scattering of solar radiation. Less attenuation, therefore, takes place on a clear sky and maximum radiation is received at the earth surface.

There are different paths of how solar irradiance is propagated, leading to different types of radiation (figure 2-10). Solar radiation received at the earth surface with no change in direction, i.e. in line with the sun is known as direct radiation. Diffuse radiation is the radiation received at the earth surface after being subjected to scattering in the atmosphere. The sum of direct radiation and diffuse radiation is known as total or global radiation. The global radiation and the proportion of diffuse radiation to direct radiation are greatly affected by clouds, the condition of the atmosphere (e.g. haze and dust layers), as well as climatic and geographic conditions (Li et al., 2015).

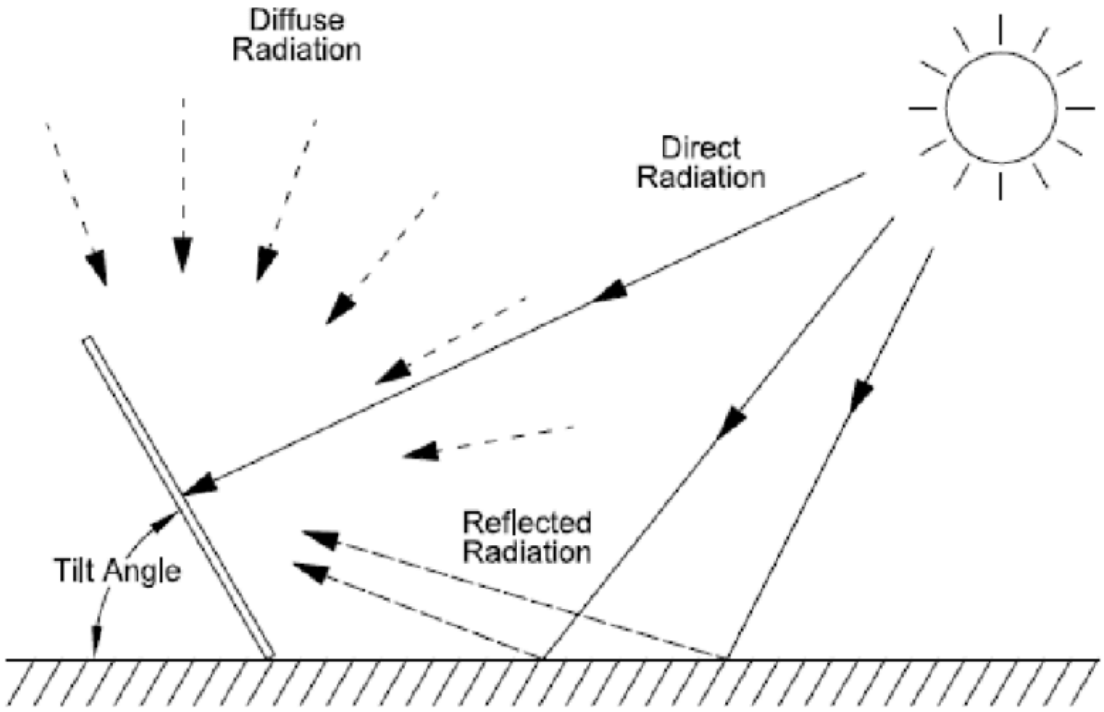

Figure 2-10: Different paths of solar radiation propagation to the earth surface

2.3.1.2 Solar resource assessment

Solar resource assessment is the characterisation of solar irradiance available for energy conversion in a region or specific location over a period of interest. This assessment enables the evaluation of the amount of solar irradiation received by a specific area and the seasonal variations. Solar resource assessment is an important decision tool before the implementation of any solar technology, which enables to determine the feasibility of a project and the design parameters, such as the required land, as well as to predict the performance of the plant or dryer. For this, the characteristics of the location that are susceptible to have an effect on the solar irradiance received must be determined: landscape, topography, vegetation, latitude, longitude, elevation above the sea level, among other. In the same way, the characteristics of the technology to implement must be defined.

2.3.1.3 Classification of weather

The duration of the sunshine and its intensity depend on the period of the year, weather conditions and the geographical position. Weather is defined as the state of the atmosphere at a given place or time in regards to sunshine, heat, cloudiness, wind and rain. The weather is dependent on climate, seasons and other factors. Weather days are categorized into the following major categories (Badescu, 2014);

- Sunny: characterized by the sun shining and giving warmth to the land with little or no cloud presence.
- Cloudy: clouds form a barrier to block rays from the sun and also trap heat from the ground.
- Windy: majorly formed as a warm air mass rises upward and masses of cold air flows to fill the vacuum. Windy weather can be observed through a breeze or swaying of vegetation in one direction.
- Rainy/snowy: arises when heavy clouds cannot hold any more water/snow, so they fall in the form of raindrops in case of rain or snowflakes in the case of snow.

Windy conditions can also possibly co-exist with either sunny or cloudy weather.

2.3.2 Solar dryers

The objective of a solar dryer is to collect and harness the solar thermal energy. This provides adequate amount of heat energy for drying, i.e. more than ambient temperature under given humidity. Increase in temperature of drying product causes increase of the vapour pressure of the moisture confined within the drying product. This consequently leads to decrease of the relative humidity of the drying air and the moisture carrying capacity of the air is increased. The air is conveyed through the dryer by natural or forced convection. The air can be pre-heated and then after partially cooled as it catches moisture from the drying product. Pre-heated air holds more moisture than cold air at the same relative humidity, this means amount of moisture removed is dependent on the temperature to which the air is pre-heated as well as its humidity ratio.

The performance of solar dryers is significantly dependent on weather conditions. The heat required for removing the moisture is supplied by the solar energy. For technologies with forced convection inside the dryer, heat energy from the sun can also be used for driving the fans through photovoltaic conversion of the solar energy into electricity. The drying time is shorter under sunny conditions and consequently longer during cloudy weather conditions. The variation in drying capacity between dry and rainy season has to be taken into consideration for the calculation of the yearly capacity of the dryer (Lingayat et al., 2017). Dry seasons typically involve long hours of sun and thus increased heat energy available of drying as compared to the rainy seasons.

Solar dryers are most commonly classified depending on their heating modes and the manner in which the solar thermal energy is utilized. In broad terms, solar dryers can be classified into four major groups (Kant et al., 2016, Mustayen et al., 2014), namely:

- Direct solar dryer, which expose the material to be dried to direct sun rays through a transparent cover of high transmittance. This transparent cover creates a greenhouse effect. This is necessary to reduce heat losses and increase amount of heat energy available for drying, and it simultaneously gives the drying product protection from rain and dust.

- Indirect solar dryer, in which the wet product is dried by a hot convective air stream that has been heated by the use of solar energy.

- Mixed-mode solar dryer, in which the wet product is dried through a combination of direct solar radiation and a hot convective air stream that has been pre-heated by solar energy.

- Open sun drying, which involves spreading the drying product on open ground. The product is dried by direct solar radiation from the sun. The wet product could be covered with a shelter as a protective measure from rain or extreme winds. Open sun drying does not use a solar thermal system.

Solar dryers can also be classified depending on how the flow of the drying air is induced, i.e. forced convection and natural convection solar dryers (Sharma et al., 2009). In natural

convection, drying airflow is caused by forces that occur naturally during the heating of the system, such as buoyancy forces. In forced convection, the air is forced to flow over the drying material by external means such as a pump or fun.

2.3.3 Recent developments on solar thermal drying

In recent years, there is hardly any literature published in regards to solar thermal drying processes and kinetics for faecal sludge. A few studies could be traced concerning solar thermal drying for sewage sludge. However, solar thermal drying has been widely applied in the agricultural sector as a means of preservation and improving quality of agricultural products. Numerous studies have highlighted the benefits and drawbacks of solar thermal drying for agricultural products (Tiwari, 2016). The benefits include; higher temperatures, higher air flowrates and lower humidity, as compared to open sun drying, which result in higher drying rates thus smaller drying area; relatively lower capital and operational costs than conventional thermal drying systems. The drawbacks of solar thermal drying include; lower performance compared to conventional thermal drying systems, possible operation only during day time in the presence of the sun or requiring of a backup heat source for continuous drying during the night and adverse weather conditions.

Poblete and Painemal (2020) studied solar drying processes for landfill leachate sludge. A comparison was made for solar drying with thermal storage to solar drying without thermal storage. Stabilization of the mass of sludge using thermal storage was obtained faster than without thermal storage. Drying experiments were carried out on different days and nights with different values of solar irradiation. There was no mass reduction during the nights for experiments without thermal storage due to absence of solar energy during night hours. Wang et al. (2019) investigated solar drying processes for sewage sludge within a stainless-steel chamber. Experiments were conducted in Shanghai, China with a mean annual solar radiation of 500W/m^2 at noon. Average solar irradiance values ranged between 300 and 700W/m^2. Sewage sludge was dried in thin layers for varying thicknesses (0.5, 1 and 5cm). Drying chamber temperatures ranged between 16.5 to 81.5°C and recorded humidity was in the range 35 to 73%. The velocity of air flow within the drying chamber was not monitored. Belloulid et al. (2019) worked on a site-specific study of solar drying of wastewater sludge within a greenhouse effect in the region of Marrakesh in Morocco. Drying studies were undertaken during both summer and winter seasons. A maximum dry solids concentration of 80% was reached in 32 hours during summer and 57 hours during winter. Therefore, solar radiation significantly affected the drying time. Shrinkage effect in the drying sludge was observed after 12hours in summer and after 24hrs in winter. Shrinkage effect therefore was highest at higher drying rates. After 72hours of drying, volume reduction was approximately 90% during summer and 83% during winter. An investigation of the performance of direct and indirect solar drying of sewage sludge under natural convection was done in Algeria by Ameri et al. (2018). Drying experiments were conducted at ambient air temperature and air humidity (15-20%). Average temperature outside the drying chamber was 24°C. Peak temperatures of the drying samples were 44°C during indirect drying and 41°C for direct drying. This represents a temperature gain of 20°C and 17°C for indirect and direct solar drying respectively. Peak temperatures for air in the chamber were 67°C and 50°C during indirect and direct solar drying respectively. In all these studies, there was no investigation on the air conditions within the drying chamber and this would have a significant effect on the drying processes (section 2.1.3).

2.4 Literature review conclusion

Faecal sludge is mainly comprised of moisture on proportions depending on the type of on-site technology, geographical location and user habits. Drying of faecal sludge is necessary to reduce the volume, ease its handling and neutralise its pathogen content. From this review, it can be noted that drying, a fundamental process in faecal sludge treatment, can be performed using solar thermal energy as the primary source of power. Solar thermal energy offers the advantage of being a free, sustainable and environmentally friendly energy resource. The amount of power needed for drying depends on the sludge to be dried and the technique used. Solar drying not only plays a significant role in the drying of faecal but also has potential in killing the pathogens in the sludge due to the high temperatures involved.

Drying is basically the process of moisture removal from a wet product through evaporation. Wet products are categorised into two basic groups in accordance to their drying behaviour, i.e. granular/ crystalline solids that hold moisture in open pores between particles, and fibrous/amorphous solids that tend to dissolve moisture or trap moisture in fibres or very fine pores. Feacal sludge corresponds rather to a granular/crystalline solid. Moisture within the sludge can be held within its open pores or trapped within the sludge cellular structure.
Moisture inside the faecal sludge differs in physical, chemical, and biochemical properties, which may significantly affect the drying process. Presence of moisture within faecal sludge could be bound (bonded to the solid matrix) or unbound. Unbound water usually represents the majority of water in undried faecal sludge. This unbound moisture can be removed through mechanical dewatering.

The rate at which drying occurs depends on the power supplied by the heating source, nature of the moisture interactions inside the sludge and the conditions influencing the transfer rates, such as the characteristics of the solid (geometry, size, porosity) and the external conditions (air temperature, velocity and humidity). This research study was therefore conducted during both sunny and overcast weather condition to allow for the variation in solar irradiance that was the main heating source. Additionally, the temperature and velocity of the airstream inside the solar dryer were varied.

When a wet product is subjected to thermal convective drying, heat and mass transfer processes occur simultaneously within the product being dried and in the boundary layer of the solid with the environment. The heat provided from the surrounding is used to raise the temperature of the wet solid and evaporate the moisture. Mass transfer is achieved by moisture migration from the interior of the solid out to the surface. In this study, the heat from the solar radiation and the airstream is expected to induce a temperature rise within the sludge, causing migration of moisture from the core to the surface and its evaporation. The heat and mass transfers will be characterized through the quantification of the heat and mass transfer coefficients, and the moisture effective diffusivity.

The removal of moisture from the faecal sludge induces mechanical stresses and a re-arrangement of the dry bone structure. This is reflected by perceivable morphological changes such as; collapse of the sludge structure (shrinkage), cracking of the top surface of the sludge and development of a hard skin layer (crust) on the sludge surface. This study therefore includes an investigation into the occurrence of these morphological changes in relation to the different operating parameters.

Whereas there is vast literature concerning solar drying processes and kinetics for agricultural products, there is hardly published research regarding solar drying processes and kinetics for

faecal sludge. The few of the studies performed to date are focused on solar drying for sewage sludge within a greenhouse effect. This study shall therefore be centred around the drying kinetics and characteristics for faecal sludge solar thermal convection drying process. Modelling is an important tool to predict the drying process kinetics for the design, operation, optimization and improvement of solar thermal systems. There are numerous empirical models developed to describe thin layer drying for wet products. These models shall be confronted to experimental drying curves for faecal sludge.

3 MATERIALS AND METHODS

This chapter is about the description of the methodology from this investigation. The faecal sludge used in the experiments and the equipment with the experimental procedures are described. The analytic methods for the treatment of the experimental data are also presented.

3.1 Material: Faecal sludge

Faecal sludge from ventilated improved pit (VIP) and urine diversion (UD) toilets was used for this study. Samples were collected from a black soldier fly (BSF) faecal sludge treatment plant (FSTP) located in Isipingo, KwaZulu-Natal province, South Africa. The sludge is issued from the regular VIP and UD pit emptying activities within eThekwini municipality (Durban metropolis). Pit emptying is usually done manually and involves hand equipment like shovels to dig and pitchfork for removing the large trash particles. No water was added to the sludge during the emptying process. In fact, in the BSF plant, the sludge from the different toilets is put together in a pile. Therefore, we can assume that there is a certain degree of mixing. Since samples were grabbed from the mixture, it could be considered that the samples were an average of the sludge from various toilets, so it can be deemed as representative from the region.

About 20 kg of each sample was put in sealed plastic containers, transported to the laboratory from where it was screened with a 5 mm sieve to remove any trash that was disposed in the pit by the toilet user (frequent habit in the region of Durban). Samples were thereafter stored in a laboratory cold room at a temperature of 4°C to deter any possible biological action/degradation and also maintain sludge properties to the possible extent (Strande et al., 2018) until when required for the experiments.

The samples were analyzed for initial chemical and physical properties before the experiments. These analyses included: moisture content, water activity, density, total volatile solids (TVS), ash content, total carbon oxygen demand (COD), pH and electrical conductivity. All these tests were undertaken according to Standard Operating Procedure (SOP) of PRG accessible at http://prg.ukzn.ac.za/laboratory-facilities/standard-operating-procedures.

Table 3-1 shows results of the selected chemical and physical analyses on the sludge samples. The values of the measured parameters were similar to those reported in literature for typical faecal sludge (Strande et al., 2018, Brouckaert et al., 2013, Rose et al., 2015). The average moisture content recorded, i.e. 73% for VIP and 71% for UD sludge meant the largest proportion of sludge consisted of moisture. Initial water activity results, i.e. 0.9866 for VIP and 0.9824 for UD were close to 1 which indicated a significant amount of free moisture in the sludge available for microbial action (section 2.1.2.3).

Table 3-1: Composition and characteristics of faecal sludge used for the experiments

Sludge type	**VIP**	**UD**	Ranges in literature (Strande et al., 2018, Brouckaert et al., 2013, Rose et al., 2015)
Moisture content	75% (3g/g)	71% (2.7g/g)	66 - 95%
Water activity	0.9866	0.9824	0..8 - 1
Density	1090kg/m^3	1120kg/m^3	540 - 2400 kg/m^3
Ash content	10%	13%	5 - 56%
TVS	84%	83% (100% - 17%)	60-85%
pH	7.9	7.7	6.9-8.5
Total COD	< 5000mg/l	< 5000mg/l	1200 – 50000 mg/l

3.2 Description of solar drying rig

Experiments were undertaken within a laboratory-scale solar thermal drying set-up (Figure 3-1) used previous studies (Septien et al., 2018). This setup consists of a cylindrical glass drying chamber, electric heater, mass balance and interface to record data automatically into the computer software. On the contrary to the previous investigation (Septien et al., 2018), the setup was modified with an automatic control flow system, consisting in an electronic flowmeter, proportional valve and controller.

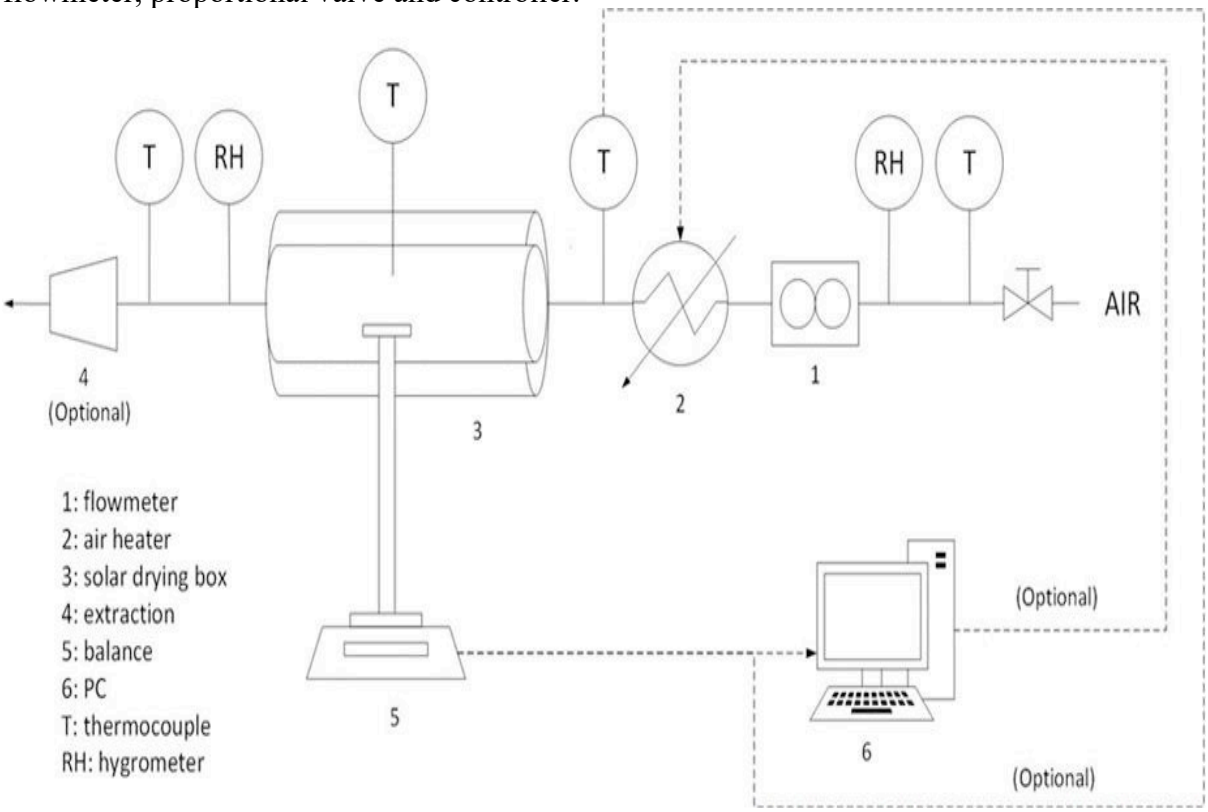

Figure 3-1: A Schematic layout of the solar thermal drying rig set-up

The different components of the solar thermal convection experimental setup are described here below:

a) Drying chamber: The drying chamber was made out of silica glass, cylindrical in shape with dimensions 500 mm length and 140 mm internal diameter. The chamber was fitted with 2 ports within the center, each 20 mm diameter to allow linking of the balance and temperature sensors to the sample. The transmittance of the chamber material is estimated to be 80% according to the previous investigation with the same apparatus (Septien et al., 2018).

b) Airflow system: The air stream in the drying chamber was supplied by the compressed airline from the Chemical Engineering building at a maximum pressure of 4 bar. This pressure was adequate to achieve the desired air flowrates (0.5 and 1 m/s). The airstream was introduced in the drying chamber by multi-entries inlet that enabled an even distribution of the air velocity along the cross-section.

c) Mass balance: A digital balance (Model *ACB 3000*) with accuracy of ±0.01 g was used for measuring sample mass. This balance was enclosed in a wooden box to protect the mass reading from external perturbations, in particular wind, and to avoid overheating from the exposure to solar radiation.

d) Air heater: Before introduction into the drying chamber, the air stream could be heated in a custom-designed electric 20A air heater. The heater was linked to a data interface through which the required air temperature was set.

e) Temperature measurement: Temperature sensors *pt*100 were fixed at both the inlet and the outlet of the drying chamber to track air temperatures into and out of the chamber. Type-k thermocouples of 0.3 mm diameter were employed in the measurement of the temperatures of the sludge samples and air in the drying chamber. The length of the thermocouples wire was covered by glass fibre in order to avoid heat losses that can lead to an inaccurate temperature reading. Type-K thermocouples were opted during measurements of sludge sample temperatures (as opposed to pt100 probes that offer higher accuracy at low temperatures) because of their small diameter (0.3 mm) that could easily fit the small sample thicknesses (5 mm).

f) Humidity measurement: Humidity probes model *HPP809A031* from *TE Connectivity* and *HP474ACR* from *Delta Ohm* were used to measure air humidity at the inlet and outlet of the drying chamber.

g) Flowrate measurement: The air flowrate was varied by a *Burkert* proportional 2- way solenoid valve with a *Burkert 8605* flow controller and flow measured by *Alicat M-1000SPLM-D/10V* mass flowmeter that was connected in series to the flow controller.

h) Air velocity measurement: Airflow velocity at the chamber outlet was monitored at hourly intervals by a hot air anemometer model *ET-961*.

i) Irradiance measurement: Incident solar radiation (W/m^2) throughout the experimental process was determined by a second-class silicon photo-electric pyranometer, model *CMP3* from *Kipp & Zonen* with accuracy ±15 W/m^2

j) Sample crucible: Samples were dried on a cylindrical acrylic glass crucible with dimensions 110 mm diameter and 10 mm thickness.

k) Data interface: A software written in LabVIEW was installed on a computer to create an interface between the computer and measuring instruments. The sensitive balance, thermocouples, temperature sensors, humidity meters and the pyranometer transferred the measurements to the computer via data loggers. All the data loggers were contained in a data acquisition box together with the power supply and control for the air heater.

This set-up was installed at the roof-top of the Chemical Engineering building (latitude: 29°52'08.1" S; longitude: 30°58'46.6"E) at the Howard College campus, University of Kwa-Zulu Natal (UKZN), Durban, South Africa. The solar assessment of the experimental site was done in the previous investigation (Septien et al., 2017) and found that the irradiation levels at this site were high enough to perform solar drying experiments. Experiments were conducted in open space to ensure there was no shading. Figure 3-2 shows a photograph of the solar drying rig during one of the experiments.

Figure 3-2: Photograph of the experimental drying set

3.3 Experimental procedure

Drying experiments were carried out for 5 hours daily from 10:00 to 15:00. Experiments were conducted during sunny and overcast weather days during the months of October, November 2019 (during spring) and January, February, March 2020 (during summer).
Typical solar irradiance values ranged between 400 to 600 W/m2 during overcast weather days, and between 800 to 1350 W/m2 during the sunny weather days.

3.3.1 Experimental protocol

Before the experiments, sludge samples from the cold room were exposed to open air inside a shed for 30 minutes so as to achieve room temperatures. The drying apparatus and parameters to be investigated were also set 15 minutes beforehand to allow for stabilization of the drying conditions.
During the experiments, a sludge sample was placed on a crucible to a thickness of 5 mm and exposed to the solar radiation inside the transparent cylindrical chamber. The crucible was linked to a mass balance, as displayed in figure 3-3, so as to measure and record the changes in mass during the drying process every 60 s. The airstream at a selected temperature and velocity was introduced to the chamber so as to remove the evaporated moisture and enhance the drying process. Detailed Standard Operating Procedure (SOP) for experiments can be seen in Appendix B.

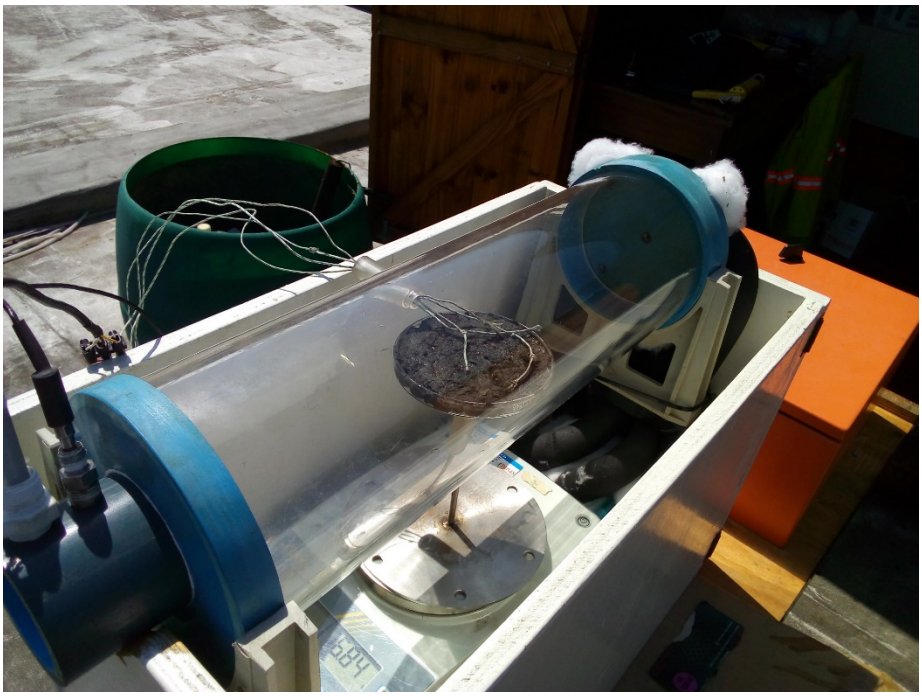

Figure 3-3: Photograph of a sample setup during the drying experiments

At the end of the drying experiment, thickness of dried samples was measured using a foot ruler calibrated in millimeters. Dried samples were visually inspected for presence of crust layer, cracks and odour. Dried samples were also tested for water activity.

3.3.2 Operating conditions

All experiments were conducted at relative humidity of 0% which was the prevailing humidity of dry compressed air. The operational parameters for the experiments were;

1. Weather conditions: Sunny and overcast. Sunny weather days were days with little or no clouds in the sky while overcast weather days were marked by a cloud covering of a large part of the sky.

2. Air flowrate: 0.5 m/s and 1 m/s. The desired air flowrate was achieved by setting the flow control valve half-open (0.5 m/s) and fully open (1 m/s).

3. Air temperature: ambient temperature, 40°C and 80°C. The desired air temperature was set directly at the data interface. Dry air was heated within the air heater box to the set temperatures before reaching the drying chamber.

The following experiments were considered for the control:

i. Open sun drying experiments with a similar crucible and same amount of sample compared to the experiments inside the solar drying rig were undertaken and changes in mass manually recorded every 1 h using an LCD display precise digital scale. The open sun experiments were carried out at the same time than the experiments inside the solar thermal drying rig during sunny weather, with the samples placed to the drying setup. These experiments were conducted in order to draw a comparison between solar drying inside the thermal solar system and solar drying at the open-air.

ii. Experiments were also conducted within the solar drying rig without solar radiation for varying air temperatures (ambient, 40°C and 80°C) and airflow of 0.5 m/s, to determine the effect of solar radiation on drying. This experiment was done by placing a layer of thick black cloth and aluminum foil on top of the drying chamber to block the solar radiation.

iii. Experiments were also conducted without the supply of an air stream into the drying chamber (0 m/s air velocity) to investigate the effect of convection on the drying process. This experiment was conducted by fully closing the flow control valves.

Table 3-2 shows an experimental summary plan for the undertaken experiments. In order to determine the repeatability of results, experiments at the same operating conditions were conducted in duplicates. Average ambient air temperature was 23°C.

Table 3-2: Summary of operational parameters for each experiment

Experiment	Air temperature (°C)	Airflow rate (m/s)	Air humidity (%)	Weather condition	Sludge type
1	Ambient	0.5	0	Sunny	VIP
2	40	0.5	0	Sunny	VIP
3	80	0.5	0	Sunny	VIP
4	Ambient	1	0	Sunny	VIP
5	40	1	0	Sunny	VIP
6	80	1	0	Sunny	VIP
7	Ambient	0.5	0	overcast	VIP
8	Ambient	0	0	Sunny	VIP
9	Ambient	0.5	0	Sunny	UD
10	40	0.5	0	Sunny	UD
11	80	0.5	0	Sunny	UD
12	Ambient	0.5	0	no sun	VIP
13	Open drying			Sunny	VIP

3.4 Kinetic data analysis methods

From the solar drying experiments, data of mass, temperature and solar irradiance as a function of time was obtained. This section describes the methods that were considered for the treatment and modelling of the data to achieve useful information and meet the study objectives.

3.4.1 Moisture content

Moisture content is defined as the amount of moisture present in the sludge samples at any given time of the drying process. From the recorded sample mass reading, the evolution of percentage moisture content on wet basis M_{wb} and on dry basis M_{db} was deduced using equation 2-1 and equation 2-2 (section 2.1.2.1)

3.4.2 Moisture ratio

Moisture ratio (MR) of the drying sludge samples at any given time during drying was calculated according to equation 2-3 (section 2.1.2.1)

3.4.3 Drying rate

The drying rate DR was calculated in terms of the mass of moisture removed from sludge per unit time per unit area of the sludge sample. This rate was determined as the difference between two consecutive moisture contents (in dry basis) in a given drying time interval, as shown in equation 2-4 (section 2.1.5.3). Drying behaviour was determined using graphs of drying rate versus drying time.

Before computation of drying rate, the raw drying curves were smoothened using Microsoft Excel trendlines so as to remove the noise within the data. On Microsoft Excel, the drying curve was decomposed into two sections; a first section where it evolves linearly, and a second section where it loses its linearity. For the first section a linear regression line was fitted. This was achieved by choosing two points. The first point was the initial mass of wet material (i.e., at t = 0), while the second was a random point on the plane containing the data. The initial moisture content could not be altered, thus, the *'x'* and *'y'* coordinate of the second point were manually adjusted so that the straight line fits the experimental data. For the second section, an exponential regression line was fitted. The constant rate period section corresponded to the derived equation from straight line and the falling rate period section corresponded to the derived equation from the exponential equation.

The inflection point on the drying rate curve i.e., point at which a perceptible deviation from a straight line to exponential curve was observed is called the critical point. The moisture content at the critical point was referred to as the critical moisture content ($M_{critical}$). The time taken from the start of drying to the critical point ($t_{critical}$) was considered as the time taken to reach critical moisture content

The critical moisture content was determined by using a linear interpolation formula as in Equation 3-1 below

$$\frac{M_{critical} - M_1}{t_{critical} - t_1} = \frac{M_2 - M_1}{t_2 - t_1} = slope\ of\ liner\ fit \qquad (3-1)$$

Where $M_{critical}$ represents the critical moisture content (g/g db) and $t_{critical}$ is the drying time taken to reach critical moisture content. (M_1, t_1) and (M_2, t_2) correspond to values of moisture content and time respectively for two random points on the linear section (constant rate period) of the drying curve.

Interpolation of raw drying curve data through linear and exponential trendlines for the calculation of the drying rates can be seen in detail in appendix D.

3.4.4 Modelling of the drying curves

Regression analysis was done to fit the drying curves to the already existing thin layer drying models. This was undertaken so as to compare the solar drying kinetics for faecal sludge to tested drying models that are reported in literature.

Six tested thin layer drying models, i.e. Newton model, Page model, modified Page model, Henderson and Pabis model, Logarithmic model, and the Two-term model were investigated for the thin layer solar drying of faecal sludge. These models were selected because they are regarded as the most accurate in describing various food material as well as sewage sludge (Wan et al., 2009, Bahammou et al., 2019) and also because of the simplicity for the determination of the coefficient(s) involved using a regression method. The data was normalized using the moisture ratio (*MR*). The respective model equations were applied as explained in section 2.1.5.2.

The SOLVER (GRG2 method) optimization tool available in Microsoft Excel 2016, was used for the regression of the parameters of each of the models by minimizing the sum of the square differences between the experimental and the calculated values.

The models were investigated by comparison with the experimental data using the goodness of fit statistical measure. The coefficient of determination R^2 was used to evaluate how well each model fitted the experimental data, and the root mean square error ($RSME$) and reduced chi-square (X^2) were calculated to reflect the dispersion in the obtained data. These three statistical models were determined, as shown below in equations 2-5, 2-6 and 2-7 (section 2.1.5.3)

The best-fitting model was considered to have the smallest values of X^2 and $RSME$, and the largest value for R^2.

3.5 Morphology of dried sludge

The methods used to characterize the morphological properties of the dried sludge are described in this section. The physical characteristics of dried sludge investigated included; shrinkage, density, qualitative observations (crust, cracking, colour, odour, reflectivity) and water activity

3.5.1 Shrinkage

Shrinkage occurs as a result of the removal of moisture from the sludge which leads to stresses in the sludge solid structure. This causes the structural collapse, volume change, shape deformation, and capillaries contraction.

Shrinkage *S* (%) was calculated as the ratio of change in volume of sludge after drying to the initial volume of sludge sample as in equation 3-2.

$$S = \frac{V_0 - V_d}{V_0} \times 100 \qquad (3-2)$$

Where V_0 (mm^3) represents initial volume of the sludge sample and V_d (mm^3) represents volume at the end of drying period. Given that the crucible with the sludge sample was cylindrical, volume can be expressed as a product of base area and thickness as displayed in equations 3-3 and 3-4.

$$V_0 = \pi r^2 l_o \quad (3-3)$$

$$V_d = \pi r^2 l_d \quad (3-4)$$

The entire base area of the crucible remained occupied by sludge through the experiments, therefore it was considered that sample base area at the start and end of drying period was the same. Therefore, substituting equations 3-3 and 3-4 in equation 3-2 gives equation 3-5. Therefore, for this study, shrinkage (%) was computed using equation 3-5.

$$S = \frac{(l_0 - l_d)}{l_0} \times 100 \quad (3-5)$$

Where l_0 (mm) is the initial sample thickness and l_d (mm) is the sample thickness at the end of the drying experiment. Sample thicknesses were measured using a foot ruler. It should therefore be noted that the measurements were a rough estimate given that the measurement method was not precise.

3.5.2 Density

Density refers to the mass per unit volume of the dried sludge samples. Density d (g/mm^3) was determined as in equation 3-6:

$$d = \frac{m_d}{V_d} \quad (3-6)$$

Where m_d is the mass of sludge sample at the end of the drying period as recorded from the mass balance and V_d is the volume of dried sample as in equation 3-11. Similar to shrinkage, density values were also considered as rough estimates as the methods for measurement were not precise.

3.5.3 Qualitative observations

A qualitative analysis was carried out on the dried samples. Parameters for this analysis included; presence of cracks and crust layer on the dried sample surface, colour, odour and reflectivity of the dried sludge.

Cracks were depicted by presence of fracture lines on the dried sludge surface along which the sludge split without breaking apart.

Formation of crust was depicted by presence of a thick skin-like layer of top of the dried sludge. Hardness of this layer was estimated by the force required to drive a needle through the top surface. The needle was introduced manually into the dried sludge sample and the force required for penetration was based on the perception of the experimenter.

The colour and odour (smell) of the dried samples was compared to those from the initial sludge sample before drying.

The reflectivity of dried sludge samples was determined by the shininess and brightness of the top surface of dried sludge when exposed to light, and compared to the sludge before drying.

3.5.4 Water activity

A tuneable diode laser water activity meter model *4TEV* from AQUALAB was used for the water activity tests. Water activity tests for each sample were carried out in duplicates and the average of the duplicates was considered.

3.6 Characterization of the performance of the solar thermal drying process

Characteristics of the solar convection drying set-up are presented in this section. The system was characterized by the fallowing elements: flow regime, convective heat and mass transfer coefficients, energy efficiency.

3.6.1 Flow regime, heat and mass transfer parameters

Dimensionless numbers that is Reynolds number, Schmidt number and Sherwood number, were used to characterise the hydrodynamic conditions within the drying chamber and the mass transfer coefficients.

3.6.1.1 Flow Regime

To determine the flow regime inside the drying chamber, hydraulic Reynolds number Re was calculated according to equation 3-7.

$$Re = \frac{\rho u L}{\mu} \qquad (3-7)$$

Where ρ is the density of air (kg/m^3), u is the airflow velocity (m/s), L is the characteristic length, i.e. diameter of the drying chamber (m) and μ is the dynamic viscosity of air (kg/m.s).

The hydraulic regime of airflow within the drying chamber was determined from the values of Reynolds number. Reynolds number less than 2100 indicates a laminar flow while Reynolds number greater than 4000 indicates a turbulent flow while values of Reynolds number between 2100 and 4000 depict a transitional flow.

3.6.1.2 Mass transfer coefficients

Particle Reynolds number was calculated to characterize the flow regime at the nearby of the sludge sample surface and compute the heat and mass transfer coefficients as in equation 3-7 but using characteristic length L as the diameter of the drying sample.

Schmidt number Sc is the ratio of kinematic viscosity and mass diffusivity and was determined from equation 3-8.

$$Sc = \frac{v}{D} = \frac{\mu}{\rho D} \qquad (3-8)$$

Where D is the diffusion coefficient of water vapor air (m^2/s).

Sherwood number Sh represents the ratio of the convective mass transfer to the rate of mass transport by diffusion (equation 3-9). It was deduced from the results of Schmidt's number and Particle Reynold's number using the equation 3-10. Equation 3-10 corresponds to external forced convection flow over a flat plate for $0.6 \leq Sc < 50$

$$Sh = \frac{h_m}{D/L} \qquad (3-9)$$

$$Sh = 0.664Re^{1/2}Sc^{1/3} \quad (3-10)$$

Where h_m is the convective mass transfer coefficient (m/s).

The mass transfer coefficient h_m was determined by combining equation 3-9 and equation 3-10 into equation 3-11.

$$h_m = \frac{ShD}{L} \quad (3-11)$$

3.6.1.3 Heat transfer coefficients

Prandtl dimensionless number P_r was calculated according to equation 3-12.

$$P_r = \frac{v}{\alpha} = \frac{\mu}{\rho\alpha} \quad (3-12)$$

Where α represents the thermal diffusivity of air (m^2/s).

The Nusselt dimensionless number N_u was computed using the formula used by Nems et al. (2017) as shown in equation 3-13. This corresponds to fluid flow over a flat plate for Re smaller than 10,000 and P_r between 0.6 and 2000.

$$N_u = 0.664 * Re^{\frac{1}{2}} * P_r^{\frac{1}{3}} \quad (3-13)$$

The convective heat transfer coefficient h_c ($W/m^2.K$) was determined using the expression in equation 3-14.

$$h_c = \frac{N_u * K_v}{L} \quad (3-14)$$

Where K_v is the thermal conductivity of dry air (W/m.K).

The properties of air at ambient temperature (~ 23°C), 40°C and 80°C used in the dimensionless numbers calculations are presented in table 3-3.

Table 3-3: Air physical properties at varying temperatures

	Ambient temperature	**40°C**	**80°C**
Density, ρ (kg/m^3)	1.184	1.127	0.9994
Dynamic viscosity, μ x10^{-5} (kg/m.s)	1.849	1.918	2.096
Kinematic viscosity, ν x10^{-5} (m^2/s)	1.534	1.692	2.248
Diffusion coefficient of water vapour in air, D x10^{-5} (m^2/s)	2.420	2.815	3.600
Thermal diffusivity, α x10^{-5} (m^2/s)	2.141	2.346	2.931
Thermal conductivity, K_v (W/m.K)	0.02551	0.02662	0.02953

3.6.2 Moisture diffusivity

The moisture diffusivity was computed for the regions of the drying curves at the falling rate period. The analytical solution of the flat slab geometry was used in the determination of the effective diffusivity due to its simplicity in relation to the other geometries and also considering the initial shape of the sludge samples (section 2.1.4.3). The temperatures for the analysis were 30 (ambient), 40 and 80 °C while the airstream was operated at a constant air velocity of 0.5 and 1 m/s. The following assumptions were adopted for this analysis (Koukouch et al., 2017):

a) the transport of moisture from within the sludge core structure carries out only by diffusion;
b) the diffusion coefficient and temperature of sludge have constant values;
c) the sludge was homogenous, and therefore the initial moisture distribution was uniform;
d) the shrinkage effect was neglected.

The analytical solution of Fick's second law, i.e. equation 2-8 (section 2.1.7.1), was developed for the case of an infinite plate of a given thickness to give equation 3-15 (Mghazli et al., 2017):

$$MR = \frac{8}{\pi^2}\sum_{n=0}^{\infty}\frac{1}{(2n+1)^2}exp\left[-(2n+1)^2\frac{\pi^2 D_{eff}t}{4l^2}\right] \qquad (3-15)$$

Where D_{eff} is the effective moisture diffusivity (m^2/s), t is the drying time (s), and l is sludge sample thickness (m).

Taking consideration that only the first term of the series is significant for longer drying periods, the solution from equation 3-15 becomes as follow (Koukouch et al., 2017, Mghazli et al., 2017):

$$MR = \frac{8}{\pi^2} exp\left[\frac{-\pi^2 D_{eff} t}{4l^2}\right] \quad (3-16)$$

or

$$\ln MR = \ln\frac{8}{\pi^2} - \frac{\pi^2 D_{eff} t}{4l^2} \quad (3-17)$$

Using equation 3-17, the graph of ln MR versus the drying time t was plotted and the effective moisture diffusivity was determined from the slope of the curve after linear regression using equation 3-18;

$$D_{eff} = -\frac{B4l^2}{\pi^2} \quad (3-18)$$

Where B is the slope of the straight line obtained after linear regression.

3.6.3 Activation energy

The activation energy describes the relationship between moisture diffusivity and temperature. This was computed based on Arrhenius type equations as displayed in equation 3-19;

$$D_{eff} = D_0 exp\left(-\frac{E_a}{R_g T}\right) \quad (3-19)$$

where E_a is the activation energy (kJ/mol), D_0 is the Arrhenius constant in (m^2/s) and R_g is the perfect gas constant which is 8.314 $Jmol^{-1}K^{-1}$.

From equation 3-19 the graph of ln D_{eff} versus $\frac{1}{T}$ was plotted for varying drying air velocities. Linear regression analysis was applied to give a straight line of best fit with a slope C. The activation energy at each air velocity was determined using equation 3-20.

$$C = -\frac{E_a}{R_g} \quad (3-20)$$

D_0 corresponded to the intercept for the line of best fit with the y-axis.

3.6.4 Power and efficiency

The solar convection drying system received two sources of power; from the solar radiation (radiative heat power) and from the convection of the heated air stream (convective heat power).

The convective power P_c (W) was determined using equation 3-21.

$$P_c = (h_c * \Delta T) * A \quad (3-21)$$

Where ΔT is the average temperature difference between the temperature T at the sludge surface and the air temperature T_c in the drying chamber (°C) during the drying experiment, A is the surface area of the sample (m^2), h_c is the convective heat transfer coefficient ($W/m^2.K$) as calculated in section 3.6.1.

The solar radiative power P_s (W) was determined according to equation 3-22:

$$P_s = 0.8 * I * A \quad (3-22)$$

Where I is the average solar irradiance (W/m^2) recording during the experiment and 0.8

represents the transmittance of the drying chamber (section 3.2).

The total power of the system P (W) is the sum of the solar radiative and convective power, as calculated in equation 3-23.

$$P = P_c + P_s \qquad (3-23)$$

The efficiency η (%) of the solar convection drying system was a comparison of the power utilized for drying to the total power received by the samples. The efficiency was computed according to equation 3-24

$$\eta = \frac{P_{out}}{P} \times 100 \qquad (3-24)$$

It was assumed that all the energy received by the sludge (P_{out}) was used for moisture evaporation (latent heat) and not for its heating (sensible heat). This was a reasonable assumption since the sensible heat was much lower than the latent heat, so the sensible heat could be neglected.

$P_{out}$was computed from the average drying rates during the experiment according to equation 3-25.

$$P_{out} = L_v * D_r * m_d * A \qquad (3-25)$$

Where L_v is the latent heat of vaporization of water (2260 J/g) and D_r is the average drying rate (g/g.s.m^2) of sludge sample during the experiment and m_d is the sample dry mass (g).

4 RESULTS AND DISCUSSIONS

Within this chapter, data from faecal sludge solar convection drying experiments are presented, analyzed and compared to findings reported from previous studies.

4.1 Drying Kinetics of solar convective sludge drying

The results at varying operation conditions are presented in this section. Parameters investigated included: weather conditions (sunny/overcast), convection air stream conditions (temperature, velocity) and type of sludge (UD/VIP). Each experiment at the same conditions was carried out twice (duplicates) and both sets of results, i.e. run 1 and run 2 are presented. Experimental results at the same operating conditions were not averaged due to the variation of solar irradiance even at similar weather conditions. Table 4-1 presents a summary of the results of solar irradiance, temperatures within the sludge and drying chamber, drying rates and final moisture content achieved at the end of the experiment. The average results from the beginning to the end of each experiment are presented.

Table 4-1: Summary of the results of the average solar irradiance, average sludge and air chamber temperature, final moisture content and average drying rates during each experiment

Experiment	Average irradiance (W/m^2)	Average internal sludge temperature (°C)	Average drying chamber temperature (°C)	Final moisture content (g/g db)	Average drying rates (g/g $min.m^2$)
1 run 1	835	26.3	36,8	1.51	0.53
run 2	1189	29.6	43.6	1.38	0.66
2 run 1	952	34.9	39.3	1.29	0.67
run 2	1219	38.6	41.9	1.16	0.69
3 run 1	1016	42.1	50.3	0.94	0.81
run 2	1107	44.4	51.2	0.99	0.76
4 run 1	1064	32.3	36.2	1.03	0.71
run 2	1195	36.3	43.6	0.93	0.77
5 run 1	1020	41.7	44.1	0.92	0.84
run 2	1147	43.0	44.6	0.73	0.94
6 run 1	1051	45.3	48.7	0.71	0.97
run 2	1332	48.6	50.4	0.60	0.99
7 run 1	418	24.6	27.2	1.78	0.41
run 2	595	26.2	27.6	1.84	0.43
8 run 1	966	42.6	41.3	1.85	0.40
run 2	848	40.3	39.2	1.79	0.42
9 run 1	1120	43.5	40.7	1.60	0.30
run 2	985	42.9	38.9	1.58	0.29
10 run 1	1141	45.2	43.8	1.52	0.33
run 2	1009	41.4	40.3	1.47	0.31
11 run 1	1149	55.7	52.5	1.44	0.37
run 2	924	52.0	50.4	1.43	0.35
12 run 1	0	23.35	31.6	2.13	0.31
run 2	0	23.01	34.3	2.04	0.34
13 run 1	835	N/A	N/A	1.15	0.62
run 2	1189			1.12	0.60

The operating conditions for each of the experiments i.e. experiment 1 to 12 were as stated in table 3-2. Initial moisture content was 3 g/g for experiments 1-8, 12 and 13 (with VIP sludge) and 2.7g/g for experiments 9, 10 and 11 (with UD sludge) as described in table 3-1.

4.1.1 Effect of weather condition

Experiments were carried out with VIP sludge during sunny, overcast and without solar radiation, at the same operating conditions (ambient temperature and air velocity of 0.5 m/s). Figure 4-1 shows the solar irradiance recorded during the experiments at different weather conditions. The average solar irradiance recorded was 1012 W/m^2 and 506 W/m^2 during sunny and overcast. As expected, the greatest solar irradiance was received during sunny weather. Experiments were conducted during the peak hours of daylight (10.00 to 15.00 h). The irradiance maintained an almost constant value through the experiments at sunny conditions. High irradiance fluctuations were observed during overcast weather (particularly for run 2), which were attributed to the alternance between clouds and sunlight. The value recorded for solar irradiance during the experiments without radiation can be assumed to be zero, because if the drying chamber is covered, we could assume that no sunlight could reach the sample. The small irradiation values recorded during the experiments at zero radiation, i.e. ± 15 W/m^2, were due to the measurements from the pyranometer that were out of its accuracy range (section 3.2).

It should be noted that all irradiance curves (even during similar weather conditions) showed unique trends and not all experimental cases followed the trends described above. This was because of the uniqueness/variability of the irradiance on each experimental day. This demonstrated why the duplicates experiments could never be carried out with identical irradiance.

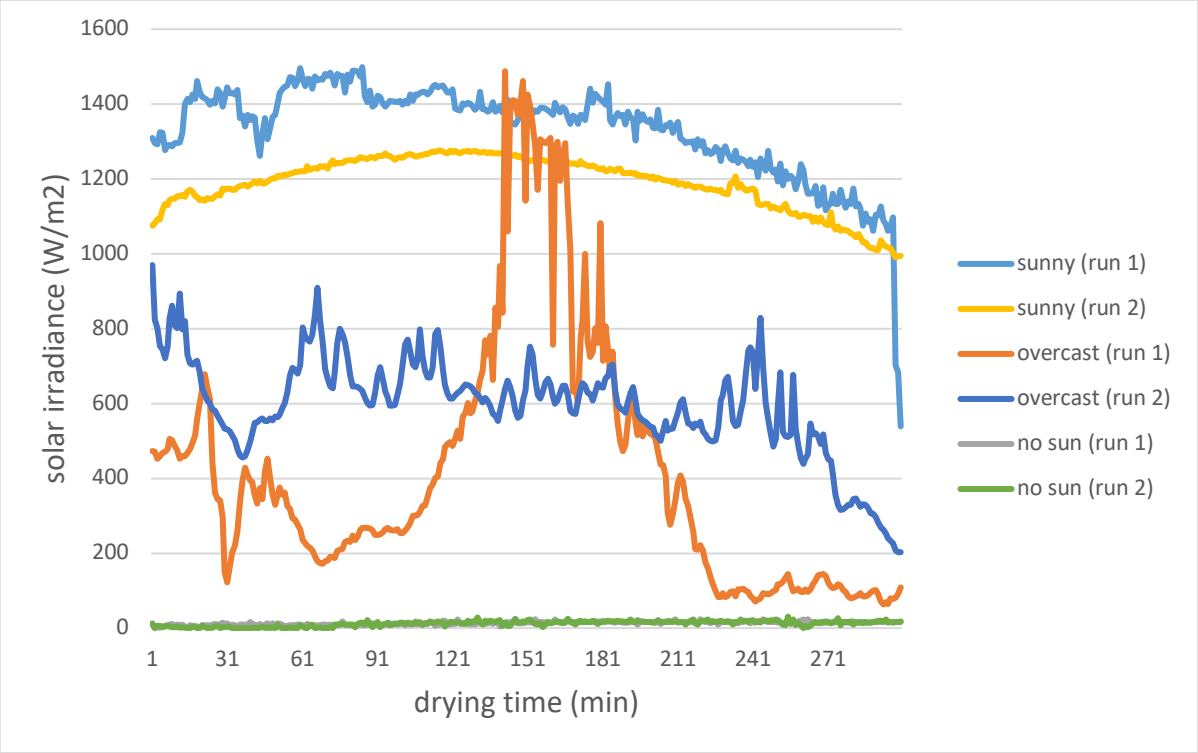

Figure 4-1: Solar irradiance recorded during solar drying experiments for sunny and overcast weather conditions at ambient temperature (23°C) and 0.5 m/s air velocity

Figure 4-2 shows the respective drying curves at the varying weather conditions. The final moisture content recorded was on average 1.47 g/g db at sunny weather, 1.83 g/g db at overcast conditions, and 2.09 g/g db without radiation. The greatest reduction in moisture content was observed for drying experiments at sunny conditions followed by overcast, and least moisture content reduction for drying experiments at zero irradiation. As shown in Figure 4-1, sunny weather resulted in higher solar irradiance and so more heat was available for the evaporation of the moisture from the sludge. These results are similar to research by Mathioudakis et al. (2013) and Hassine et al. (2017), who concluded that drying for sewage sludge was faster at higher solar radiation intensities.

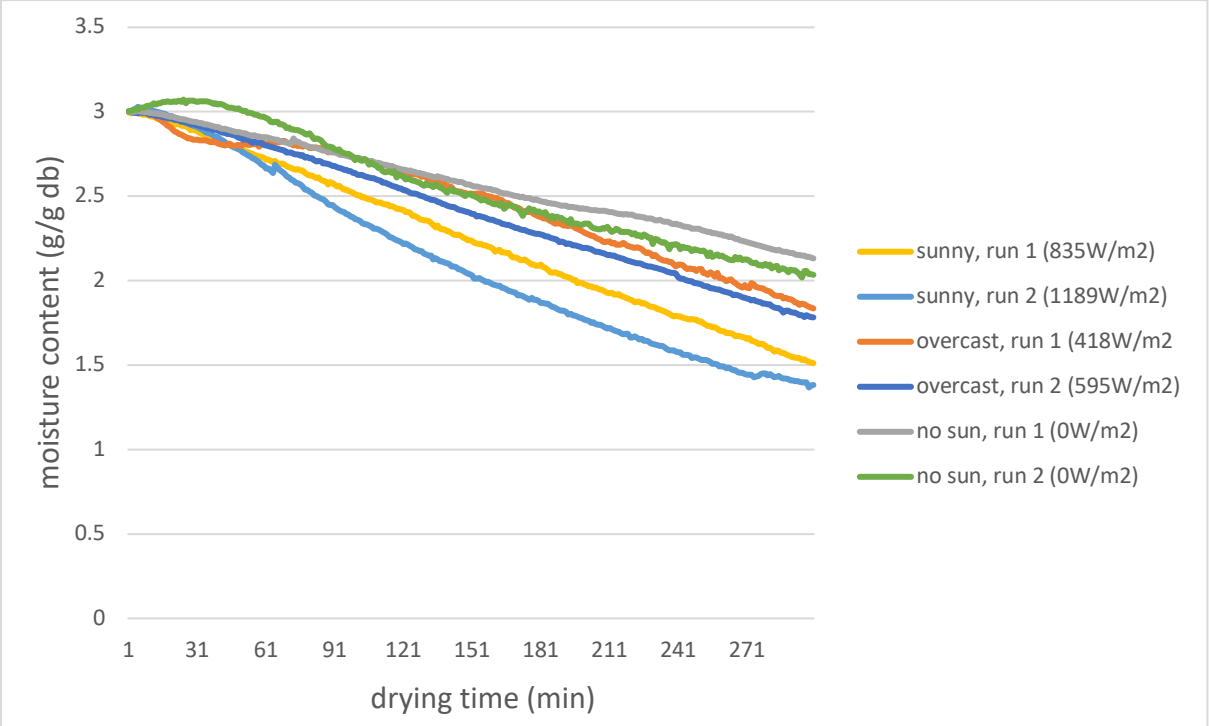

Figure 4-2: Drying curves during solar drying experiments for VIP sludge at 0.5m/s air velocity, ambient air temperature (23°C) and varying weather conditions

4.1.2 Effect of air temperature

Effect of air temperature on solar drying for faecal sludge was investigated through experiments with VIP samples at varying airflow temperatures, i.e. ambient (23°C), 40°C and 80°C, at constant air velocity (0.5 m/s) and similar weather condition (sunny). Air temperature was varied so as to simulate a solar thermal system with both direct and indirect solar drying. Figure 4-3 shows the variation of moisture content with drying time at 0.5 m/s airflow while figure 4-4 represents the drying curves at 1 m/s airflow. After 5 hours of drying, the moisture content at 0.5 m/s air velocity (figure 4-3) on average was 1.47 g/g db at ambient temperature, 1.23 g/g db at 40°C, and 0.97 g/g db at 80°C. At an air velocity of 1 m/s (figure 4-4), the final recorded moisture contents were on average 0.98 g/g db at ambient air, 0.83 g/g db at 40°C, and 0.66 g/g db at 80°C.

When air temperature increased, there was a greater reduction in moisture content; thus, the drying times were reduced. Drying was faster by increasing air temperatures due to enhanced vapour pressure in the sludge and increased heat transfer rates, causing that the removal of moisture from the sludge occurred at a higher rate. This trend is similar to that reported by Ameri et al. (2018) for solar drying of sewage sludge. In figure 4-3, the drying rate was similar

between the experiments conducted at ambient temperature (run 2) and 40°C (run 1), which could be attributed to the fact that solar irradiance at ambient air temperature (1189 W/m^2) was significantly greater than at 40°C (958 W/m^2). This suggested that variability of the solar irradiance could have obscured some of the critical observations of the effects of air temperature on the drying performance.

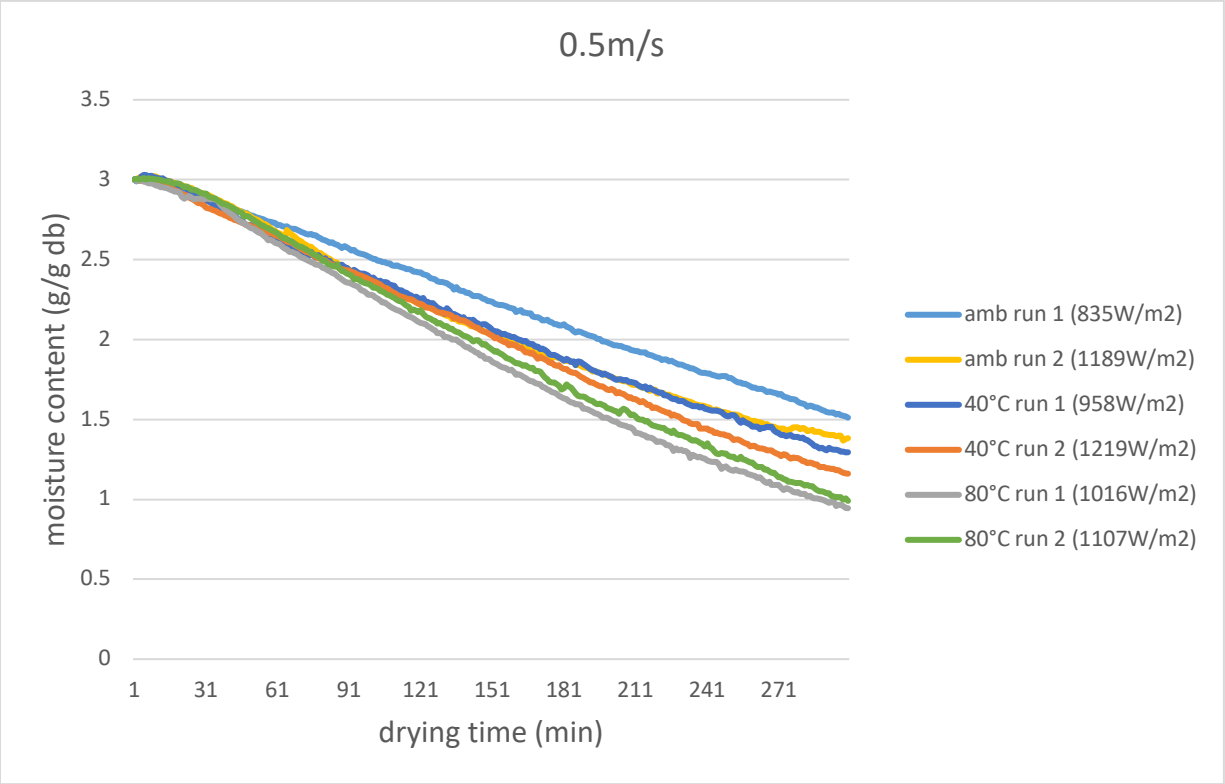

Figure 4-3: Drying curves showing variation of moisture content with drying time for VIP sludge dried during sunny weather conditions, 0.5m/s airflow and at varying conditions of air temperature (ambient 23°C, 40°C and 80°C)

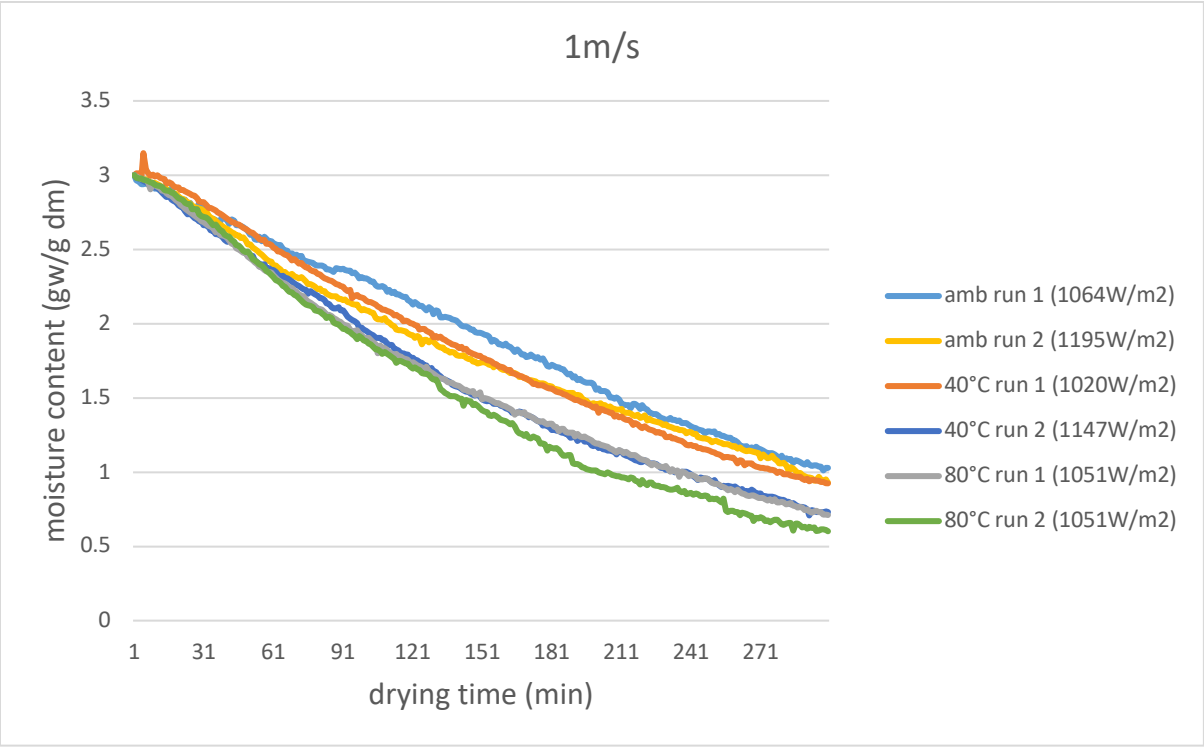

Figure 4-4: Drying curves showing variation of moisture content with drying time for VIP sludge dried during sunny weather conditions, 1m/s airflow and at varying conditions of air temperature (ambient 23°C, 40°C and 80°C)

4.1.3 Effect of air velocity

The effect of air velocity on faecal sludge solar drying was investigated through experiments with VIP sludge at similar weather conditions (sunny) and air temperature, while the air velocity was varied at 0, 0.5 and 1 m/s. Figure 4-5, 4-6 and 4-7 show the drying curves for the different air velocities at ambient temperature, 40°C and 80°C respectively. Experiments at a null air velocity (0 m/s), could only be carried out at ambient conditions.

At ambient air temperature, moisture contents achieved were on average1.82 for 0m/s air velocity, 1.47 for 0.5m/s, and 0.98 for 1m/s. At 40°C air temperature, final moisture contents were 1.23 at 0.5m/s, and 0.83 at 1m/s air velocity. At 80°C air temperature, final moisture contents were on average 0.97 at 0.5m/s, and 0.66 at 1m/s air velocity.

All results showed that the lowest moisture contents were achieved at 1 m/s air velocity followed by 0.5 m/s and, at the last, the experiment without the introduction of airflow rate. This indicated that drying for faecal sludge was faster with increasing air velocity. This was explained by the fact that the increase in air velocity decreased the boundary layer thickness, which enhanced the heat and mass transfer rates, thereby leading to faster moisture evaporation from the sludge sample surface and faster heating in the case of preheated air (Aral and Bese, 2016).

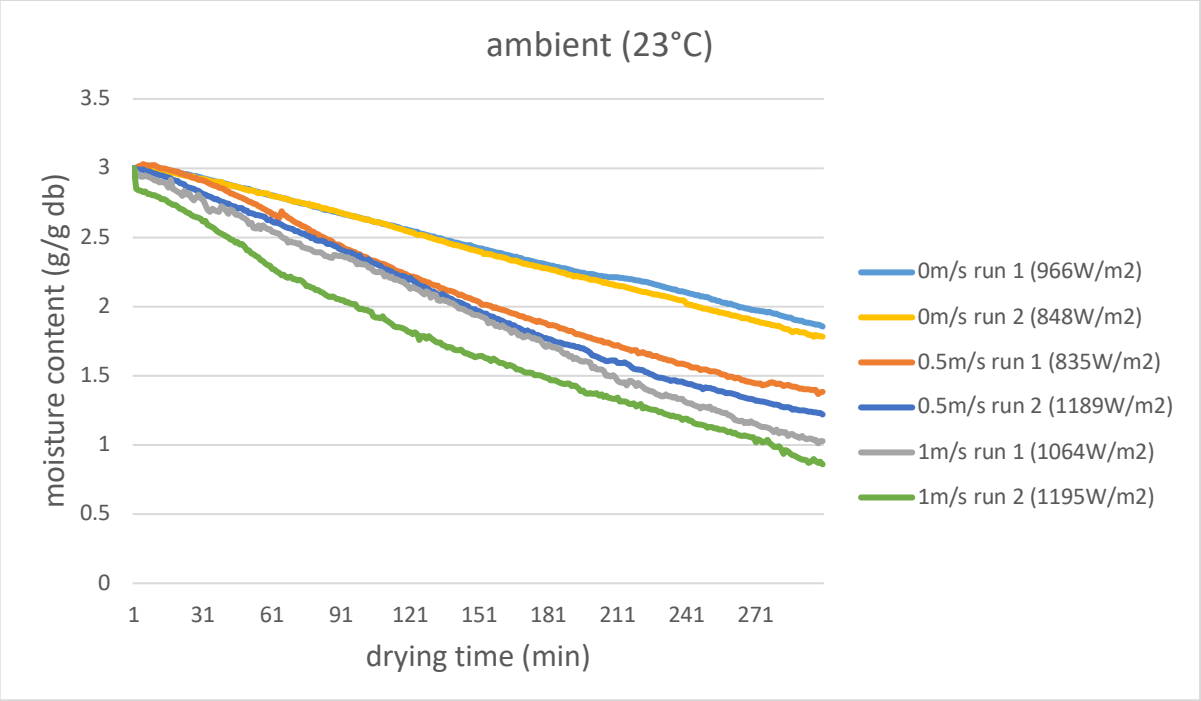

Figure 4-5: Drying curves showing variation of moisture content with drying time for VIP sludge dried during sunny weather conditions, ambient air temperature and varying conditions of air flow (0, 0.5, 1m/s)

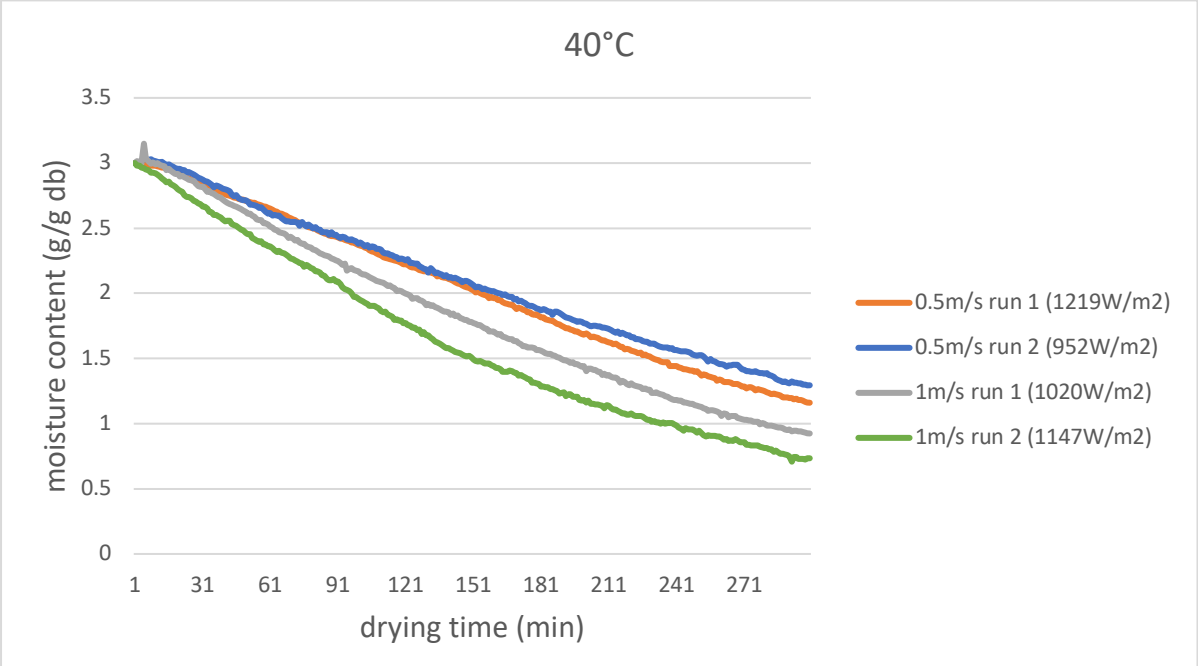

Figure 4-6: Drying curves showing variation of moisture content with drying time for VIP sludge dried during sunny weather conditions, air temperature 40°C and varying conditions

of air flow (0.5, 1m/s)

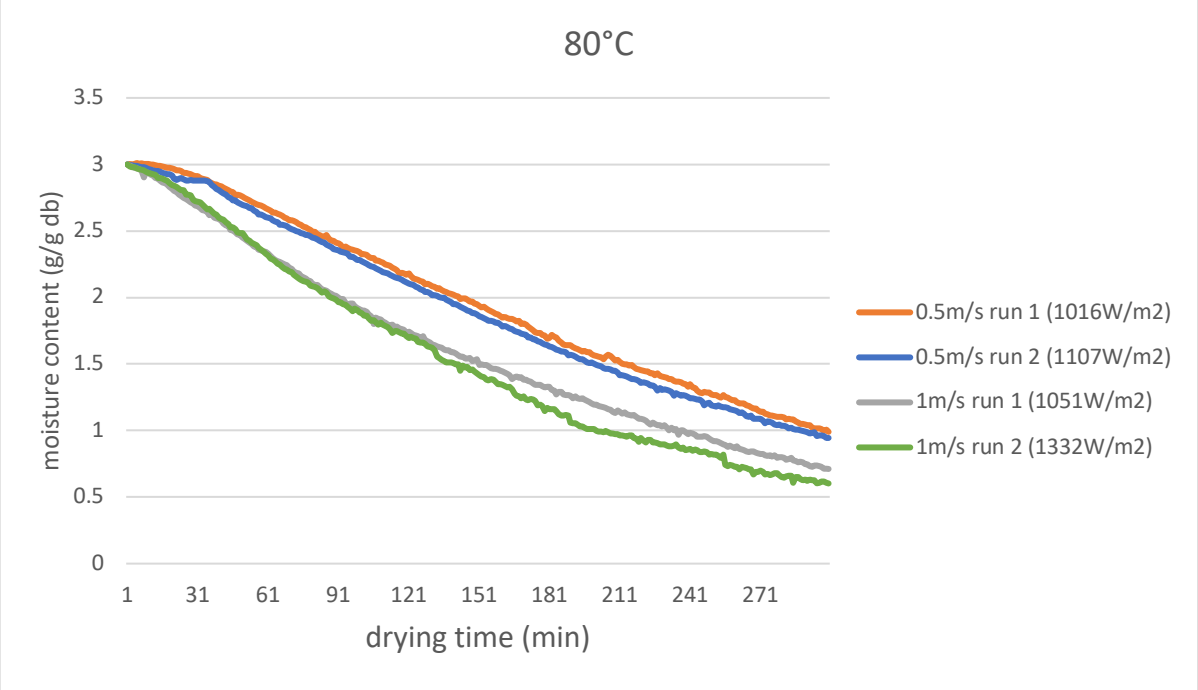

Figure 4-7: Drying curves showing variation of moisture content with drying time for VIP sludge dried during sunny weather conditions, air temperature 80°C and varying conditions of air flow (0.5, 1m/s)

4.1.4 Drying rates at varying conditions of air temperature and velocity

Figures 4-8 and 4-9 show the variation of drying rates with moisture ratio (Krischer curves) for VIP sludge at 0.5 and 1 m/s air velocities, respectively, at different air temperatures (ambient, 40°C and 80°C). As shown from both figures, the drying rates were constant and then declined after certain time. This trend suggested that drying of VIP sludge occurred in the constant rate period until the critical moisture ratio was achieved, beyond which the falling rate period started. The exception of this trend was the experiment 'ambient (run 1)' that showed only a constant drying rate as possibly the critical moisture ratio was not achieved. Ameri et al. (2020) investigated the drying behaviour for sewage sludge within a natural convection solar dryer and reported a similar trend.

The constant rate period in all the samples occurred when the entire surface of the sludge was saturated in moisture that continuously evaporated and was replaced immediately by moisture from inside the particle. But beyond a certain moisture ratio (corresponding to the critical moisture ratio), sludge sample surface was no longer saturated and thus moisture from the surface of the sludge started to evaporate at a faster rate than it could be replaced from inside the sludge sample, causing a decrease of the drying rate, and therefore the falling rate period (section 2.1.5).

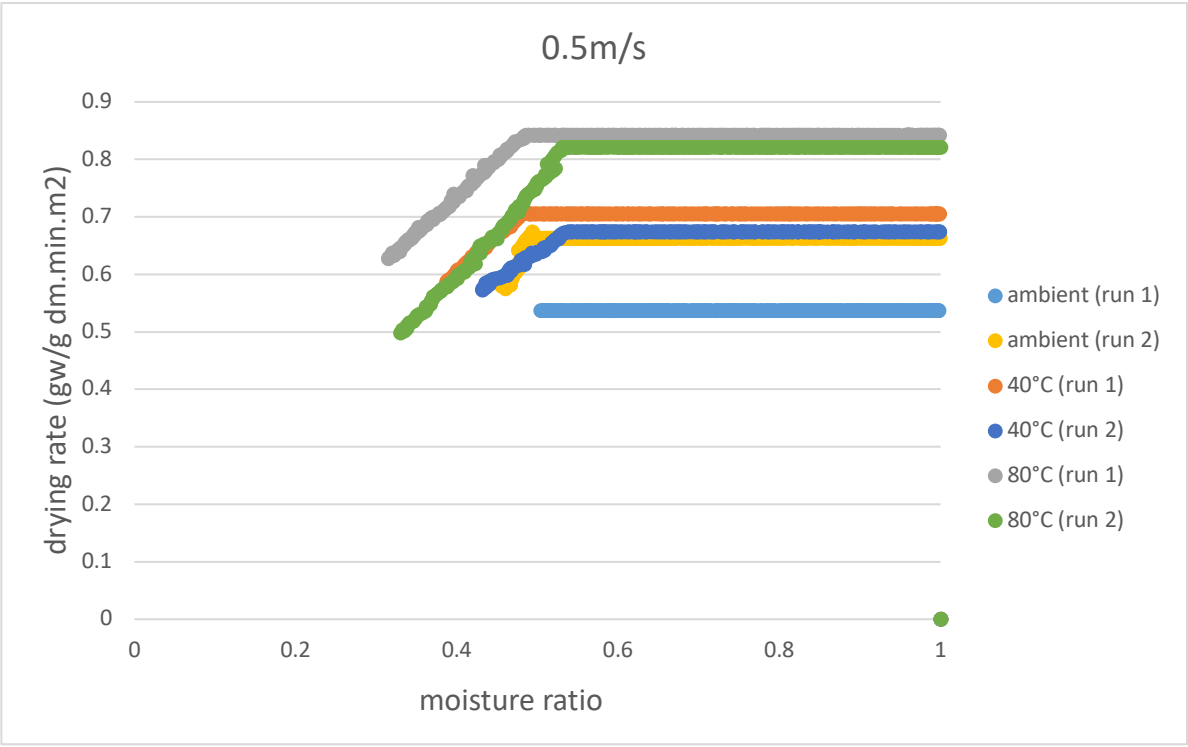

Figure 4-8: Krischer curves showing variation of drying rates with moisture ratio for VIP sludge during sunny weather, 0.5 m/s air velocity and varying air temperature (ambient, 40°C and 80°C)

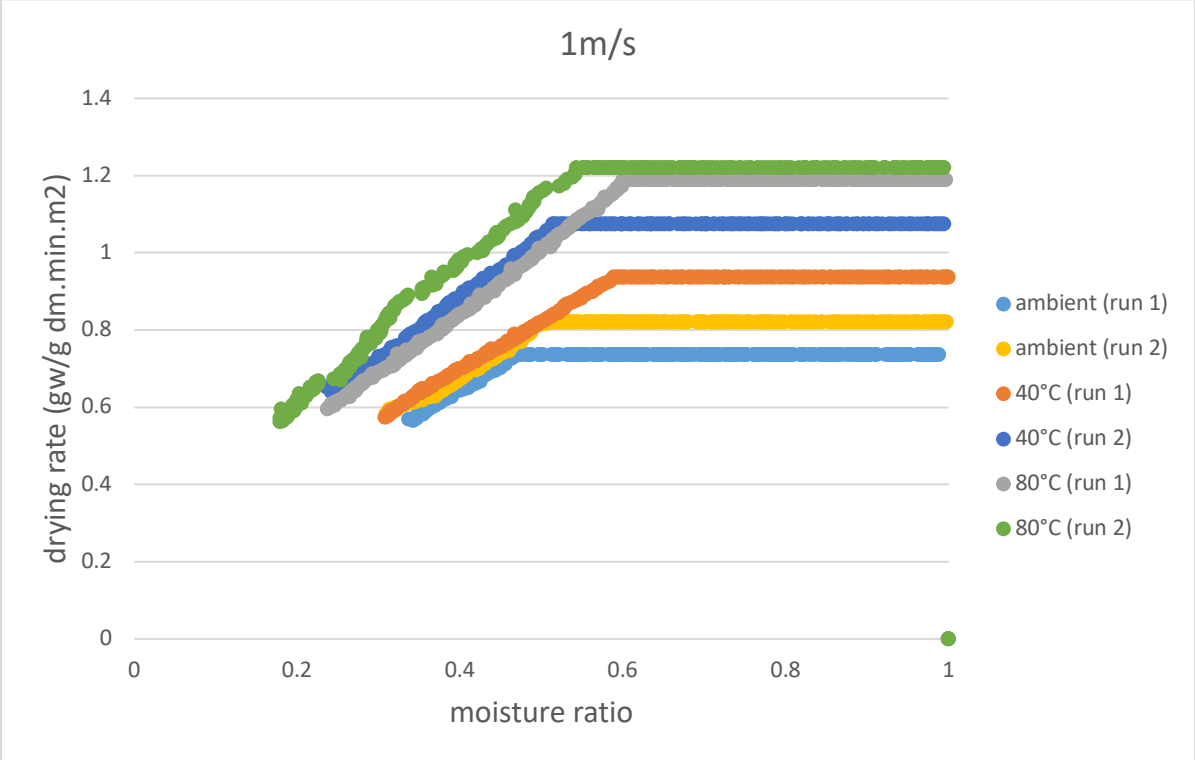

Figure 4-9: Krischer curves showing variation of drying rates with moisture ratio for VIP sludge during sunny weather, 1m/s air velocity and varying air temperature (ambient, 40°C and 80°C)

It was also observed that drying rates in figure 4-9 (1 m/s) were higher than rates in figure 4-8 (0.5 m/s), and in both cases the rates were the greatest at 80°C and the lowest at ambient temperature. Drying rates, therefore, increased with increasing air velocity and temperature, which is in accordance to the observations from section 4.1.2 and 4.1.3.

The estimated constant rate period duration and critical moisture content at the different air velocities and temperatures were tabulated in table 4-2. These parameters were determined at the point on the drying curve where the decrease of moisture content was not further linear. The variation of the drying rates as a function of time can be seen in appendix E.

The estimated constant rate period duration and critical moisture content at the different air velocities and temperatures were tabulated in table 4-2.

Table 4-2: Estimated constant rate period durations and critical moisture content for VIP sludge solar drying during sunny weather at different air velocities and temperatures

Air velocity (m/s)	Air temperature (°C)	Estimated drying time for constant rate period (mins)	Critical moisture content (g/ g db)	Critical moisture content (% wet basis)	Average solar irradiance
0.5	ambient	N/A 260	N/A 1.4070	N/A 58.5	835 1189
	40	240 230	1.4338 1.5650	58.9 61.0	952 1219
	80	205 195	1.4413 1.5985	59.0 61.5	1016 1107
1	Ambient	220 190	1.7857 1.5989	64.1 61.5	1064 1195
	40	152 145	1.7164 1.5129	63.2 60.4	1020 1147
	80	110 125	1.4314 1.4113	58.9 58.5	1051 1332

From table 4-2, the constant rate period was shorter with increasing drying air temperature and velocity. This result could be explained by the higher air temperature and velocity associated to higher moisture removal rates (sections 4.1.2 and 4.1.3), leading to lower time to reach unsaturated levels at the surface as compared to samples dried at lower air temperature and velocity.
Critical moisture content was in the range 1.4 to 1.8 g/g on dry basis and 58-64% on wet basis. The differences in critical moisture content values could be due to experimental uncertainties or explained by the fact that critical moisture content is not entirely a material property, but also depends on drying conditions (solar irradiation, air temperature and air velocity) as reported by (Mujumdar and Devahastin, 2011).

4.1.5 Internal temperature profile

Three thermocouples were inserted at three different points (center and edges) within the drying sample to track the temperature changes within the sludge during the drying process. The three internal temperature readings for each sample were averaged to provide an estimate of the evolution of internal sludge temperature with time.

Figures 4-10 shows the evolution of internal temperatures alongside moisture content for VIP sludge solar drying during a sunny weather, at 0.5 m/s air velocity and varying air temperatures (ambient, 40°C and 80°C). It was observed that there was a great increase in internal temperature at the early drying stages (first 30 minutes), which coincided with a slight reduction in moisture content. Thereafter, the internal temperature increased at a slower rate and stabilized. This behavior was because the temperature gradients between the sludge and air was high at the beginning of the experiments causing a steep temperature rise in the samples as all of the heat energy is absorbed to heat it to the wet-bulb temperature. As the process progressed, the temperature gradient gradually reduced and most of the absorbed heat was used in moisture evaporation. This consequently led to greater reduction in moisture content and slower increase in internal sludge temperature as it moved towards the wet-bulb temperature. Earlier research by Flaga (2005) on municipal sludge also found internal temperature profile followed this similar trend and was independent of sludge type, with the wet-bulb temperature ranging from 50-85° C.

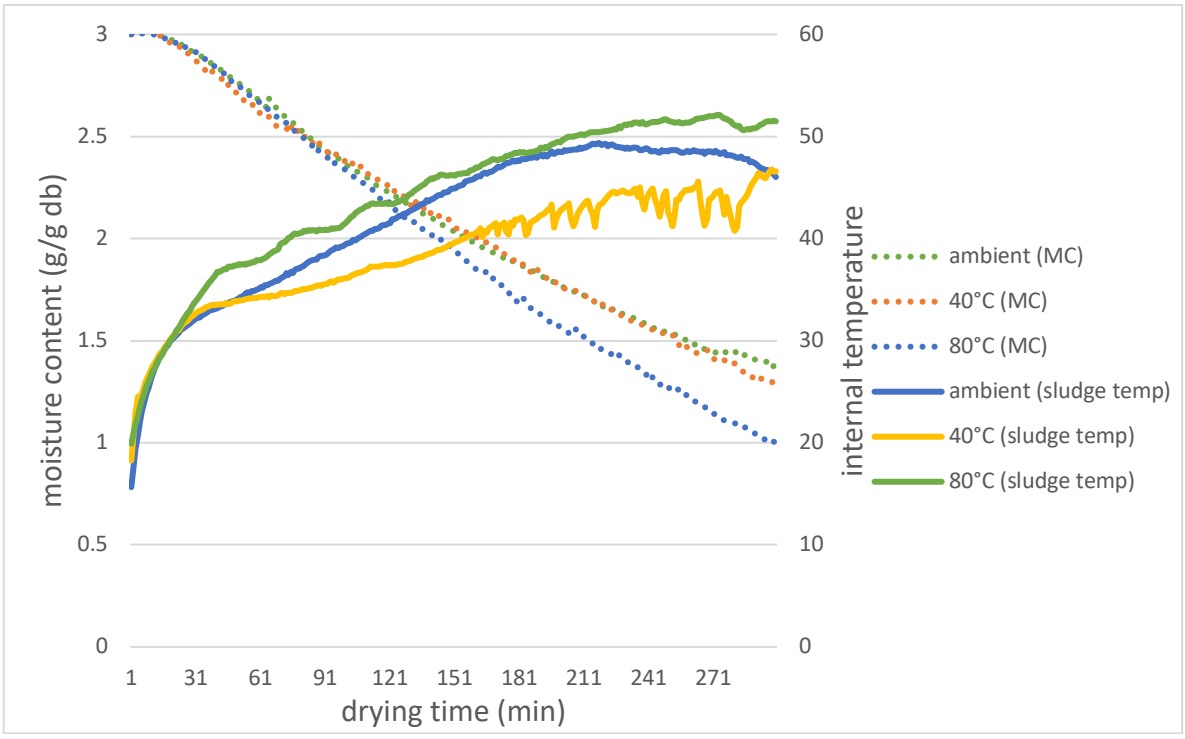

Figure 4-10: Drying curves showing evolution of internal sludge temperature and moisture content with drying time for VIP sludge during sunny weather, 0.5m/s air flow and varying air temperature (ambient, 40°C and 80°C

It was also observed from figure 4-10 that though similar patterns, the internal temperatures generated within the sludge were greatest for experiments conducted at 80°C drying air temperatures followed by 40°C and least for experiments at ambient air temperatures. This was because higher air temperatures result in higher wet bulb temperature as can be seen in the psychrometric chart (section 2.1.3.2).

4.1.6 Comparison between UD and VIP sludge

To determine the variation on drying behavior between different types of faecal sludge, experiments were also conducted with UD sludge samples under similar operating conditions than with VIP sludge. Drying curves for UD and VIP sludge samples during similar weather conditions (sunny), constant air velocity (0.5 m/s) and different air temperatures (ambient, 40°C and 80°C) are shown in figure 4-11. It was observed that moisture reduction progressed at a similar rate for both UD and VIP sludge during the early drying stage. However, after about 30 minutes of drying time, moisture reduction in UD samples progressed at a much slower rate than in VIP sludge samples. At the end of the 5 hours experimental drying period, the final moisture ratios recorded at ambient, 40°C and 80°C temperature were 0.65, 0.62, 0.59 for UD sludge and 0.45, 0.42 and 0.31 for VIP sludge respectively. The corresponding final moisture content (g/g db) recorded at ambient, 40°C and 80°C temperature was 1.59, 1.50 and 1.44 for UD sludge and 1.45, 1.23 and 0.97 for VIP sludge respectively. The slower drying rate of the UD sludge can be explained by the formation of a hard shell or crust layer on the top surface of the sample during the early stages of the process. The hardness of the crust was estimated by the force required to drive a pin through the top sample layer at the end of the experiments. This hard crust layer potentially created an impermeable barrier and trapped moisture within the UD sludge, limiting the mass transfer of moisture to the environment. Additionally the hard crust layer could also have acted as a resistance for the penetration of heat into the UD sludge core for moisture evaporation (Sharma et al., 2018).

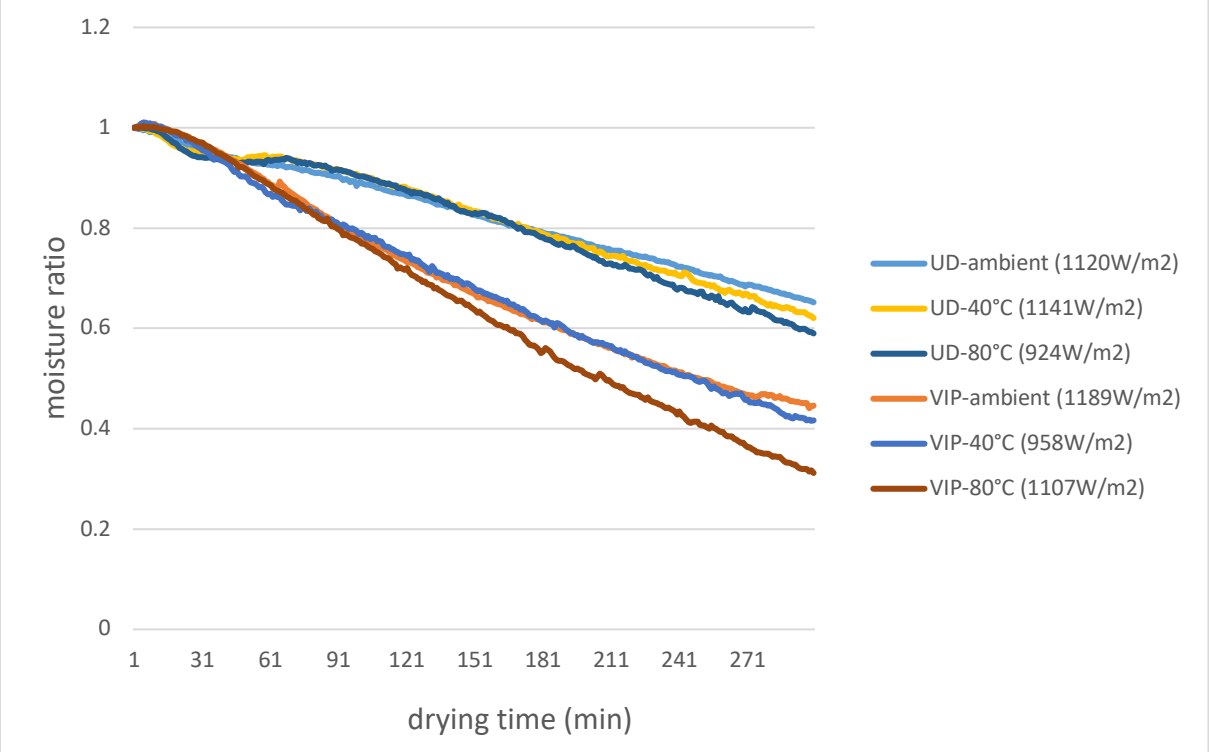

Figure 4-11: Drying curves showing variation of moisture ratio with drying time for both UD and VIP sludge during sunny weather, 0.5m/s air velocity and for air temperatures ambient, 40°C and 80°C

Figures 4-13 presents the variation of the internal sludge temperature during drying of the VIP and UD sludge. It shows that the internal temperature of the UD sludge samples peaked at a higher value during the beginning of drying as compared to that of the VIP sludge. This

suggested that the UD samples achieved the wet-bulb temperature in less time than the VIP sludge. The greater temperature of the UD samples may have led to faster drying on the surface of the sludge, which could have formed the crust layer on the UD samples in an earlier stage as compared to the VIP samples (Lu et al., 2008, Siebert et al., 2018).

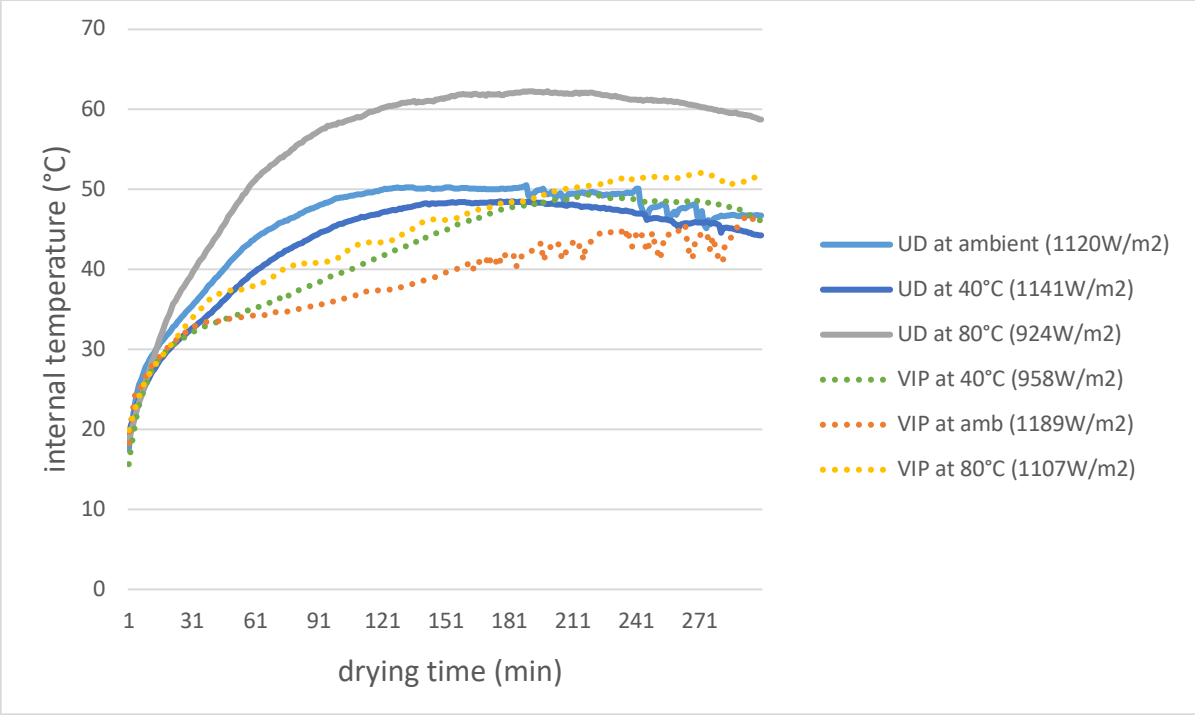

Figure 4-12: Internal temperature profiles for UD and VIP sludge during drying at sunny weather, 0.5m/s air flow for air temperatures ambient, 40°C and 80°C

4.1.7 Effect of uncontrolled operating conditions on the drying process for faecal sludge

Open sun drying experiments were undertaken to determine the effect of uncontrolled operating conditions that is air temperature and air velocity. Open sun experiments involved exposure of the samples to direct sun rays under uncontrolled/prevailing air conditions. A comparison was made between drying curves from open sun experiments versus experiments within the solar thermal drying rig for VIP sludge with the air stream at ambient temperature (no preheating) and at a velocity of 0.5 m/s. Open sun drying experiments were carried out at the same time than those in the drying rig and therefore solar irradiance could be considered equal. Figure 4-13 shows the variation of moisture content with drying time for open sun experiments and solar convection experiments.

The final moisture content was on average 1.14 g/g db for open sun drying and 1.45 g/g db for drying in the solar thermal system. Moisture content reduction was slightly higher in open sun experiments as compared to the experiments in solar thermal drying rig. A study by Septien et al. (2018) reported that drying occurs faster inside the solar thermal drying chamber than at the open air, for sunny conditions (no windy) and overcast conditions. The unexpected faster drying in open air than inside the solar thermal system was therefore explained by the high winds during the experimentation days (noted by the experimenter but not quantified), which caused high convection above the sample surface exposed at the open air, so enhancing the mass transfer of the evaporated moisture from the sludge surface to the environment. Summer wind speeds have been reported to average over 4 m/s in the Southern Africa region (Mosetlhe

et al., 2018).

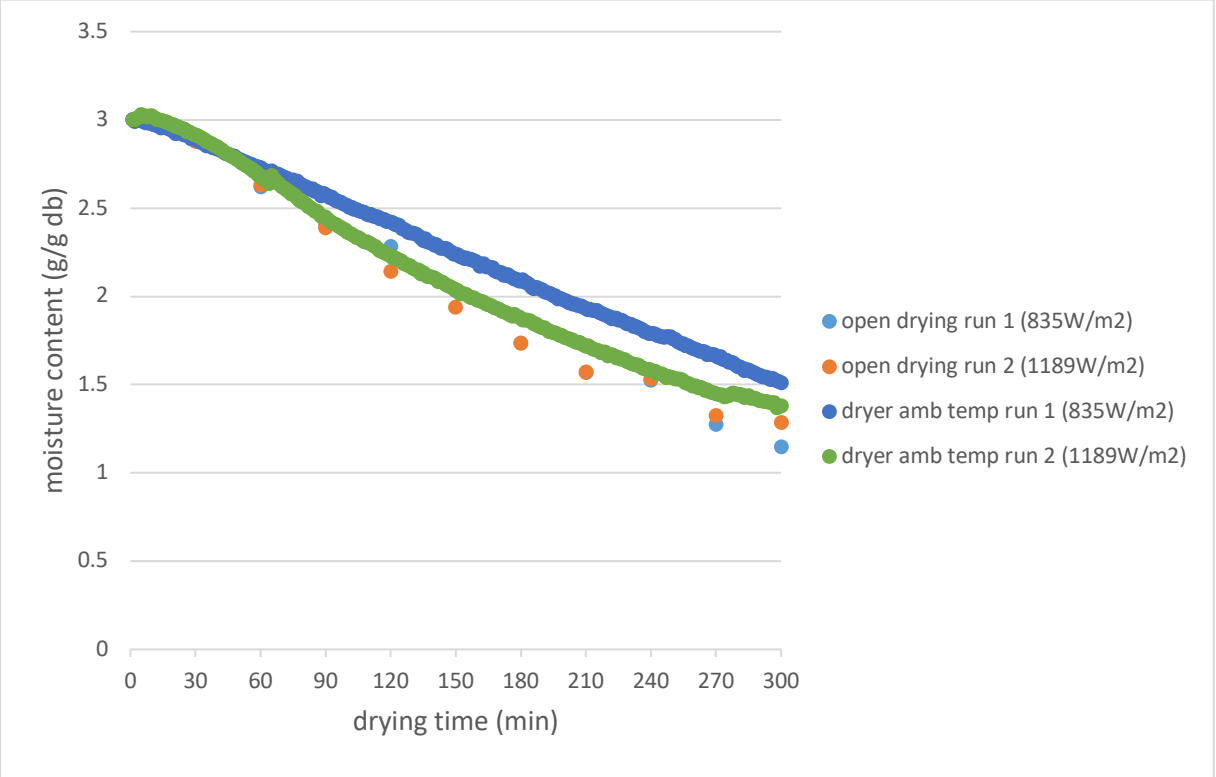

Figure 4-13: Drying curves showing moisture content variation as a function of time during the open air sun drying and controlled solar drying in the rig (0.5m/s air velocity and ambient air temperature) of VIP sludge under sunny weather conditions.

4.1.8 Regression analysis of experimental data

The kinetic drying data obtained from the sludge drying process was fitted to some common empirical drying models, which were the Newton model, the Page model, the modified Page model, the Henderson and Pabis model, the Two-term exponential model and the Logarithmic model. This was undertaken to find the best empirical model for solar thermal drying of sludge to guide future model developments.

Non-linear regression was used to determine the model constants; this was performed using the Solver function in Microsoft excel 2016. Table 4-3 shows the computed values of the model parameters, reduced chi-square (X^2), root mean square error ($RMSE$), the coefficient of determination (R^2) and model constants for the various thin layer drying models corresponding to the drying curves from VIP sludge during sunny weather and at 0.5 m/s air velocity for varying air temperatures (ambient temperature, 40°C, 80°C).

Table 4-3: Model constants and results of the goodness of fit statistical analysis

Model name	**Temperature**	**Model constants**	X^2 **(x10^{-4})**	***RMSE***	R^2
Newton	Ambient	k = 0.0021	3.56	0.0188	0.8123
	40	k = 0.0028	6.27	0.0250	0.8848
	80	k = 0.0033	16.08	0.0400	0.8407
Page	Ambient	n = 1.1976 k = 0.0007	0.55	0.0074	0.9644
	40	n = 1.2402 k = 0.0008	0.18	0.0042	0.9886
	80	n = 1.3564 k = 0.0005	0.28	0.0053	0.9840
Henderson and Pabis	Ambient	a = 1.0410 k = 0.0023	0.48	0.0069	0.9933
	40	a = 1.0518 k = 0.0031	0.17	0.0132	0.9789
	80	a = 1.0845 k = 0.0038	4.86	0.0220	0.9625
Logarithmic	Ambient	a = 1.0410 b = 0 k = 0.0023	0.48	0.0069	0.9542
	40	a = 1.0518 b = 0 k = 0.0031	1.75	0.0132	0.9332
	80	a = 1.0845 b = 0 k = 0.0038	4.88	0.0219	0.9625
Modified Page	Ambient	n = 1 k = 0.0020	4.52	0.0212	0.7474
	40	n = 1 k = 0.0030	11.33	0.0335	0.8885
	80	n = 1 k = 0.0036	22.71	0.0475	0.8021

Two Term	Ambient	$k_1 = 0$ $k_2 = 0.0020$ $a = 0$ $b = 1.0030$	4.29	0.0201	0.9520
	40	$k_1 = 0$ $k_2 = 0.0030$ $a = 0$ $b = 1.0900$	11.28	0.0334	0.9623
	80	$k_1 = 0$ $k_2 = 0.0038$ $a = 0$ $b = 1.0844$	4.90	0.0220	0.9481

The results in Table 4-3 show that Page model best describes the solar convective drying of VIP sludge with the Henderson and Pabis model coming second. These models were found to have the least values reduced chi-square (X^2), and root mean square error ($RMSE$) as well as highest values of coefficient of regression (R^2). Page model has also previously been identified as the most suited model for drying of sewage sludge, according to Wan et al. (2009). It was also observed that the model constants were different for each temperature as these models do not factor in varying drying conditions. The variation between the predicted moisture content ratio from the models and the experimental values of sludge samples at the different air temperatures is showed in Appendix G.

4.2 Morphological and physical characteristics of sludge during solar convective drying

The morphological and physical changes of faecal sludge as a result of solar convection drying are presented in this section. The studied parameters were both quantitative (shrinkage, density, water activity) and qualitative (crust formation, cracking, reflectivity, colour)

4.2.1 Shrinkage

Shrinkage was due to an inward contraction of sample material resulting from inner stresses and mechanical in-equilibrium between the top and core of the sludge sample as drying progressed (Aprajeeta et al., 2015). Initial and final thicknesses of the drying sample were recorded from which final percentage shrinkage factors were deduced. Shrinkage values were considered rough estimates as the measurement method was not precise. Figure 4-14 shows the relationship between shrinkage and final moisture content for all the experiments. Shrinkage values were higher for samples with the lowest final moisture content values. This is because higher moisture reductions are associated with a greater loss of the volume that was occupied by the evaporated moisture. The reduction in volume translates into a collapse or shrinkage of the sludge samples (Lu et al., 2008). This pattern of increasing shrinkage with reducing moisture content was similar to that reported by Krokida and Maroulis (1997) on various food products. Shrinkage values for UD sludge were not influenced by the operating conditions.

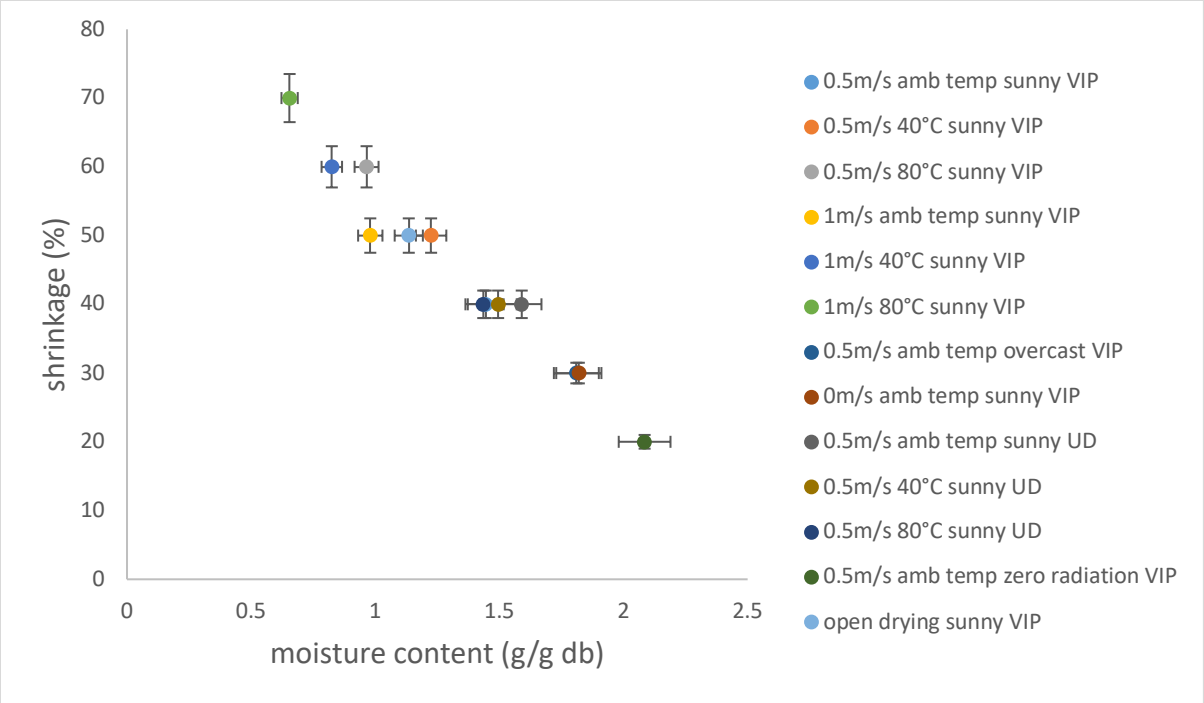

Figure 4-14: Shrinkage versus final moisture content for UD and VIP sludge samples at varying drying conditions

The final shrinkages of VIP sludge samples at varying air temperature and flowrate are shown in figure 4-15. Final shrinkage was estimated at 40%, 50%, 60% at 0.5 m/s air velocity and 50%, 60% and 70% at 1 m/s air velocity, at ambient temperature, 40°C and 80°C respectively. Shrinkage increased with increasing drying air temperature and air velocity. This trend was the result of higher air temperatures and higher air velocity that resulted in greater moisture reduction during drying (sections 4.1.2 and 4.1.3).

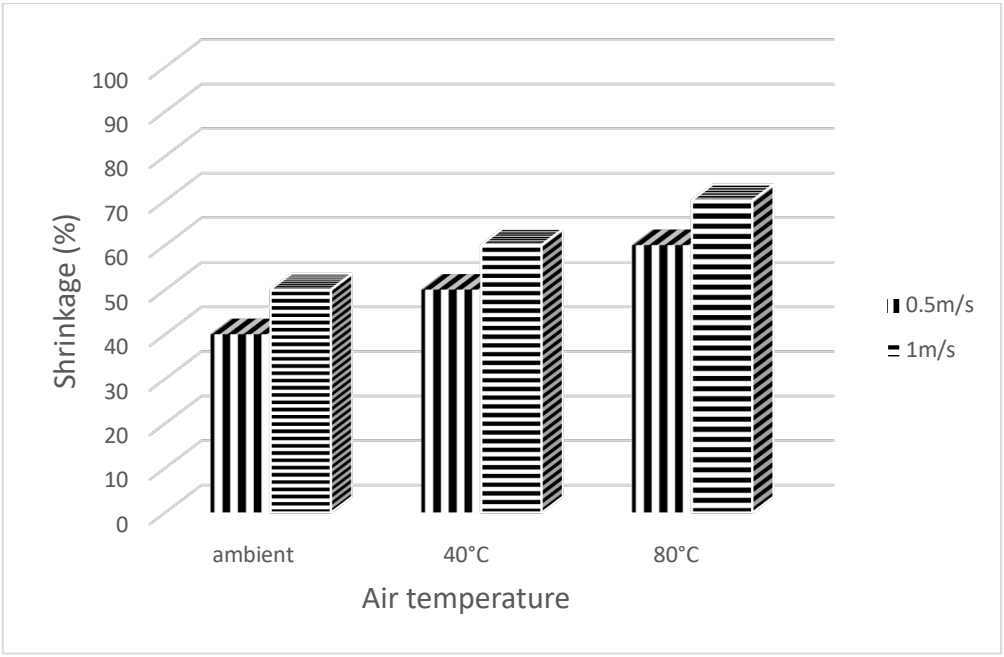

Figure 4-15: Shrinkage as a function of drying air conditions (temperature and velocity) for VIP sludge solar drying during sunny conditions

4.2.2 Density

For this study density was analysed in terms of apparent density which is the mass of the dried sample divided by its external volume (sum of the pore and solid volume).

Figure 4-16 shows the variation of density with moisture content after solar drying of sludge under the various experimental conditions. Density of dried sludge samples ranged between 1678 kg/m^3 at 2.09g/g db moisture content to 1228 kg/m^3 at 0.66g/g db moisture content which is similar to values reported by O'Kelly (2005) for dewatered sewage sludge. From figure 4-16 there is a general trend of decrease in density with reducing moisture content. This implied that density of sludge samples decreased as drying progressed. This trend is with exception of two experiments (1m/s amb temp sunny VIP and 1m/s 40°C sunny VIP) which could be a result of experimental inaccuracies/outliers. Decrease in density as drying progressed was an indication of general lower reduction in sludge mass as compared to volume as moisture content reduced. There was no specific pattern between sludge density and operating parameters.

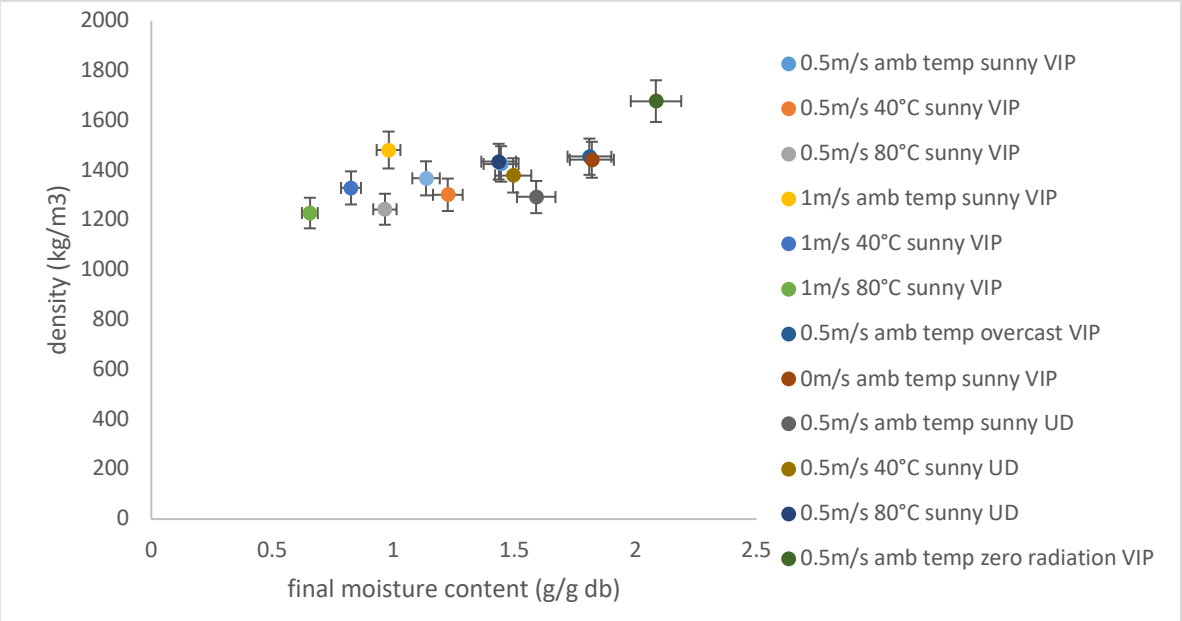

Figure 4-16: Variation of density with final moisture content for both UD and VIP sludge samples at the varying drying conditions

4.2.3 Qualitative analysis

A qualitative investigation of the dried samples was undertaken to determine the formation of cracks, crust layer, and changes in odour, colour and reflectivity of the dried samples in relation to its initial aspect. Figure 4-17 displays photographs of the initial and final aspect of VIP sludge dried at an air velocity of 0.5 m/s and at different temperatures. Initially, sludge was a deformable material with soft paste-like consistency. Its aspect was similar to the typical appearance of VIP sludge as reported in the literature (Schoebitz et al., 2014). After drying, sludge turned to a hard, crystal-like, less deformable structure with cracks on the surface

Cracking was observed particularly for the samples dried at 80°C and in a lower extent for the samples dried at ambient temperature. This result could be explained by the lower moisture reduction at ambient conditions and a possible uniform moisture distribution at the sludge surface. This reduced internal stresses within the sludge structure and thus caused less cracking. In addition, at higher temperatures the drying of sludge was at more advanced stages and thereby more cracking (S. Abbasi, 2011).

Case hardening or formation of a crust layer on the sludge surfaces was also observed. The crust formation was possibly related to internal moisture transfer limitations. Indeed, if the

internal moisture transport is not fast enough to feed the external surface, a superficial desiccation can occur hardening the top surface of the sludge (Leonard et al., 2004). The crust layer was more significant for UD samples as compared to VIP (section 4.1.6).

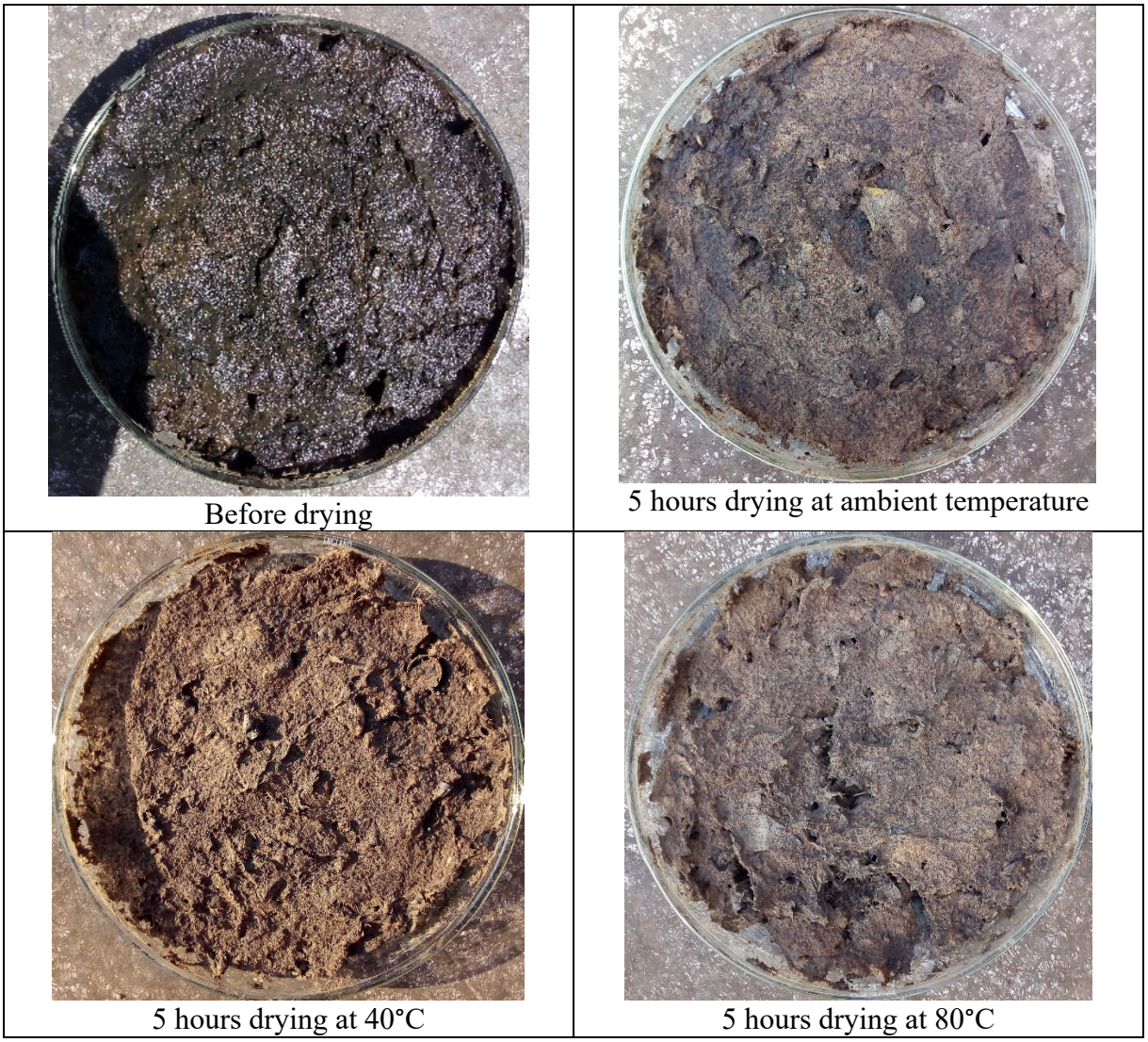

Figure 4-17: Photographs of VIP sludge samples before drying and after drying during sunny conditions, at varying air temperatures

From visual observation, initial sludge surface was shinny with a relatively high light reflectivity. This shinny surface faded gradually as drying progressed. The fading of the shiny surface was attributed to the gradual loss of surface moisture as drying progressed and this could be an indicator of a potential increase of solar irradiance absorbance of the material as drying progressed. The change in colour varied from a dark black in the wet samples to a dark brown in the dry samples. Foul odour/smell from the sludge samples was also noticed to gradually cease as drying progressed. Changes in the colour and odour of the dry sludge was in agreement to that reported in literature (Getahun et al., 2020). There was no noticeable relationship between colour and odour of sludge with the operating operators.

4.2.4 Water activity

Water activity a_w indicates the amount of unbound water that is available in the sludge for microbial growth. Figure 4-18 shows the relationship between water activity and final moisture

content for all the experimental conditions. Average values from the experiments done in duplicates are presented. From the results in figure 4-18, there is a slight decrease in water activity with decreasing moisture content. However, since uncertainty bars overlap, statistically no significant difference between water activities at the varying experimental conditions. Water activity values were highest for 80°C drying air temperature and least for ambient air (23°C) drying air temperatures. This agrees with results from (Serowik et al., 2017) who reported that water activity is significantly reduced with increasing dry air temperatures. There was no specific relationship between water activity and drying air velocity.
Water activity for all dry samples was in the range 0.9374 to 0.981, which is close to 1. This result meant that moisture within all the dry samples was predominantly slightly bound. This water activity from this study were within the values reported in literature by (Getahun et al., 2020) for VIP and UD sludge at similar moisture content values.

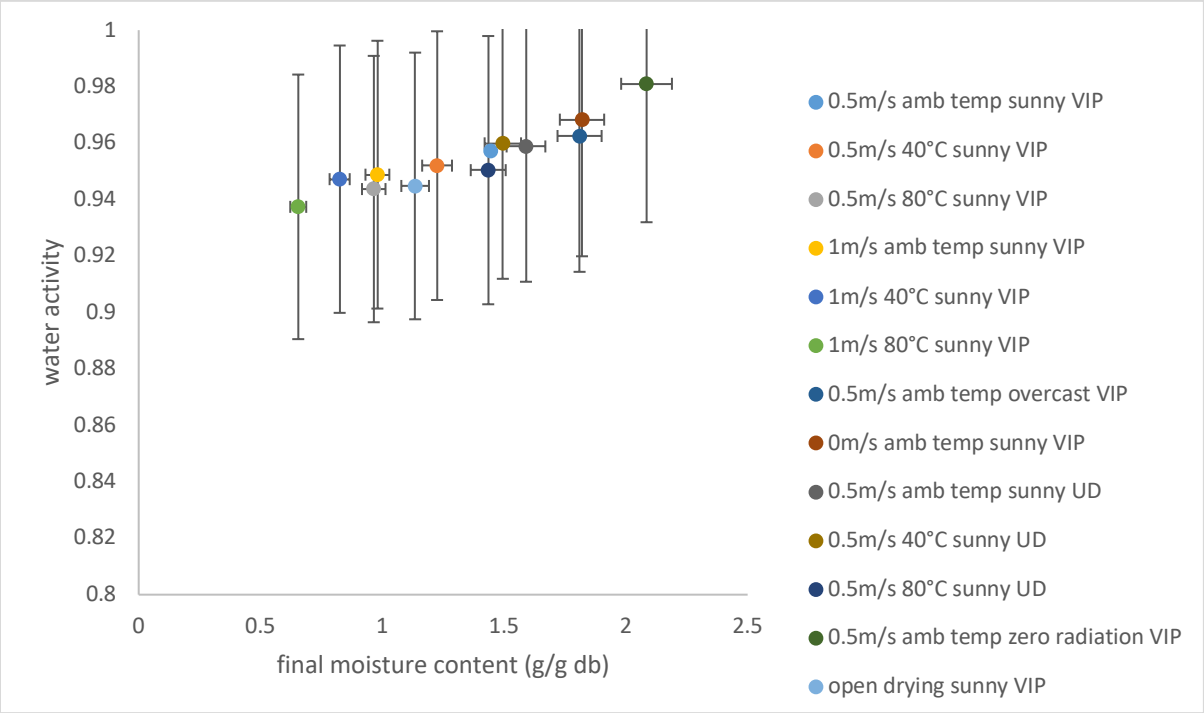

Figure 4-18: Water activity versus final moisture content for both UD and VIP sludge samples at all the experimental conditions of weather, air temperature and airflow

4.3 Performance parameters of the solar convective drying system

The solar thermal drying system was characterized in this section. Parameters for characterization included the flow regime of the air stream within the drying chamber, the convective heat and mass transfer coefficients, the effective moisture diffusivity and the activation energy. The performance of the drying system was also evaluated through the determination of the generated power and process efficiency at the various experimental parameters.

4.3.1 Heat and mass transfer coefficients

Dimensionless numbers were used to determine the flow characteristics of the convective air stream within the sludge drying chamber. Hydraulic *Re* was obtained with a characteristic length of 140 mm (diameter of drying chamber) and Particle *Re* was calculated using 110 mm as the characteristic length (diameter of sludge sample). Transfer parameters were quantified based on the particle Reynolds number. Table 4-4 presents the computed values of hydraulic and particle Reynold numbers, Schmidt number *Sc*, Sherwood number *Sh* as well as convective mass transfer coefficients h_m at different drying conditions of air flow and air temperature.

Table 4-4: Dimensionless numbers of Reynolds, Schmidt and Sherwood, and convective mass transfer coefficients for solar convective drying of sludge at varying air velocity and temperature

Airflow rate (m/s)	Temperature (°C)	Hydraulic Re	Particle Re	Sc	Sh	h_m (m/s)
0.5	Ambient (23)	4481	3521	0.64	33.95	7.47×10^{-3}
	40	4113	3231	0.60	31.83	8.15×10^{-3}
	80	3338	2623	0.62	28.99	9.49×10^{-3}
1	Ambient (23)	8963	6840	0.64	47.32	1.04×10^{-2}
	40	8226	6463	0.60	45.02	1.15×10^{-2}
	80	6676	5245	0.62	41.01	1.34×10^{-2}

According to table 4-4, the hydraulic regime of flow during the experiments conducted at 0.5 m/s air velocity was transitional, i.e. a mixture of both lamina and turbulent flow since the values of hydraulic Reynolds number were between 2000 and 5000. Hydraulic airflow regime for experiments at 1m/s was found to be turbulent since all values of Reynolds number were above 5000.

Schmidt number varied within a range 0.60 to 0.64 and this is familiar to the typical Schmidt number of roughly 0.7 reported for gas-liquid systems (Treybal, 1980).

From table 4-4, the convective mass transfer coefficients ranged from 7.47×10^{-3} to 9.49×10^{-3} m/s at 0.5 m/s air velocity and 1.04×10^{-2} to 1.34×10^{-2} at 1 m/s. These values are similar ranges to those reported by Koua et al. (2019) during solar drying of agricultural produce at similar conditions of air velocity and temperature. No literature could be obtained regarding mass transfer coefficients for sludge within the experimental conditions studied. It was also noted that coefficient of mass transfer values increased with increasing air temperature and increasing airflow. This is behaviour is in agreement to results of increased moisture removal rate from sludge at increasing air temperatures and velocity, as discussed in sections 4.2.1 and 4.2.2, respectively.

Table 4-5 presents the computed values of Prandtl number *Pr*, Nusselt number *Nu*, as well as convective heat transfer coefficients h_c at different drying conditions.

Table 4-5: Dimensionless numbers of Prandtl and Nusselt, and convective heat transfer coefficients for solar convective drying of sludge at varying air velocity and temperature

Airflow rate (m/s)	Temperature (°C)	Pr	Nu	h_c (W/m^2.K)
0.5	Ambient (23)	0.730	35.48	8.23
	40	0.725	33.91	8.21
	80	0.715	30.41	8.16
1	Ambient (23)	0.730	49.45	11.47
	40	0.725	47.95	11.60
	80	0.715	43.00	11.54

Prandtl number varied in the range 0.715 to 0.73 as expected for air. Nusselt number varied in the range 30 - 36 for experiments at 0.5 m/s air velocity and in the range 43 - 50 for experiments at 1 m/s air. A larger Nusselt number corresponds to a higher heat transfer by convection compared to thermal conductivity.

From table 4-5, convective heat transfer coefficients significantly increased when air velocity was increased i.e. from around 8 W/m^2.K at 0.5 m/s to 11 W/m^2.K at 1 m/s. This was attributed to the increase of the heat transfer by increasing convection (i.e. increasing air velocity).

4.3.2 Moisture diffusivity

Moisture diffusivity is an important parameter for the analysis of drying processes for various materials. According to the experimental drying rate curves in this study, both constant and falling rate period could be observed for almost all the experiments. Fick's second law was used to describe the drying behaviour in the falling rate period. This analysis was applied for VIP sludge solar drying under sunny weather conditions at 0.5 and 1 m/s air velocity, and different air temperatures. Linear regression was performed on the drying curves and lines of best fit determined. Figure 4-19 shows the logarithm of the moisture ratio versus drying time at the different air temperatures and 0.5 m/s air velocity. Figure 4-20 shows the same data at 1 m/s air velocity. The Results are presented in duplicates that are run 1 and run 2.

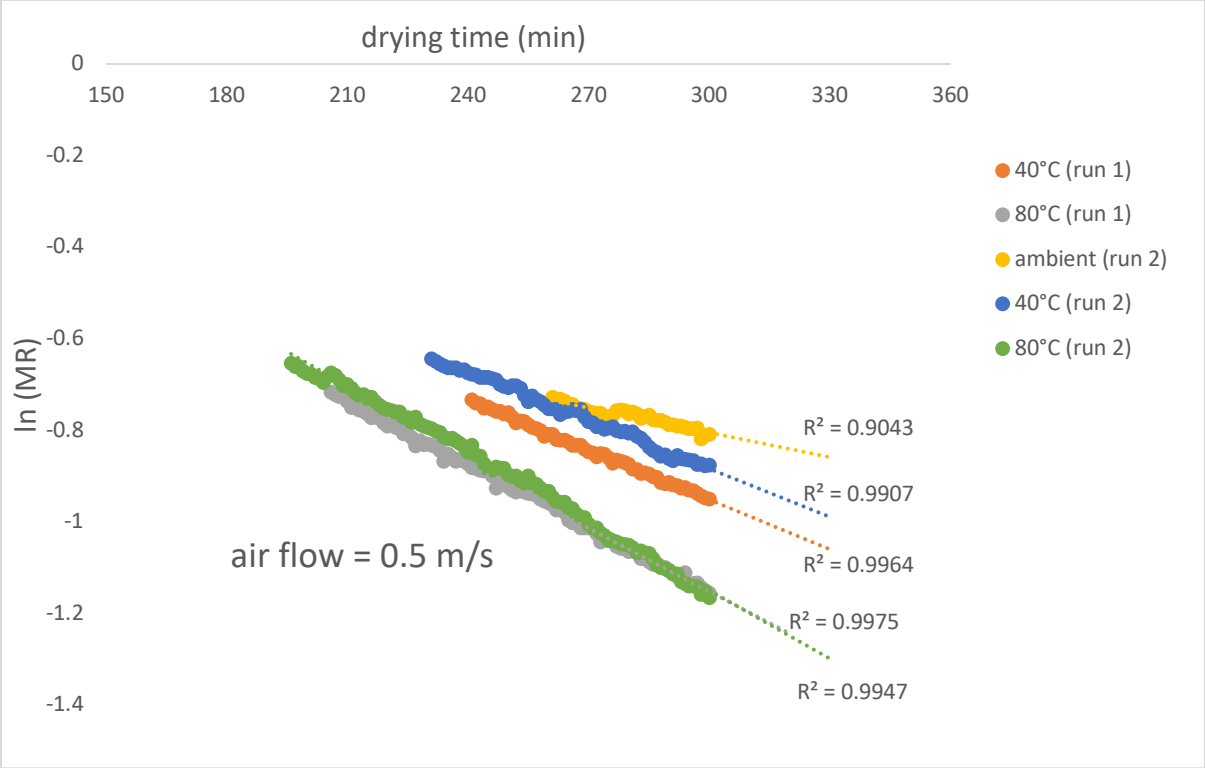

Figure 4-19: Logarithm of the moisture ratio versus time for VIP sludge solar drying during sunny weather conditions, at 0.5 m/s air velocity and varying air temperature during the falling rate period

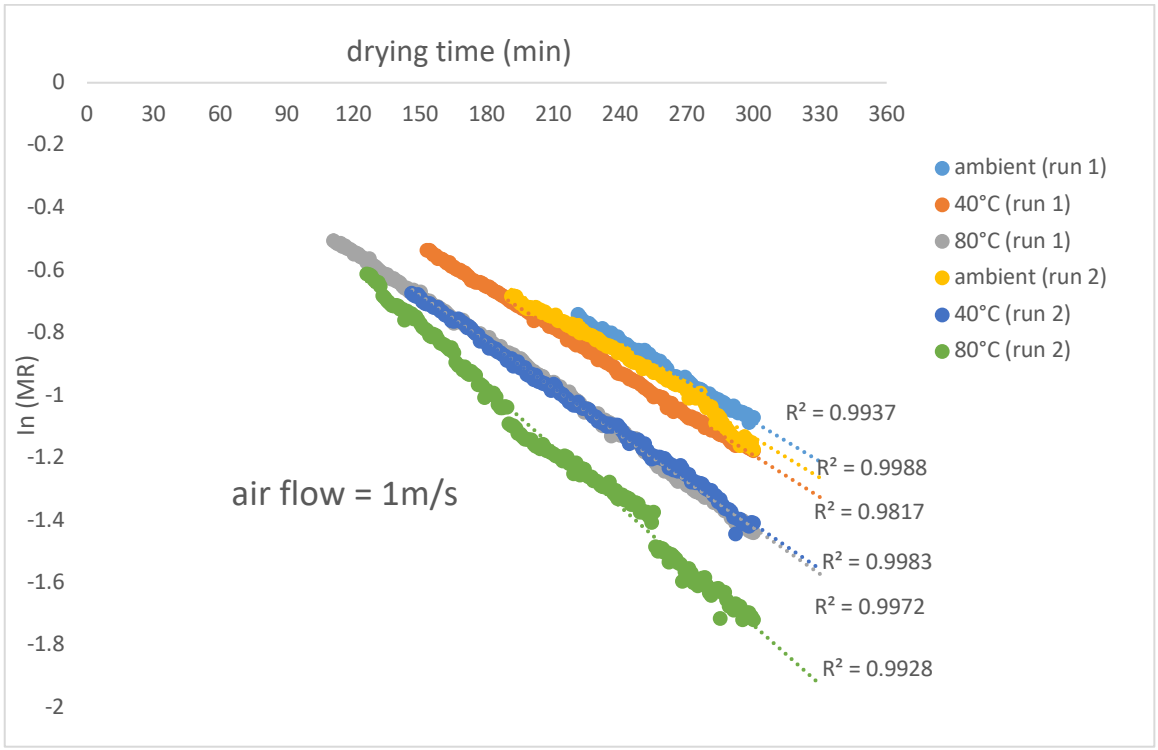

Figure 4-20: Logarithm of the moisture ratio versus drying time for VIP sludge at sunny weather, 1m/s air velocity and varying air temperature during the falling rate period

From both figures 4-19 and 4-20, straight lines described the graphs with reasonable accuracy with a coefficient of determination R^2 at least 0.904. It can be deduced that drying of sludge under the studied conditions took place with relatively constant diffusivity during the falling rate period.

Effective moisture diffusivity was calculated using equation 3-25 for 5 mm sludge sample thickness from the equation of the trendlines in Figure 4-19 and 4-20. The average length of diffusion of moisture was considered to be half the sample thickness. The values of the effective moisture diffusivity D_{eff} of VIP sludge at different drying conditions of are shown in table 4-6. Results for D_{eff} and R^2 are presented as an average of the duplicates.

Table 4-6: Effective moisture diffusion coefficients for VIP sludge during sunny weather at varying velocity and temperature air conditions

Air velocity (m/s)	**Air temperature (°C)**	**D_{eff} (m^2/s)**	**R^2**
0.5	Ambient (23)	4.56×10^{-9}	0.904
	40	8.99×10^{-9}	0.994
	80	1.22×10^{-8}	0.997
1	Ambient (23)	1.09×10^{-8}	0.997
	40	1.18×10^{-8}	0.995
	80	1.42×10^{-8}	0.995

As shown in Table 4-6, the D_{eff} values varied with temperature from 4.56×10^{-9} m^2/s at ambient temperature to 1.01×10^{-8} m^2/s at 80°C for 0.5 m/s air velocity, and from 9.37×10^{-9} to 1.52×10^{-8} m^2/s for 1 m/s air velocity in the same temperature range. These results showed that D_{eff} increased with increasing drying temperature, as it could be expected. The reason for this is that a rise in temperature increases the kinetic energy of moisture molecules within the sludge, facilitating the movement of moisture within the sludge during drying and thereby increasing the mass transfer to the environment.

According to table 4-6, the D_{eff} values varied also by increasing the air velocity from 0.5 to 1 m/s, from 4.56×10^{-9} to 1.04×10^{-8} m^2/s at ambient temperatures, from 7.70×10^{-9} to 1.29×10^{-8} m^2/s at 40°C, and air from 1.01×10^{-8} to 1.52×10^{-8} m^2/s at 80°C. The increase of air velocity consequently led to an increase of the D_{eff} values. This may be explained by the fact that an increase in air velocity reduces the boundary layer on the sludge sample surface and thus facilitates heat transfer between the core structure and surface of the sludge sample. A higher heat transfer increases the internal temperature within the sludge, leading to a higher diffusion of moisture (section 4.1.3).

The values of D_{eff} during faecal sludge solar drying from this study (4.56×10^{-9} to 1.52×10^{-8} m^2/s) are within the reported range of diffusivities for faecal sludge according to a previous research by Makununika, (2017) and for fruits and vegetables (Mghazli et al., 2017, Aral and Bese, 2016, Koukouch et al., 2017) but considerably less than diffusivity ranges for wastewater

sludge (1.53×10^{-7} to 7.67×10^{-7} m^2/s) as reported by Bennamoun et al. (2015). This suggested that the faecal sludge samples dried slower than wastewater sludge from literature.

4.3.3 Activation energy

The values of lnD_{eff} versus $1/T$ according to the linearized Arrhenius equation were plotted for different conditions of air velocity and temperature in figure 4-21. Linear regression analyses were used to fit the equations to the experimental data to obtain a linear relationship.

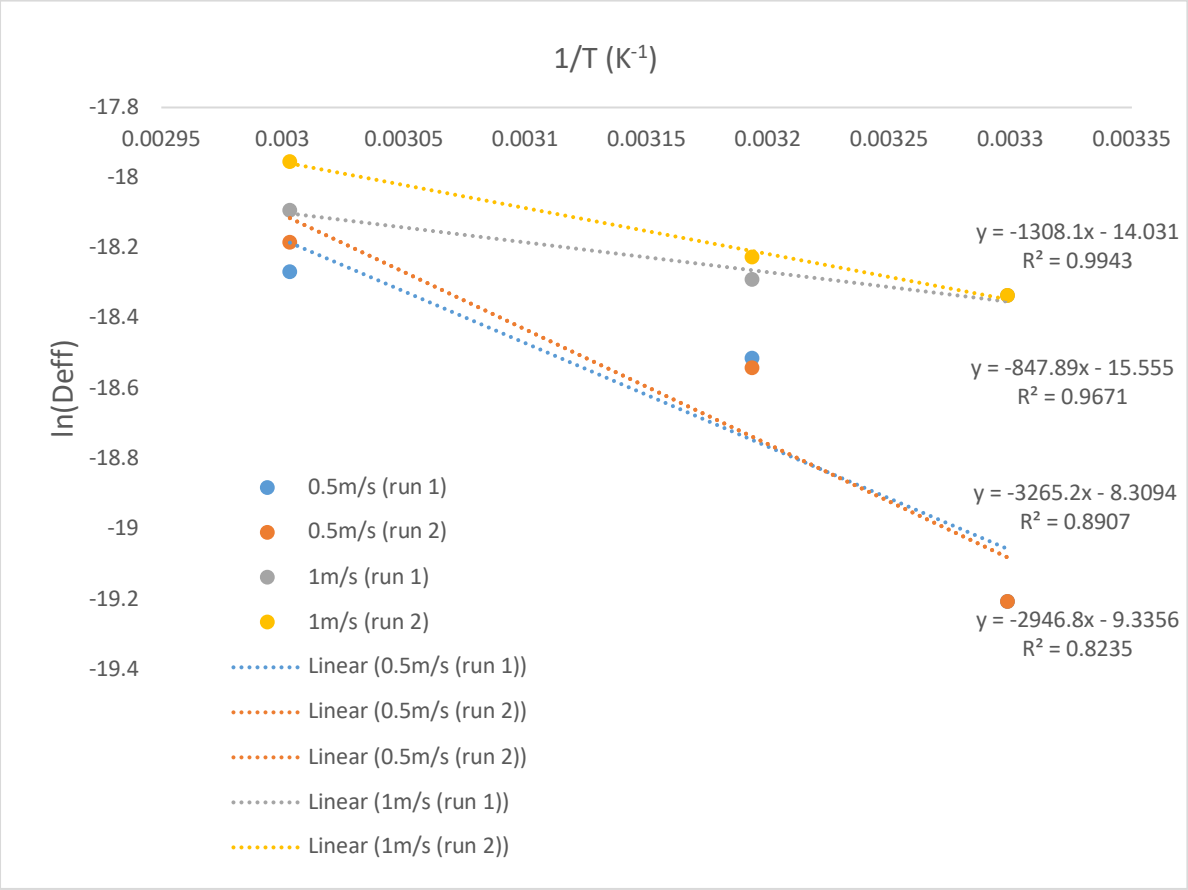

Figure 4-21: Variation of lnD_{eff} versus 1/T for VIP sludge at sunny weather, at air velocity of 0.5 and 1m/s during the falling rate period

In figure 4-21, the least coefficient of correlation (R^2) value after linear regression was 0.855 which is within the acceptable range for linearity. This verified that the Arrhenius equation (section 3.4.4) could be used to describe the relationship between moisture diffusivity and temperature of the sludge under the explored conditions.

The values of the activation energy, E_a, and Arrhenius constant, D_0, were estimated from the slopes of the lines by use of equation 3-27. Table 4-7 shows the activation energy values obtained for sludge for different drying conditions of air velocity. The values are presented as an average of the duplicates.

Table 4-7: Values of activation energy and Arrhenius constant for VIP sludge solar drying at 0.5 and 1 m/s air velocity

Air velocity (m/s)	**0.5**	**1**
E_a (kJ/mol)	25.82	8.97
D_0 (m^2/s)	1.67×10^{-4}	4.91×10^{-7}

The results from table 4-7 indicated that activation energy was greater at 0.5 m/s (25.82KJ/mol) as compared to 1 m/s air velocity (8.97KJ/mol). The higher activation energy for the experiments at 0.5 m/s showed a higher temperature dependency compared to the 1 m/s experiments. The Arrhenius constant values were 1.67×10^{-4} at 0.5 m/s, and 4.91×10^{-7} m^2/s at 1 m/s. All the values obtained for activation energy and Arrhenius constant are within the range available in literature for faecal sludge (Makununika, 2017) for sewage sludge (Lijuan et al., 2019).

4.3.4 Power and efficiency

In this study, the power was referred to the energy transferred to the drying chamber from the air preheating and solar radiation. Power was in form of radiative power P_s (received from the sun) and convective power P_c (received from the air stream). Efficiency η was described as a comparison of the total power input (both radiant and convective) to the useful power used in the drying process for moisture evaporation (P_{out}).

Equations 3-29, 3-28, 3-32 and 3-31 were used to compute P_s , P_c , P_{out} and η respectively. Average solar irradiance and average drying rates for the different experiments were showed in table 4-1. The evolution of temperature of sludge samples and temperature of air within the chamber with drying time as used in the computation of convective power P_c can be seen in appendix G. Table 4-8 shows the computed values for power input (convective and radiative power), power output and efficiency of solar convection drying for faecal sludge at the various experimental parameters.

From table 4-8, convective power values were negative for experiments with UD sludge and experiments at 0 m/s (no airflow). This meant that the sludge temperature was higher compared to the surrounding air and consequently sludge lost heat energy to the surrounding air. Experiments involving VIP sludge and an airflow (0.5 and 1 m/s) showed positive values for the convective power, which is an indicator that that the sludge temperature was in overall lower than the surrounding air temperature, implying that the sludge gained heat energy from the surrounding air. There was a reduction in convective power with increasing air temperature and this was because temperature difference between sludge and air reduced as air temperature increased. The highest convective power was recorded for experiments during overcast weather (experiment 7). This was because of the low solar irradiance during overcast which meant that temperature of sludge samples remained low in comparison to the air temperature. Open drying experiments (experiment 13) involved natural convection with no control of wind velocity and temperature.

Table 4-8: Values of power input (convective and radiative power), power output (power utilized in drying process) and efficiency of faecal sludge solar drying at various experimental parameters

Experiment	Convective Power P_c (W)	Radiative power P_s (W)	Power input (Radiative & convective) (W)	Power output P_{out} (W)	Efficiency (%)
1	2.65	7.80	10.35	2.13	20.8
2	1.62	8.25	9.87	2.43	24.9
3	0.83	8.07	8.90	2.81	31.6
4	1.68	8.59	10.27	2.65	26.0
5	0.87	8.24	9.10	3.19	35.1
6	0.53	9.56	10.07	3.51	34.9
7	3.34	3.85	7.15	1.51	21.2
8	-0.26	6.89	6.63	1.47	22.3
9	-0.74	8.00	7.26	1.06	14.6
10	-0.28	8.17	7.89	1.15	14.5
11	-0.52	7.88	7.36	1.29	17.6
13	N/A	7.70	7.70	2.18	29.3

From the results in table 4-8, it is evident that solar radiation was the highest source of thermal energy available for drying as compared to the convective airstream heat input. The proportion of solar thermal energy to convective thermal energy ranged between 73% to 95% during sunny weather days (experiments 1-6). During overcast weather (experiment 7), solar energy contributed around 50% to the total energy input. Experiment 12 was carried out without exposure to sun and evidently there was zero contribution of radiative energy.

Figure 4-22 shows the relationship between solar irradiance and efficiency for the different experimental conditions investigated in this research.

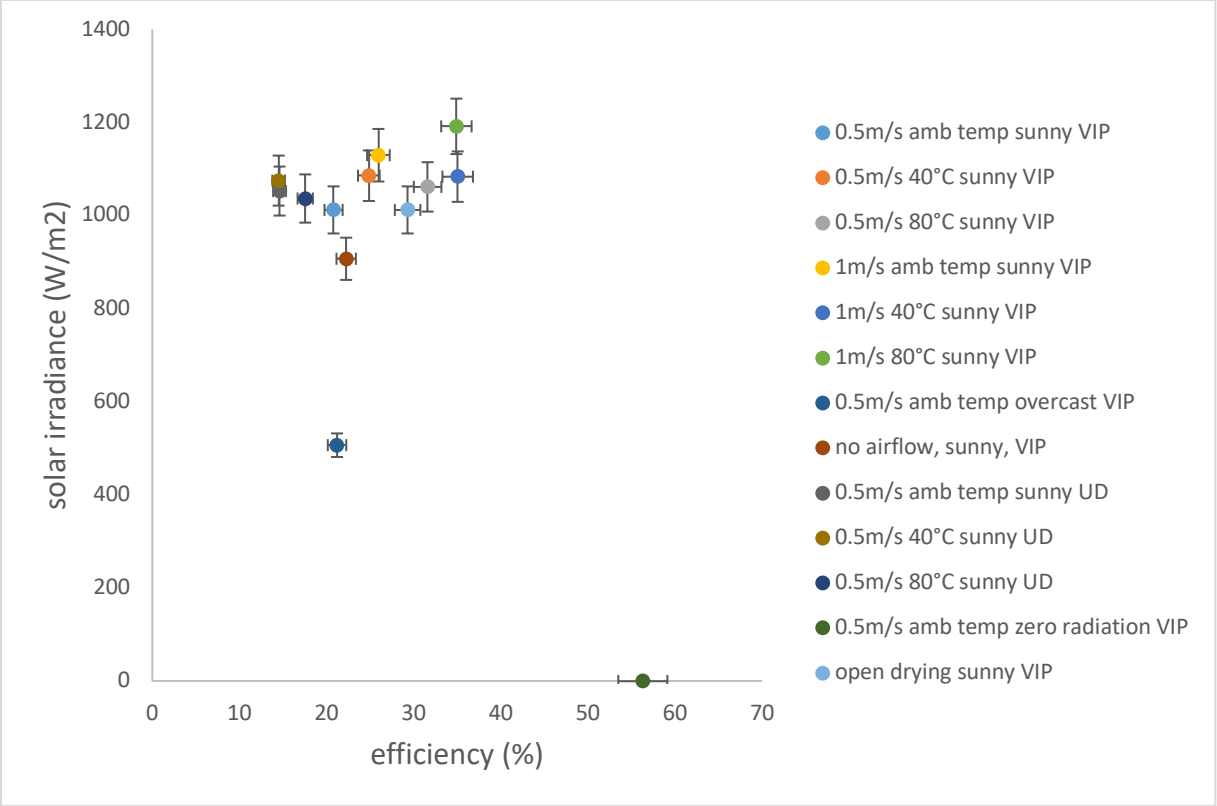

Figure 4-22: Solar irradiance as a function of efficiency for solar drying of VIP and UD sludge at varying conditions of weather, temperature and air velocity

Thermal efficiency for all experiments involving solar irradiation was in the range 13.5 to 36.6% which was within the ranges reported in literature for sludge solar drying efficiency (Poblete and Painemal, 2020). There was no observed relationship between efficiency and weather conditions (sunny and overcast). Drying experiments at zero irradiation (no sun) had the greatest efficiency (62.6 and 50%) but this corresponded with the least drying progress (section 4.1.1). There was a noticeable increase in thermal efficiency with increasing air temperature and air velocity. At similar conditions, efficiency with VIP sludge ranged between 20.8 to 35.1% while efficiency with UD sludge ranged between 14.6 to 17.6%. Efficiency with was then significantly higher VIP than UD sludge.

5 CONCLUSIONS AND RECOMMENDATIONS

This chapter discusses the conclusions of the research, the significance of the findings and possible contribution to the already existing knowledge. Also, possible areas of further research to build knowledge on the topic of faecal sludge solar drying were suggested to sanitation researchers and practitioners.

5.1 Conclusions

Conclusions on each study objective as well as an overall conclusion for the study are presented in this section.

5.1.1 Conclusions on the drying kinetics

- Solar irradiance was higher during sunny days as compared to overcast days. The values for solar irradiation ranged between 830 to 1332W/m^2 during sunny weather and between 400 to 595 W/m^2 during overcast conditions. However, every single day had a unique value and pattern for solar irradiance. Intensity of solar irradiance greatly affected the drying progress. Moisture reduction was significantly higher during sunny weather as opposed to overcast weather conditions. Under similar conditions of air stream, average final moisture content during sunny conditions was 1.40 g/g db as opposed to 1.81g/g db during overcast. Experiments conducted at without solar radiation recorded a further lower final average moisture content of 2.09 g/g db.

- Temperature and velocity of the convective air stream significantly affected the drying process. Drying rates increased with increasing air temperature and air velocity. An increase of air temperature from ambient to 40°C and from 40°C to 80 °C increased moisture reduction by 14% and 27% respectively within 5 hours, based on the final moisture content of 1.40, 1.23 and 0.97 g/g db at ambient, 40 and 80°C, respectively. Increasing the air velocity from 0.5 to 1 m/s resulted in an increase of moisture reduction rates by around 30% at ambient temperature, 40 and 80°C.

- Average drying rates for faecal sludge ranged between 0.31 and 0.99 g/g.min.m^2 depending on the operating conditions. Faecal sludge solar drying initially took place in the constant rate period, followed by a falling rate period at a later stage, which corresponded to the expected kinetic behaviour. The duration of the constant rate period ranged between 195 to 260 min during drying at 0.5 m/s and between 125 to 220 min at 1m/s. Critical moisture content values ranged between 1.41 and 1.78 g/g db. There was no trend observed relating critical moisture content and the drying operating conditions.

- Sludge temperature increased during the heating phase from drying and then stabilized. There was a great increase of the sludge temperature at the early stage of the process (first 30 minutes), which also coincided with slight reduction in moisture content. Thereafter, the increase of temperature increased at a slower rate and moved towards stabilization as drying progressed. The peak sludge temperature values were 45°C, 48°C and 55°Cat ambient, 40°C and 80°C air temperature.

- Moisture reduction was significantly higher on VIP sludge as compared to UD sludge. After 5 hours of drying, the final moisture content achieved after solar drying in sunny

conditions and at an air velocity of 0.5 m/s, were 1.45, 1.23, 0.97 g/g db for VIP sludge, and 1.59, 1.50, 1.43 g/g db for UD sludge, at ambient, 40°C and 80°C air temperatures, respectively. Low moisture reduction in UD was presumed to be due to the formation of a hard crust layer at the early stages of drying that limited its drying.

- Page model was the most appropriate empirical thin layer drying model to describe the drying curves for faecal sludge solar drying under the explored conditions. This was closely followed by Henderson and Pabis model. Page model showed the highest value of correlation coefficient and least values of root mean square error and reduced chi-square value.

5.1.2 Conclusions on the characteristics of dried sludge after solar drying

- Shrinkage increased linearly with reduction in moisture content as expected. There was no relationship between shrinkage with the experimental conditions. Shrinkage ranged between 20% and 70%, corresponding to final moisture content between 2.09 and 0.67g/g db respectively.

- Density of sludge decreased as moisture content was reduced during drying. Density of dried sludge samples ranged between 1228 kg/m^3 to 1678 kg/m^3 corresponding to moisture content of between 0.67 g/g db and 2.09 g/g db respectively.

- From visual observations, cracking and crust formation increased with reducing moisture content. Indeed, cracks and crust layer were more pronounced in samples with the least moisture content. There was no observed relationship between formation of crust or cracks and drying conditions. However, crust formation was more significant in UD sludge as compared to VIP sludge. There was also reduction in shininess (reflectivity) of the sludge surface and fading of the smells emanating from the sludge as drying progressed.

- Water activity reduced with moisture content removal. No relationship was observed between water activity and the experimental conditions. Water activity for all dried samples was in the range 0.9374 to 0.9810, which is close to 1, meaning there was still possibility of biological activity within all dried samples, making possible the development of microorganisms.

5.1.3 Conclusions on characteristics and performance of the drying system

- The hydraulic regime of flow of convective airstream was transitional at 0.5m/s air velocity and turbulent for experiments at 1m/s air velocity.

- As it could be foreseen, the convective mass transfer coefficients increased with increasing air temperature and air velocity. Convective mass transfer coefficients ranged from 7.47- 9.49×10^{-3} m/s at 0.5 m/s air velocity and 1.04-1.34×10^{-2} at 1 m/s.

- Convective heat transfer coefficients increased by increasing the air velocity but were fairly constant by varying the air temperature. Convective heat transfer coefficients were approximately 8 W/m^2.K at 0.5m/s and 11 W/m^2.K at 1 m/s.

- Effective moisture diffusivity D_{eff} increased by increasing the air temperature and velocity. D_{eff} values varied in the range of 4.56×10^{-9} to 1.01×10^{-8} m^2/s at 0.5m/s air velocity and in the range of 9.37×10^{-9} to 1.52×10^{-8} m^2/s at 1m/s.

- Activation energy was 25.82 kJ/mol at 0.5 m/s air velocity and 8.97 KJ/mol at 1 m/s. Activation energy increased by increasing the drying air velocity. Arrhenius constant values were 1.67×10^{-4} m^2/s at an air velocity of 0.5 m/s and 4.91×10^{-7} m^2/s at 1 m/s.

- The greatest contribution to the heat input into the system was from solar irradiation as compared to convective heating. The proportion of solar energy to the total energy input ranged between 73% to 95% during sunny weather days. During overcast weather, solar energy contributed around 50% of the total energy input. There was therefore notable reduction of the contribution of solar radiation in the heat input during overcast conditions

- Efficiency for all experiments involving solar irradiation was in the range 14.6% to 35.1%. There was a noticeable increase in thermal efficiency by increasing the air temperature and velocity.

5.1.4 Overall conclusion

In the solar thermal convective system, faecal sludge was dried from initial moisture content of 3.0 g/g db (75% wb) to values from 0.67 to 1.81 g/g db (37% to 58% wb) depending on the experimental parameters after 5 hours of experiment. This coincided with a sludge volume reduction (shrinkage) in the range of 20 to 70%. The highest moisture removal and shrinkage was registered for the VIP sludge dried during sunny weather conditions, at 80°C air temperature and 1 m/s air velocity. The weather conditions had the greatest effect on drying compared to the convection properties of the air stream (namely temperature and velocity). This was due to the significant difference in solar irradiance received during sunny and overcast conditions. The effect of crust formation that could limit the drying of faecal sludge was significant and this needs to be mitigated as much as possible. In addition, the decrease of the foul smell during drying indicated the need to manage such foul odour release in especially a full-scale process. Solar radiation energy was the highest contributor to the power input to the drying system as opposed to convection air. The solar thermal convection drying system had a maximum efficiency of 36.6% recorded during sunny weather at 80°C air temperature and 1 m/s air velocity, which is a typical value for a solar thermal energy system. Air velocity and temperature increased the efficiency of the system. This proved that ventilation is an important

parameter to enhance moisture removal, and also solar thermal energy could be combined with an external convective heating source as an optimal solution. Based on the maximum recorded drying rate (0.99 g/g min.m^2), an estimated 3,368 m^2 of land space would be required to dry 1 tonne of faecal sludge to an acceptable level of dryness (from 75% to 37%) within 5 hours of sunlight.

These results earmarked a great potential for use of solar thermal energy in drying for faecal sludge. The application, effectiveness and value add that comes with use of solar energy as a primary heat source in faecal sludge drying was highlighted. This investigation brings valuable information to various researchers and sanitation practitioners towards the design of solar thermal drying systems for faecal sludge.

5.2 Recommendations

The following research areas have been suggested for further investigations about solar thermal convective drying of faecal sludge. These suggestions intend to cover the limitations from this study and to increase the existing data set and body of knowledge required for the design, optimization and operation of faecal sludge solar dryers.

1. Effect of varying sludge properties to the solar drying process- Faecal sludge even from similar sources is known to be highly variable in terms of its physical, chemical and biological properties. All these properties may have an influence on the drying process. The findings from this research may, therefore, apply accurately to only VIP and UD sludge whose properties are within the same range as the one from this study. Further research must be carried out with sludge from different regions to investigate the influence of varying initial sludge physical, chemical and biological properties to the solar drying process.

2. Drying faecal sludge to maximum achievable dryness - From this investigation, maximum dryness of faecal sludge was not achieved after 5 h of experiment, since the mass stabilization of drying samples was not achieved. This was because the mode of drying was using solar irradiation, which meant a time limitation to achieve complete dryness. Drying curves, therefore, did not portray the complete drying curves. Drying experiments over several days could be explored to achieve maximum possible dryness of sludge samples i.e., when the mass of drying sample remains constant with time.

3. Effect of relative humidity - This investigation was limited to dry air. However, relative humidity could potentially influence the drying process. Indeed, in a real solar thermal drying process, the air to be used for drying would likely be ambient with a certain humidity in it. This necessitates the need to study solar thermal drying kinetics at varying conditions of air humidity. A modification of the experimental setup was proposed to include an air humidifier to allow for experiments at varying relative humidity of the air within the drying chamber for future investigations.

4. Evolution of sludge physical properties during the drying process - This research focused on the evolution of moisture and temperature of sludge as drying progressed. Analyses for shrinkage and cracking effects could only be done before and after drying because the drying rig setup was not able to track the volume changes along the process. Modifications could be made to the experimental setup to include graduated crucibles and cameras to allow for quantification of the shrinkage and detection of crack development at the different drying stages, and determine their relationship with moisture content with higher accuracy.

5. Development of an empirical model to predict the drying behavior at changing operating parameters – The Page model was identified as the best fitting model to describe solar drying processes. A variation in the model constants k and n was observed at the different operating conditions of air temperature and air velocity. It is necessary to correlate the parameters from the Page Model as a function of the operating conditions, as well as solar irradiance, in order to obtain a predictive model.

REFERENCES

Journal Articles

AKPINAR, E. K. & TORAMAN, S. 2015. Determination of drying kinetics and convective heat transfer coefficients of ginger slices. *Heat and Mass Transfer,* 52**,** 2271-2281.

AKUMUNTU, J. B., WEHN, U., MULENGA, M. & BRDJANOVIC, D. 2017. Enabling the sustainable Faecal Sludge Management service delivery chain-A case study of dense settlements in Kigali, Rwanda. *Int J Hyg Environ Health,* 220**,** 960-973.

AMAN, M. M., SOLANGI, K. H., HOSSAIN, M. S., BADARUDIN, A., JASMON, G. B., MOKHLIS, H., BAKAR, A. H. A. & KAZI, S. N. 2015. A review of Safety, Health and Environmental (SHE) issues of solar energy system. *Renewable and Sustainable Energy Reviews,* 41**,** 1190-1204.

AMERI, B., HANINI, S., BENHAMOU, A. & CHIBANE, D. 2018. Comparative approach to the performance of direct and indirect solar drying of sludge from sewage plants, experimental and theoretical evaluation. *Solar Energy,* 159**,** 722-732.

AMERI, B., HANINI, S. & BOUMAHDI, M. 2020. Influence of drying methods on the thermodynamic parameters, effective moisture diffusion and drying rate of wastewater sewage sludge. *Renewable Energy,* 147**,** 1107-1119.

APRAJEETA, J., GOPIRAJAH, R. & ANANDHARAMAKRISHNAN, C. 2015. Shrinkage and porosity effects on heat and mass transfer during potato drying. *Journal of Food Engineering,* 144**,** 119-128.

ARAL, S. & BESE, A. V. 2016. Convective drying of hawthorn fruit (Crataegus spp.): Effect of experimental parameters on drying kinetics, color, shrinkage, and rehydration capacity. *Food Chem,* 210**,** 577-84.

BADESCU, V. 2014. Solar Radiation Estimation From Cloudiness Data. Satellite Vs. Ground-Based Observations. *International Journal of Green Energy,* 12**,** 852-864.

BAHAMMOU, Y., TAGNAMAS, Z., LAMHARRAR, A. & IDLIMAM, A. 2019. Thin-layer solar drying characteristics of Moroccan horehound leaves (Marrubium vulgare L.) under natural and forced convection solar drying. *Solar Energy,* 188**,** 958-969.

BELLOULID, M. O., HAMDI, H., MANDI, L. & OUAZZANI, N. 2019. Solar drying of wastewater sludge: a case study in Marrakesh, Morocco. *Environ Technol,* 40**,** 1316-1322.

BENNAMOUN, L., CHEN, Z. & AFZAL, M. T. 2015. Microwave drying of wastewater sludge: Experimental and modeling study. *Drying Technology,* 34**,** 235-243.

BHAGWAN, J. N., STILL, D., BUCKLEY, C. & FOXON, K. 2008. Challenges with up-scaling dry sanitation technologies. *Water Sci Technol,* 58**,** 21-7.

BROUCKAERT, C. J., FOXON, K. M. & WOOD, K. 2013. Modelling the filling rate of pit latrines. *Water SA,* 39.

CAI, L., KRAFFT, T., CHEN, T. B., GAO, D. & WANG, L. 2016. Structure modification and extracellular polymeric substances conversion during sewage sludge biodrying process. *Bioresour Technol,* 216**,** 414-21.

CASTRO, A. M., MAYORGA, E. Y. & MORENO, F. L. 2018. Mathematical modelling of convective drying of fruits: A review. *Journal of Food Engineering,* 223**,** 152-167.

CASTRO, L. M. M. N. & COELHO PINHEIRO, M. N. 2015. A Simple Data Processing Approach for Drying Kinetics Experiments. *Chemical Engineering Communications,* 203**,** 258-269.

CHANDRASEKARAN, S., RAMANATHAN, S. & BASAK, T. 2013. Microwave food processing—A review. *Food Research International,* 52**,** 243-261.

CHEN, G., LOCK YUE, P. & MUJUMDAR, A. S. 2006. Sludge Dewatering and Drying. *Drying Technology,* 20**,** 883-916.

DIENER, S., SEMIYAGA, S., NIWAGABA, C. B., MUSPRATT, A. M., GNING, J. B., MBÉGUÉRÉ, M., ENNIN, J. E., ZURBRUGG, C. & STRANDE, L. 2014. A value proposition: Resource recovery from faecal sludge—Can it be the driver for improved sanitation? *Resources, Conservation and Recycling,* 88**,** 32-38.

DINCER, I. & DOST, S. 2007. An Analytical Model for Moisture Diffusion in Solid Objects During Drying. *Drying Technology,* 13**,** 425-435.

ERTEKIN, C. & FIRAT, M. Z. 2017. A comprehensive review of thin-layer drying models used in agricultural products. *Crit Rev Food Sci Nutr,* 57**,** 701-717.

GETAHUN, S., SEPTIEN, S., MATA, J., SOMORIN, T., MABBETT, I. & BUCKLEY, C. 2020. Drying characteristics of faecal sludge from different on-site sanitation facilities. *J Environ Manage,* 261**,** 110267.

HASSINE, N. B., CHESNEAU, X. & LAATAR, A. H. 2017. Numerical Simulation of Heat and Mass Transfers During Solar Drying of Sewage Sludge: Solar Radiation Effect. *Energy Procedia,* 139**,** 804-809.

IGUAZ, A., SAN MARTÍN, M. B., MATÉ, J. I., FERNÁNDEZ, T. & VÍRSEDA, P. 2003. Modelling effective moisture difusivity of rough rice (Lido cultivar) at low drying temperatures. *Journal of Food Engineering,* 59**,** 253-258.

INGALLINELLA, A. M., SANGUINETTI, G., KOOTTATEP, T., MONTANGERO, A. & STRAUSS, M. 2002. The challenge of faecal sludge management in urban areas - strategies, regulations and treatment options. *Water Science and Technology,* 46**,** 285-294.

KABIR, E., KUMAR, P., KUMAR, S., ADELODUN, A. A. & KIM, K.-H. 2018. Solar energy: Potential and future prospects. *Renewable and Sustainable Energy Reviews,* 82**,** 894-900.

KANNAN, N. & VAKEESAN, D. 2016. Solar energy for future world: - A review. *Renewable and Sustainable Energy Reviews,* 62**,** 1092-1105.

KANT, K., SHUKLA, A., SHARMA, A., KUMAR, A. & JAIN, A. 2016. Thermal energy storage based solar drying systems: A review. *Innovative Food Science & Emerging Technologies,* 34**,** 86-99.

KARAK, T. & BHATTACHARYYA, P. 2011. Human urine as a source of alternative natural fertilizer in agriculture: A flight of fancy or an achievable reality. *Resources, Conservation and Recycling,* 55**,** 400-408.

KEMP, I. C., FYHR, B. C., LAURENT, S., ROQUES, M. A., GROENEWOLD, C. E., TSOTSAS, E., SERENO, A. A., BONAZZI, C. B., BIMBENET, J.-J. & KIND, M. 2001. Methods for Processing Experimental Drying Kinetics Data. *Drying Technology,* 19**,** 15-34.

KOUA, B. K., KOFFI, P. M. E. & GBAHA, P. 2019. Evolution of shrinkage, real density, porosity, heat and mass transfer coefficients during indirect solar drying of cocoa beans. *Journal of the Saudi Society of Agricultural Sciences,* 18**,** 72-82.

KOUKOUCH, A., IDLIMAM, A., ASBIK, M., SARH, B., IZRAR, B., BOSTYN, S., BAH, A., ANSARI, O., ZEGAOUI, O. & AMINE, A. 2017. Experimental determination of the effective moisture diffusivity and activation energy during convective solar drying of olive pomace waste. *Renewable Energy,* 101**,** 565-574.

KROKIDA, M. K. & MAROULIS, Z. B. 1997. Effect of Drying Method on Shrinkage and Porosity. *Drying Technology,* 15**,** 2441-2458.

KURT, M., AKSOY, A. & SANIN, F. D. 2015. Evaluation of solar sludge drying alternatives by costs and area requirements. *Water Research,* 82**,** 47-57.

LÉONARD, A., BLACHER, S., MARCHOT, P., PIRARD, J. P. & CRINE, M. 2004. Measurement of Shrinkage and Cracks Associated to Convective Drying of Soft Materials by X-ray Microtomography. *Drying Technology,* 22**,** 1695-1708.

LEONARD, A., VANDEVENNE, P., SALMON, T., MARCHOT, P. & CRINE, M. 2004. Wastewater sludge convective drying: influence of sludge origin. *Environ Technol,* 25**,** 1051-7.

LI, D. H. W., LOU, S. W. & LAM, J. C. 2015. An Analysis of Global, Direct and Diffuse Solar Radiation. *Energy Procedia,* 75**,** 388-393.

LIJUAN, Z., JUNHONG, Y., SHANSHAN, W. & ZHONGHUA, W. 2019. CO-drying characteristics of sticky sewage sludge pre-conditioned with biomass and coal. *Drying Technology***,** 1-11.

LINGAYAT, A., CHANDRAMOHAN, V. P. & RAJU, V. R. K. 2017. Design, Development and Performance of Indirect Type Solar Dryer for Banana Drying. *Energy Procedia,* 109**,** 409-416.

LOWE, P. 1995. Developments in the Thermal Drying of Sewage Sludge. *Water and Environment Journal, Promoting of Sustainable Solutions,* 9**,** 306-16.

LU, T., SHEN, S. & LIU, X. 2008. Numerical and experimental investigation of heat and mass transfer in unsaturated porous media with low convective drying intensity. *Heat Transfer—Asian Research,* 37**,** 290-312.

MATHIOUDAKIS, V. L., KAPAGIANNIDIS, A. G., ATHANASOULIA, E., PALTZOGLOU, A. D., MELIDIS, P. & AIVASIDIS, A. 2013. Sewage Sludge Solar Drying: Experiences from the First Pilot-Scale Application in Greece. *Drying Technology,* 31**,** 519-526.

MATHLOUTHI, M. 2001. Water content, water activity, water structure and the stability of foodstuffs. *Food Control 12 (2001) 409±417*.

MEWA, E. A., OKOTH, M. W., KUNYANGA, C. N. & RUGIRI, M. N. 2018. Effect of drying air temperature and slice thickness on the physical and microbiological quality of dried beef. *Lwt,* 92**,** 484-489.

MGHAZLI, S., OUHAMMOU, M., HIDAR, N., LAHNINE, L., IDLIMAM, A. & MAHROUZ, M. 2017. Drying characteristics and kinetics solar drying of Moroccan rosemary leaves. *Renewable Energy,* 108**,** 303-310.

MOSETLHE, T., YUSUFF, A. A. & HAMAM, Y. 2018. Investigating seasonal wind energy potential in Vredendal, South Africa. *Journal of Energy in Southern Africa,* 29.

MULAUDZI, S. K., MUCHIE, M. & MAKHADO, R. 2012. Investigation of the Solar Energy Production and Contribution in South Africa. *African Journal of Science, Technology, Innovation and Development,* 4**,** 233-254.

MUSTAYEN, A. G. M. B., MEKHILEF, S. & SAIDUR, R. 2014. Performance study of different solar dryers: A review. *Renewable and Sustainable Energy Reviews,* 34**,** 463-470.

NEMS, M., NEMS, A., KASPERSKI, J. & POMORSKI, M. 2017. Thermo-Hydraulic Analysis of Heat Storage Filled with the Ceramic Bricks Dedicated to the Solar Air Heating System. *Materials (Basel),* 10.

NIWAGABA, C. B., MBÉGUÉRÉ, M. & STRANDE, L. 2014. Faecal Sludge Quantification, Characterization and Treatment Objectives. *In:* STRANDE, L., RONTELTAP, M. & BRDJANOVIC, D. (eds.) *Faecal Sludge Management: Systems Approach for Implementation and Operation.* Alliance House, 12 Caxton Street London, SW1H 0QS, UK: IWA Publishing.

O'KELLY, B. C. 2005. Mechanical properties of dewatered sewage sludge. *Waste Manag,* 25**,** 47-52.

POBLETE, R. & PAINEMAL, O. 2020. Improvement of the solar drying process of sludge using thermal storage. *J Environ Manage,* 255**,** 109883.

PRAKASH, O., LAGURI, V., PANDEY, A., KUMAR, A. & KUMAR, A. 2016. Review on various modelling techniques for the solar dryers. *Renewable and Sustainable Energy Reviews,* 62**,** 396-417.

PSKOVSKI, Z. & MUJUMDAR, A. S. 2010. Principles of Drying Theory and Technology. *Drying Technology,* 3**,** 149-151.

RADFORD, J. T. & SUGDEN, S. 2014. Measurement of faecal sludge in-situ shear strength and density. *Water SA,* 40.

RAGHAVAN, G. S. V. 1990. Review of: "DRYING: PRINCIPLES, APPLICATIONS AND DESIGN"C. Strumillo and T. Kudra Gordon and Breach Science Publishers, NY, 1987. *Drying Technology,* 8**,** 613-614.

ROSE, C., PARKER, A., JEFFERSON, B. & CARTMELL, E. 2015. The Characterization of Feces and Urine: A Review of the Literature to Inform Advanced Treatment Technology. *Crit Rev Environ Sci Technol,* 45**,** 1827-1879.

S. ABBASI, S. M. M., M. MOHEBBI3 2011. Investigation of Changes in Physical Properties and Microstructure and

Mathematical Modeling of Shrinkage of Onion during Hot Air Drying. *Iranian Food Science and Technology Research Journal,* Vol. 7, No. 1, 2011, p. 92-98.

SEROWIK, M., FIGIEL, A., NEJMAN, M., PUDLO, A., CHORAZYK, D. & KOPEC, W. 2017. Drying characteristics and some properties of spouted bed dried semi-refined carrageenan. *Journal of Food Engineering,* 194**,** 46-57.

SHANAHAN, E. F., ROIKO, A., TINDALE, N. W., THOMAS, M. P., WALPOLE, R. & KURTBOKE, D. I. 2010. Evaluation of pathogen removal in a solar sludge drying facility using microbial indicators. *Int J Environ Res Public Health,* 7**,** 565-82.

SHARMA, A., CHEN, C. R. & VU LAN, N. 2009. Solar-energy drying systems: A review. *Renewable and Sustainable Energy Reviews,* 13**,** 1185-1210.

SIEBERT, T., ZUBER, M., ENGELHARDT, S., BAUMBACH, T., KARBSTEIN, H. P. & GAUKEL, V. 2018. Visualization of crust formation during hot-air-drying via micro-CT. *Drying Technology***,** 1-10.

SIGGE, G. O., HANSMANN, C. F. & JOUBERT, E. 1998. Effect of Temperature and Relative Humidity on the Drying Rates and Drying Times of Green Bell Peppers (Capsicum Annuum L). *Drying Technology,* 16**,** 1703-1714.

SINGH, J. R. B. R. P. 1994. Optimization of Air drying Foods. *Food Enginering*.

SINGH, S., MOHAN, R. R., RATHI, S. & RAJU, N. J. 2017. Technology options for faecal sludge management in developing countries: Benefits and revenue from reuse. *Environmental Technology & Innovation,* 7**,** 203-218.

SLADE, L. & LEVINE, H. 1991. Beyond water activity: recent advances based on an alternative approach to the assessment of food quality and safety. *Crit Rev Food Sci Nutr,* 30**,** 115-360.

STRANDE, L., SCHOEBITZ, L., BISCHOFF, F., DDIBA, D., OKELLO, F., ENGLUND, M., WARD, B. J. & NIWAGABA, C. B. 2018. Methods to reliably estimate faecal sludge quantities and qualities for the design of treatment technologies and management solutions. *J Environ Manage,* 223**,** 898-907.

TAWEESAN, A., KOOTTATEP, T. & POLPRASERT, C. 2015. Effective faecal sludge management measures for on-site sanitation systems. *Journal of Water, Sanitation and Hygiene for Development,* 5**,** 483-492.

TIWARI, A. 2016. A Review on Solar Drying of Agricultural Produce. *Journal of Food Processing & Technology,* 7.

WAN, Y., NIANSU, H., PEISHENG, L., YI, H., QIAO, X., QIN, W., JUN, Y. & GUOLU, Y. 2009. Mathematical Modeling of Drying Characteristics of Sewage Sludge. *School of Power & Mechanical Engineering, Sewage Sludge and Silt Research Center Wuhan University, Wuhan 430072, P.R. China*.

WANG, P., MOHAMMED, D., ZHOU, P., LOU, Z., QIAN, P. & ZHOU, Q. 2019. Roof solar drying processes for sewage sludge within sandwich-like chamber bed. *Renewable Energy,* 136**,** 1071-1081.

WU, R., ZHAO, C. Y., TSOTSAS, E. & KHARAGHANI, A. 2017. Convective drying in thin hydrophobic porous media. *International Journal of Heat and Mass Transfer,* 112**,** 630-642.

XU, P., MUJUMDAR, A. S. & YU, B. 2008. Fractal Theory on Drying: A Review. *Drying Technology,* 26**,** 640-650.

Books

CALLAHAN, C. W., ELANSARI, A. M. & FENTON, D. L. 2019. Psychrometrics. *Postharvest Technology of Perishable Horticultural Commodities.*

MUJUMDAR, A. S. & DEVAHASTIN, S. 2011. Fundamental Principles of Drying. *Industrial Transfer Processes.* National University of Singapore.

SHARMA, M., PRAKASH, O., SHARMA, A. & KUMAR, A. 2018. Fundamentals and Performance Evaluation Parameters of Solar Dryer. *Low Carbon Energy Supply.*

TREYBAL, R. E. 1980. *Mass - Transfer Operations*, McGraw - Hill Book Company, Malaysia.

XU, P., SASMITO, A. P. & MUJUMDAR, A. S. 2020. *Heat and Mass Transfer in Drying of Porous Media*, Boca Raton: Taylor & Francis, a CRC title, part of the Taylor & Francis imprint, a member of the Taylor & Francis Group, the academic division of T&F Informa, plc, [2020] | Series: Advances in drying science and technology.

Dissertation/Thesis

MUGAURI, T. R. 2019. *Drying of faecal sludge from ventilated improved pit latrines (VIPs) using solar thermal energy.* Master of Science in Engineering (Mechanical), University of KwaZulu-Natal.

Conference papers

SCHOEBITZ, L., BASSAN, M., FERRÉ, A., VU, T. H. A., NGUYEN, V. A. & STRANDE, L. 2014. FAQ: faecal sludge quantification and characterization – field trial of methodology in Hanoi, Vietnam. *37th WEDC International Conference.* Hanoi, Vietnam.

SEPTIEN, S., MUGAURI, T. R., SINGH, A. & INAMBAO, F. 2018. Solar drying of faecal sludge from pit latrines in a bench-scale device. *41st WEDC International Conference.* Nakuru, Kenya.

Reports

EKECHUKWU, O. V. 1995. DRYING PRINCIPLES AND THEORY: AN OVERVIEW. International Centre for Theoretical Physics, Trieste, Italy.: Energy Research Centre, University of Nigeria, Nsukka, Nigeria.

PRG, X. C., CHRIS BUCKLEY 2016. SFD Report Durban, South Africa. *In:* EAWAG/SANDEC (ed.). University of KwaZulu-Natal and McGill University.

SEPTIEN, S., MUGAURI, T. R., SINGH, A. & INAMBAO, F. 2017. Drying of Faecal Sludge using Solar Thermal Energy, Water Research Comission project report. Pollution Research Group, University of KwaZulu-Natal.

WHO/UNICEF 2017. Progress on Drinking Water, Sanitation and Hygiene, Update and SDG baselines. Switzerland: World Health Organisation and the United Nations Children's Fund.

Uncategorized References

FLAGA, A. 2005. Sludge drying. *Institue of Heat Engineering and Air Protection, Cracow university of technology*.

APPENDICES

Appendix A: Invitations/confirmation of paper oral presentations at various conferences

This section includes the invitations and confirmation for oral presentation of work related to this dissertation at the various conferences.

Appendix A-1: 6th South Africa UNESCO Engineering Conference, 2019

UNESCO ENGINEERING CONFERENCE

We hereby certify that

Martin Mawejje

presented their research with the title

Solar drying of faecal sludge: Drying kinetics and underlying sludge structural changes

during the conference on 25 September 2019 in Mahikeng

Faculty of Engineering - Executive Dean

Prof. Liezl van Dyk

Appendix A-2: 6th South Africa Young Water Professionals Conference 2019

Dear Mr. Martin Mawejje,

We are pleased to inform you that your abstract/s as detailed below has been accepted and will be included in the provisional programme for the Young Water Professionals Conference 2019 to be held at Durban ICC from 20th - 22nd October 2019.

Presentations

Title	Solar drying of faecal sludge: Effect of experimental parameters on drying kinetics and physical properties
Paper Number	47
Presentation Type	Oral
Theme	4. Sanitation solutions for water scarce country: Innovative cost effective sanitation technologies
Presenting Author	Mr. Martin Mawejje Affiliations: Pollution Reserach Group, Ukzn

Specific information for your presentation(s) will follow in due course.

For the Organising Committee to finalise your participation, please ensure that you have registered and paid for your attendance by 19th August. Please note early bird registration rate has been extended for all those accepted to the 12th August.

In order to register please click on the link below and login with your email address and password and follow the prompts.

https://confco.eventsair.com/wisaywp2019/registration

Thank you for your valuable contribution to the YWP Conference 2019. It promises to be a most memorable and exciting event.

Kind regards,

YWP Conference 2019 Organising Committee
Queries - Joanne Bezuidenhout
joanne@confco.co.za
The Conference Company
Tel: +27 31 303 9852

Appendix A-3: UKZN Post Graduate Research and Innovation symposium 2019

UNIVERSITY OF KWAZULU-NATAL
INYUVESI YAKWAZULU-NATALI

16 September 2019

Via email

Dear Martin,

It gives me great pleasure to inform you that your abstract entitled:

SOLAR DRYING OF FAECAL SLUDGE: EFFECT OF EXPERIMENTAL PARAMETERS ON DRYING KINETICS AND SLUDGE PHYSICAL PROPERTIES

has been accepted for an **Oral Presentation** at the annual College of Agriculture, Engineering and Science Postgraduate Research and Innovation Symposium to be held on **Thursday 17 October 2019** from **08:30** on the Westville Campus, **T-Block**, University of KwaZulu-Natal.

You have been allocated a 20-minute time slot (15-minute presentation and 5 minutes' question time). It is important that you stay within this timeframe. Oral presentations will be run simultaneously in five lecture venues - please note which venue you will be presenting in. To ensure the process is efficient, please load your presentation between 07:30 and 08:30 on the day at the respective venues, where you will be assisted by one of the designated student helpers.

Please find the attached (abridged) programme and a map to the venue. If you requested transport from another campus you will be given final details closer to the time.

PLEASE NOTE: Should you decide not to present your work in an oral presentation, you will be required to produce a letter from your Supervisor to this effect and to pay a penalty of R300 to recover the cost of arrangements.

Yours sincerely,

Henry Mwambi

Professor H G Mwambi
Chairman: Organising Committee
PG Research and Innovation Symposium

Website: pris.ukzn.ac.za

College of Agriculture, Engineering and Science
IKolichi lezoLimo, ubuNjiniyela kanye neSayensi
Postal Address: Private Bag X01, Scottsville, 3209, South Africa
Telephone: +27 (0)31 260 7065/8740 Facsimile: 086 681 1704 Email: rajpal@ukzn.ac.za Website: caes.ukzn.ac.za

Appendix B: Ethics approval letter

UNIVERSITY OF
KWAZULU-NATAL
INYUVESI
YAKWA7ULU-NATALI

16 October 2019

Mr Martin Nyanzi Mawejje (218087129)
School of Engineering
Howard College

Dear Mr Martin Nyanzi Mawejje,

Protocol reference number: BREC/00000203/2019
Project title: Solar Drying of Faecal Sludge; Drying kinetics and underlying structural changes
Degree Purposes: Masters of Science in Engineering

EXPEDITED APPLICATIOH: APPROVAL LETTER

A sub-committee of the Biomedical Research Ethics Committee has considered and noted your application.

The conditions have been met and the study is given full ethics approval and may begin as from 16 October 2019. Please ensure that outstanding site permissions are obtained and forwarded to BREC for approval before commencing research at a site.

This approval is valid for one year from 16 October 2019. To ensure uninterrupted approval of this study beyond the approval expiry date, an application for recertification must be submitted to BREC on the appropriate BREC form 2-3 months before the expiry date.

Any amendments to this study, unless urgently required to ensure safety of participants, must be approved by BREC prior to implementation.

Your acceptance of this approval denotes your compliance with South African National Research Ethics Guidelines (2015), South African National Good Clinical Practice Guidelines (2006) (if applicable) and with UKZN BREC ethics requirements as contained in the UKZN BREC Terms of Reference and Standard Operating Procedures, all available at http://research.ukzn.ac.za/Research-Ethics/Biomedical-Research-Ethics.aspx.

BREC is registered with the South African National Health Research Ethics Council (REC-290408-009). BREC has US Office for Human Research Protections (OHRP) Federal-wide Assurance (FWA 678).

The sub-committee's decision will be noted by a full Committee at its next meeting taking place on 12 November 2019.

Yours sincerely

---------- ----- ----------
Prof V Rambiritch (Chair)

Appendix C: Standard Operating Procedure for solar thermal convection drying rig

Standard Operation Procedure – Solar Thermal Drying Experiments

1. Scope and Application

Drying is defined as a process of moisture removal from a wet product. This wet product can be in solid, semi-solid or liquid form. Drying results from evaporation of the moisture from the wet product. Evaporation happens when liquid molecules escape from the wet product and turn into a vapour. Drying of various feedstock is needed for one or several of the following reasons: the need for easy-to-handle solids, preservation and storage, reduction in the cost of transportation, achieving the desired quality of the product.

2. Brief description of the solar thermal drying rig

A laboratory-scale solar drying rig set up. This setup consists of a cylindrical glass drying chamber, electric heater, mass balance and interface to record data automatically into the computer software. On the contrary to the previous investigation, the setup was modified with an automatic control flow system, consisting in an electronic flowmeter, proportional valve and controller.

3. Safety Precautions

- All electric cables and installations should not be in contact with water
- The air heater should be switched off while there is no convection air flow
- All pipes have to be firmly connected
- Drying experiments should not be undertaken during rainy weather
- Use appropriate personal protective equipment (PPE) while handling faecal material

4. Schematic diagram

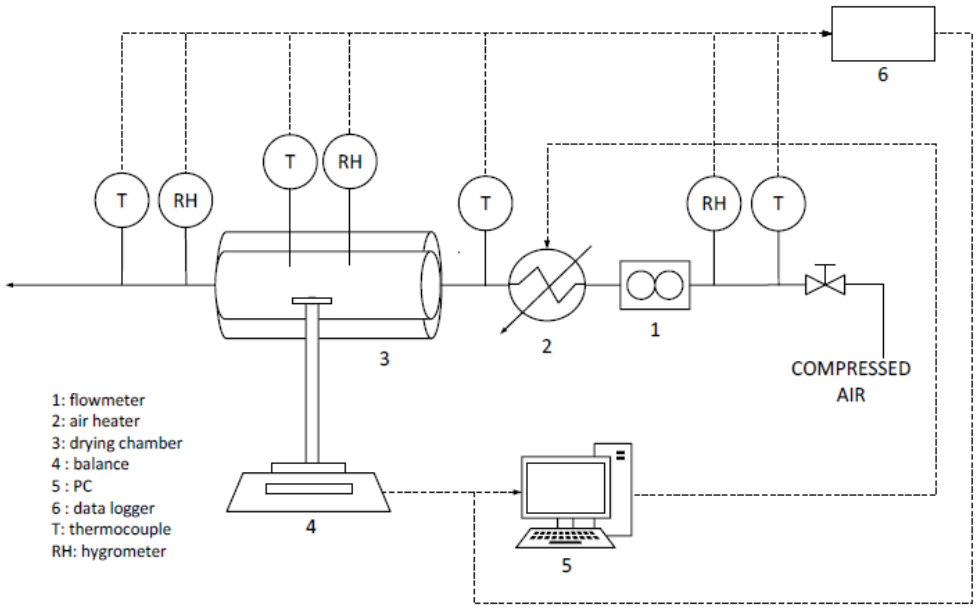

5. Experimental Procedure

Start-up

1. Turn on the computer and appropriate open software (LabVIEW) and data logger
2. Turn on the air compressor, and preset the air flowrate on the LabVIEW software
3. Set the required air temperature on the software and preheat air to this temperature
4. Turn on the mass balance and pyranometer
5. Place the sample in the drying chamber
6. Check that all temperature and humidity probes are placed at the appropriate locations

Operation

1. Log and monitor rotameter regularly

End of experiments

1. Stop the experiment on the software
2. Remove dried sample
3. Turn off air supply from the compressor
4. Turn off the computer and data logger
5. Record the thickness of the dried sludge sample
6. Observe the presence and pattern of crust layer, cracks if any and take photograph

Cleaning and Disinfecting

1. Remove holder from drying mass rig support

2. Clean holder with dump sponge
3. Disinfect holder and sore away for future use

Maintenance

Part/Apparatus	Brand Name	Model Number	Sensitivity	Special Notes
Mass Balance	BOECO	BPS51 plus	0-4500g 10mg (2dp) Max op temp = 50^0C	Recalibrate weekly
Rotameter	Tecfluid	PS-31/PVC	0-30l/s Max op Temp = 60^0C	
Pyranometer and amp box	Kipp and Zonen	CMP3	0-2000w/m^2	
Flow controller	burkert	Type 2875	<0.25% FS	

Appendix D: Interpolation of raw drying curve data through linear and exponential trendlines for the calculation of the drying rates

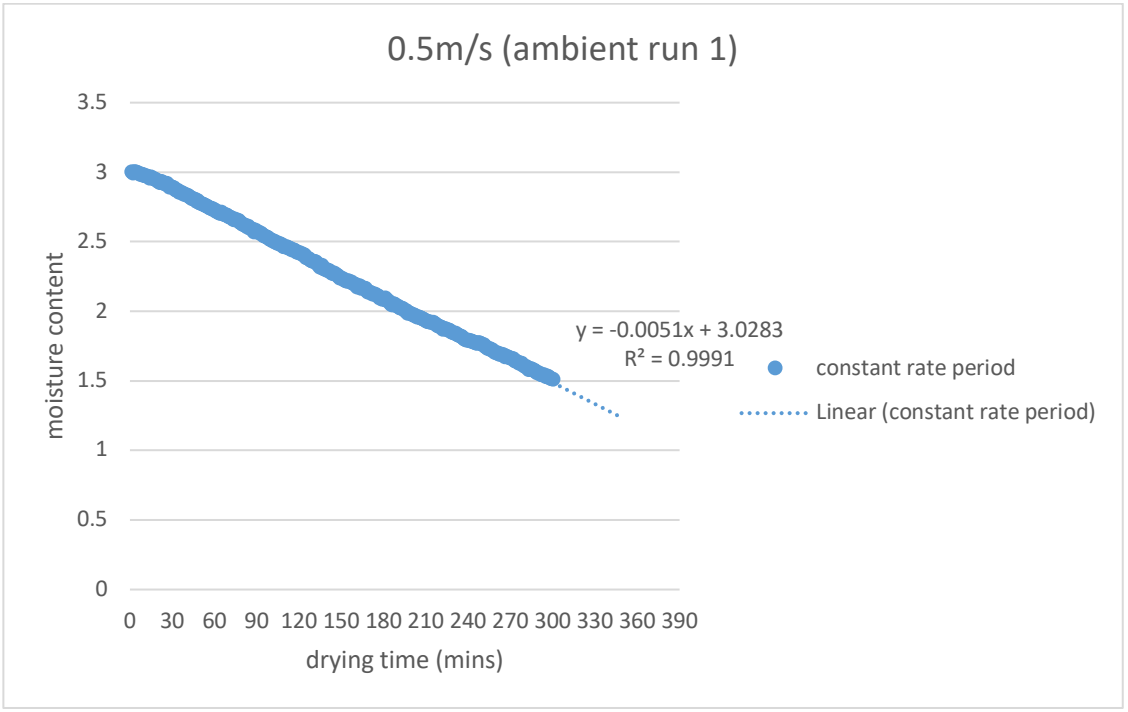

Figure D-0-1: Interpolation of drying curve for VIP sludge during sunny weather, 0.5m/s air velocity, ambient air temperature (run1)

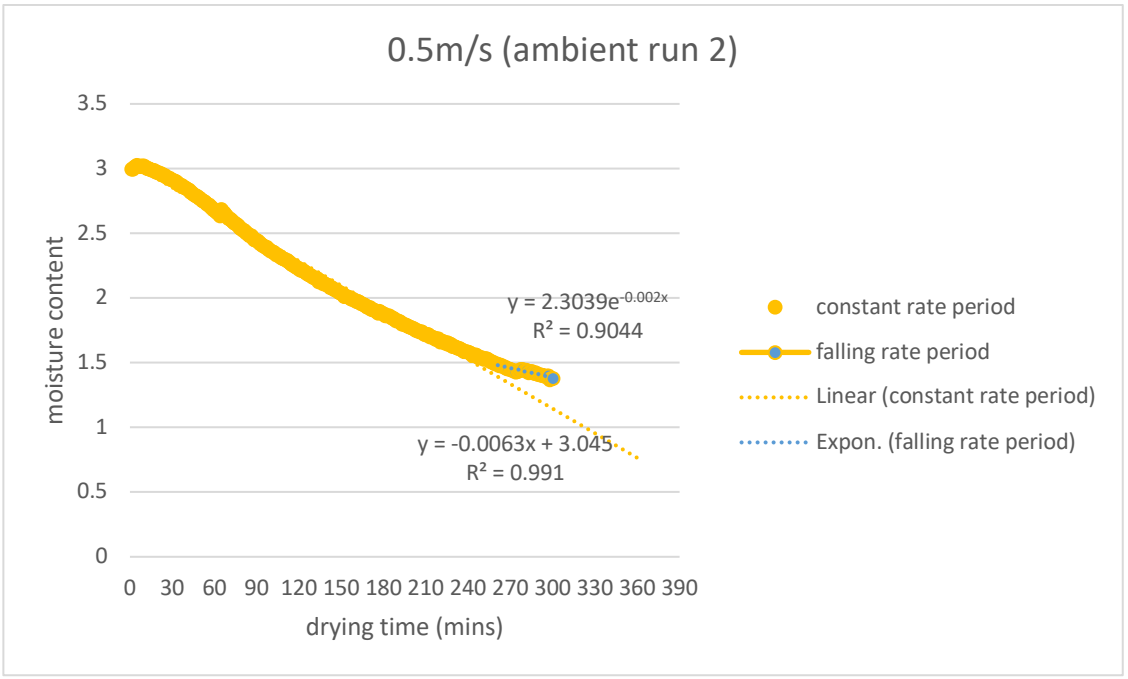

Figure D-0-2: Interpolation of drying curve for VIP sludge during sunny weather, 0.5m/s air velocity, ambient air temperature (run2)

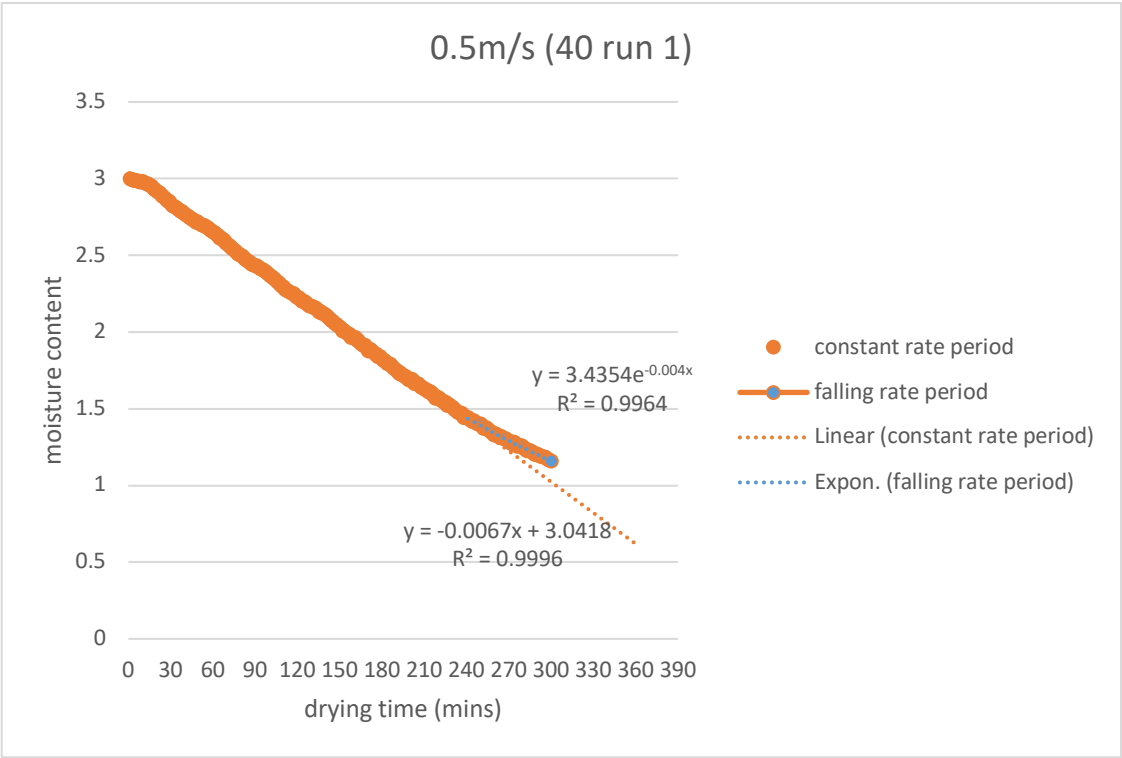

Figure D-0-3: Interpolation of drying curve for VIP sludge during sunny weather, 0.5m/s air velocity, 40°C air temperature (run1)

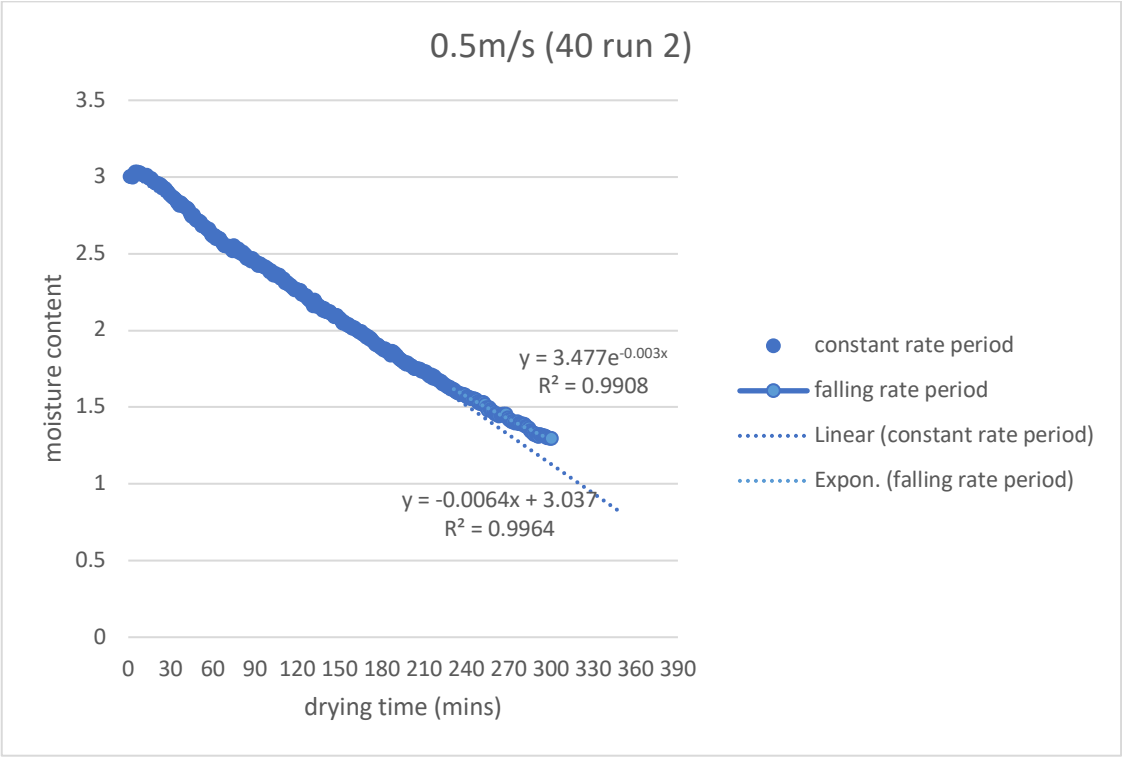

Figure D-0-4: Interpolation of drying curve for VIP sludge during sunny weather, 0.5m/s air velocity, 40°C air temperature (run2)

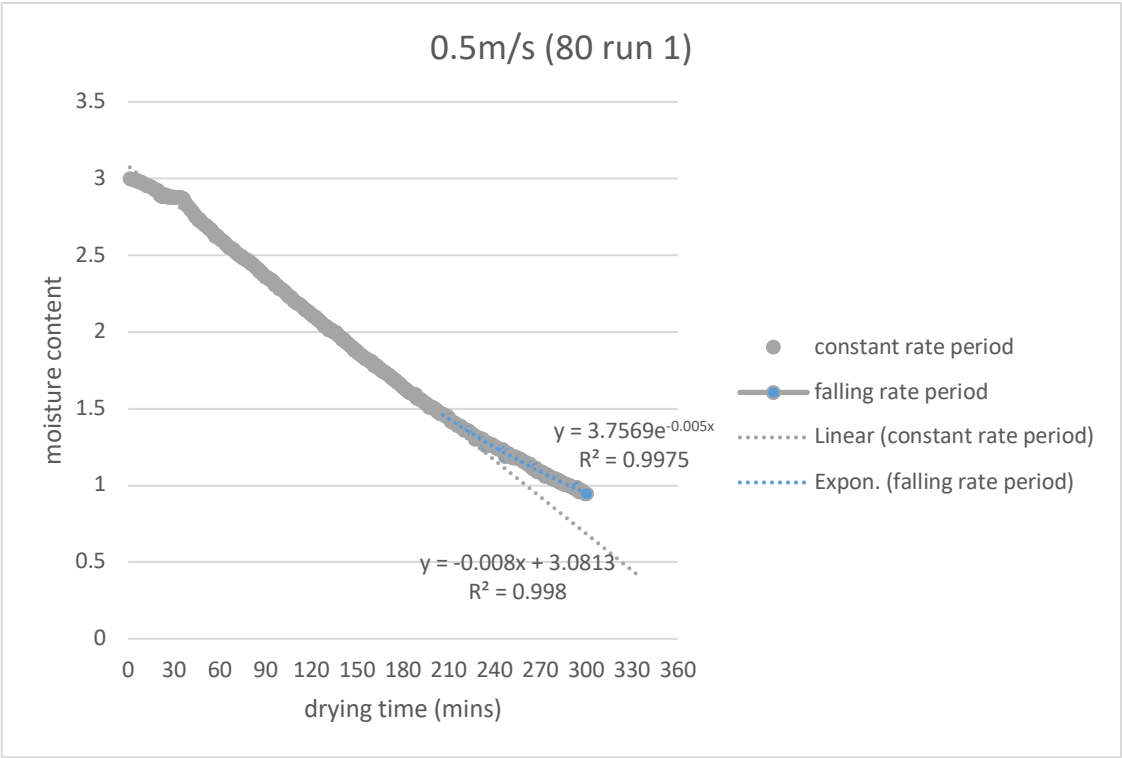

Figure D-0-5: Interpolation of drying curve for VIP sludge during sunny weather, 0.5m/s air velocity, 80°C air temperature (run1)

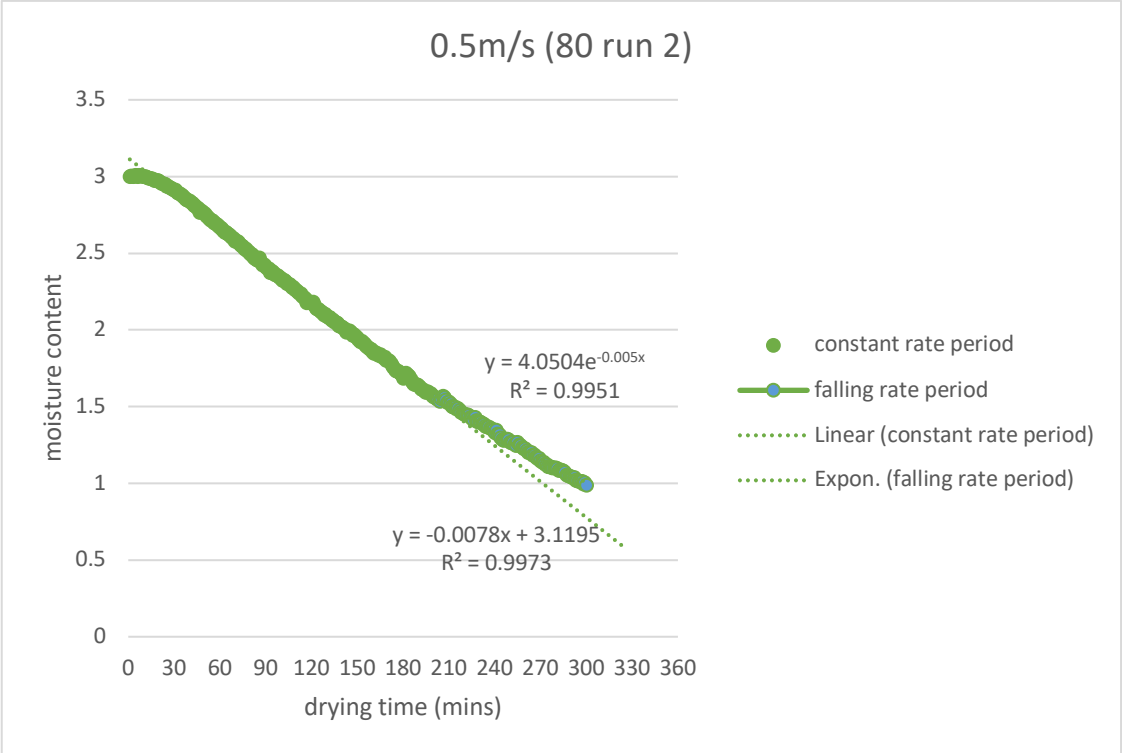

Figure D-0-6: Interpolation of drying curve for VIP sludge during sunny weather, 0.5m/s air velocity, 80°C air temperature (run2)

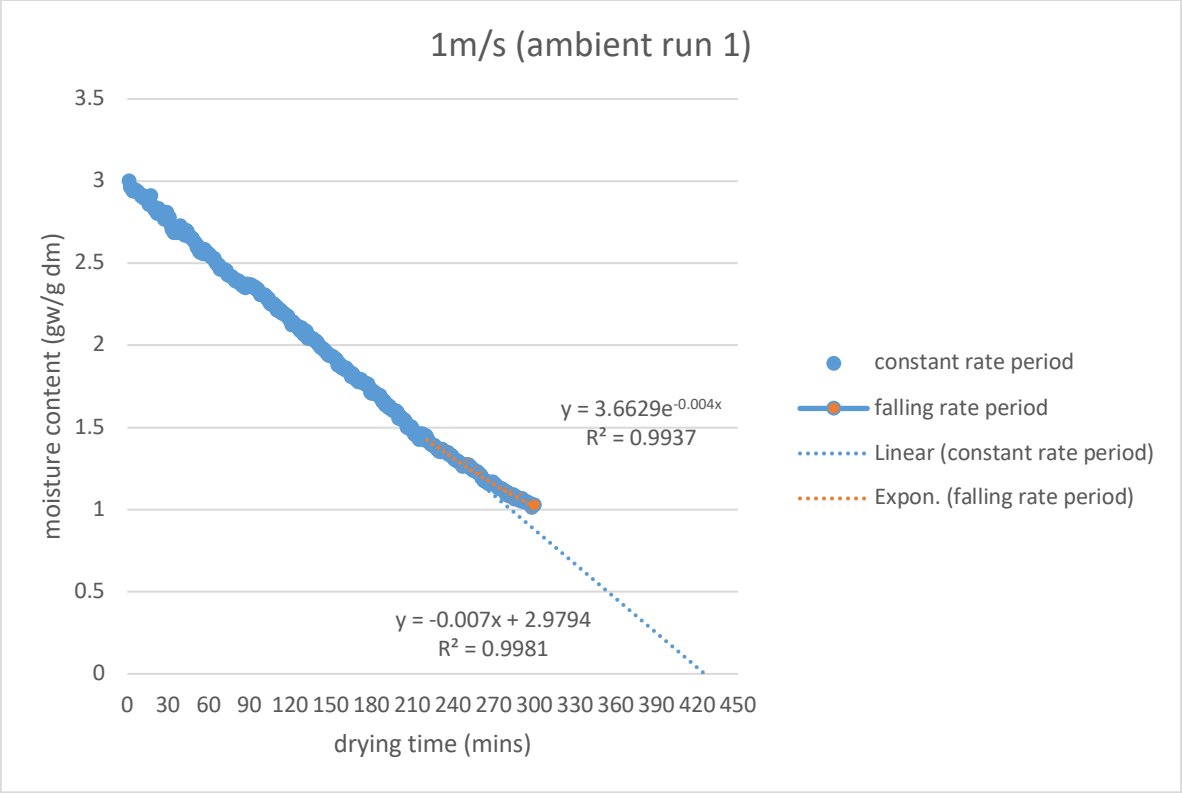

Figure D-0-7: Interpolation of drying curve for VIP sludge during sunny weather, 1m/s air velocity, ambient air temperature (run1)

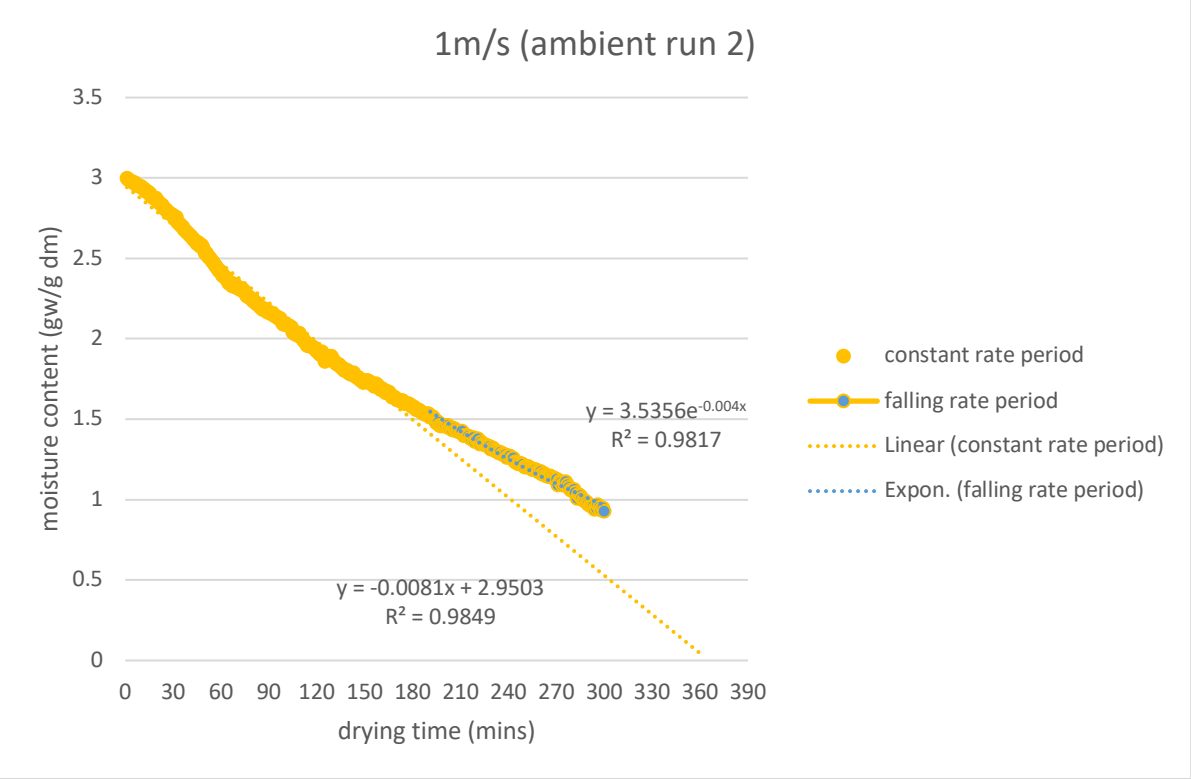

Figure D-0-8: Interpolation of drying curve for VIP sludge during sunny weather, 1m/s air velocity, ambient air temperature (run2)

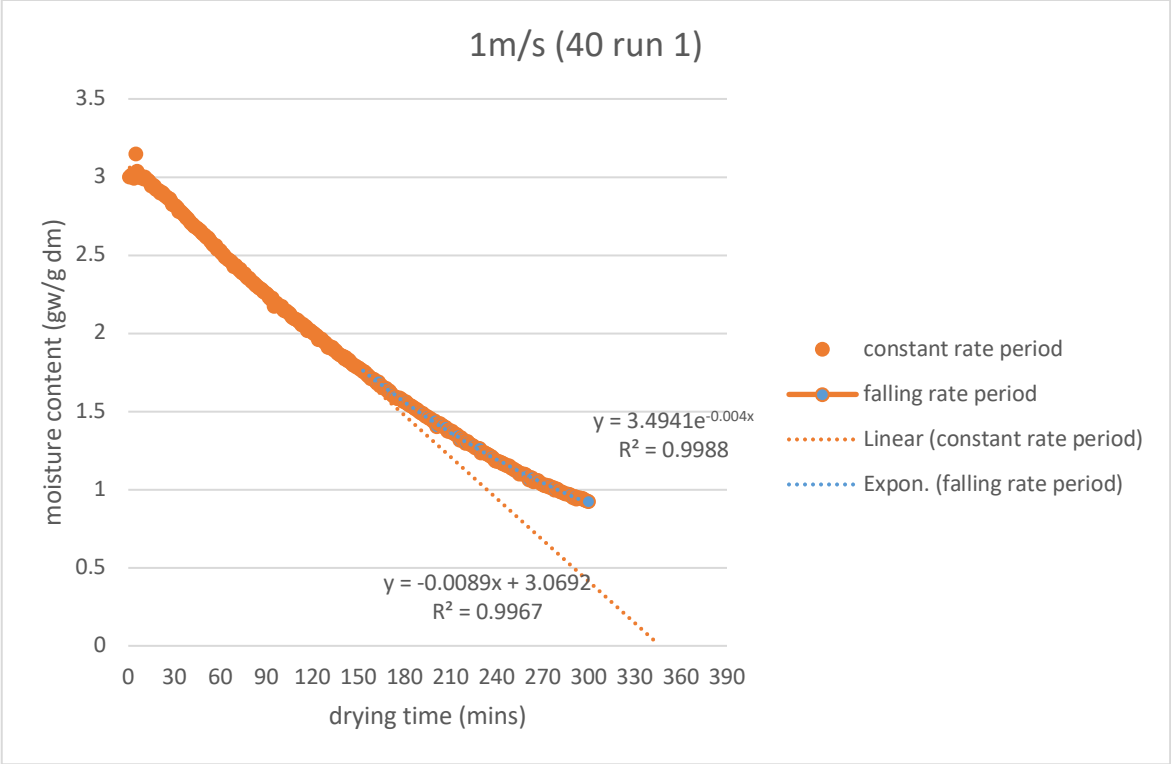

Figure D-0-9: Interpolation of drying curve for VIP sludge during sunny weather, 1m/s air velocity, 40°C air temperature (run1)

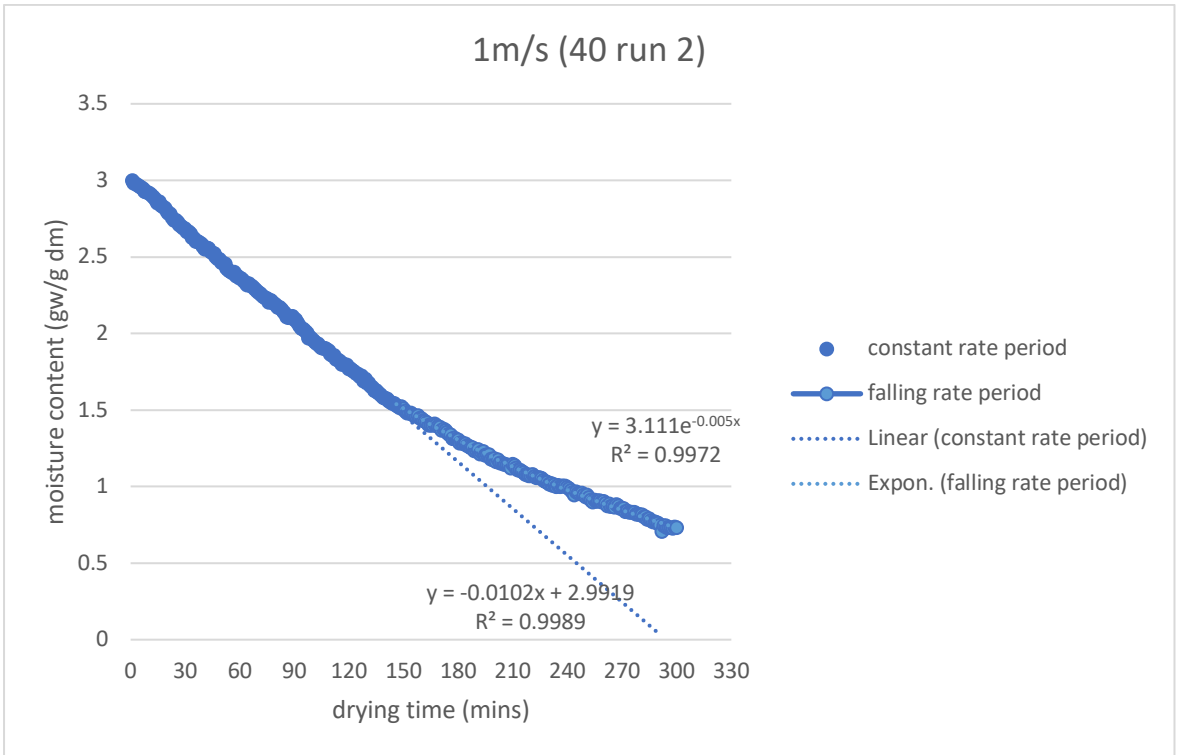

Figure D-0-10: Interpolation of drying curve for VIP sludge during sunny weather, 1m/s air velocity, 40°C air temperature (run2)

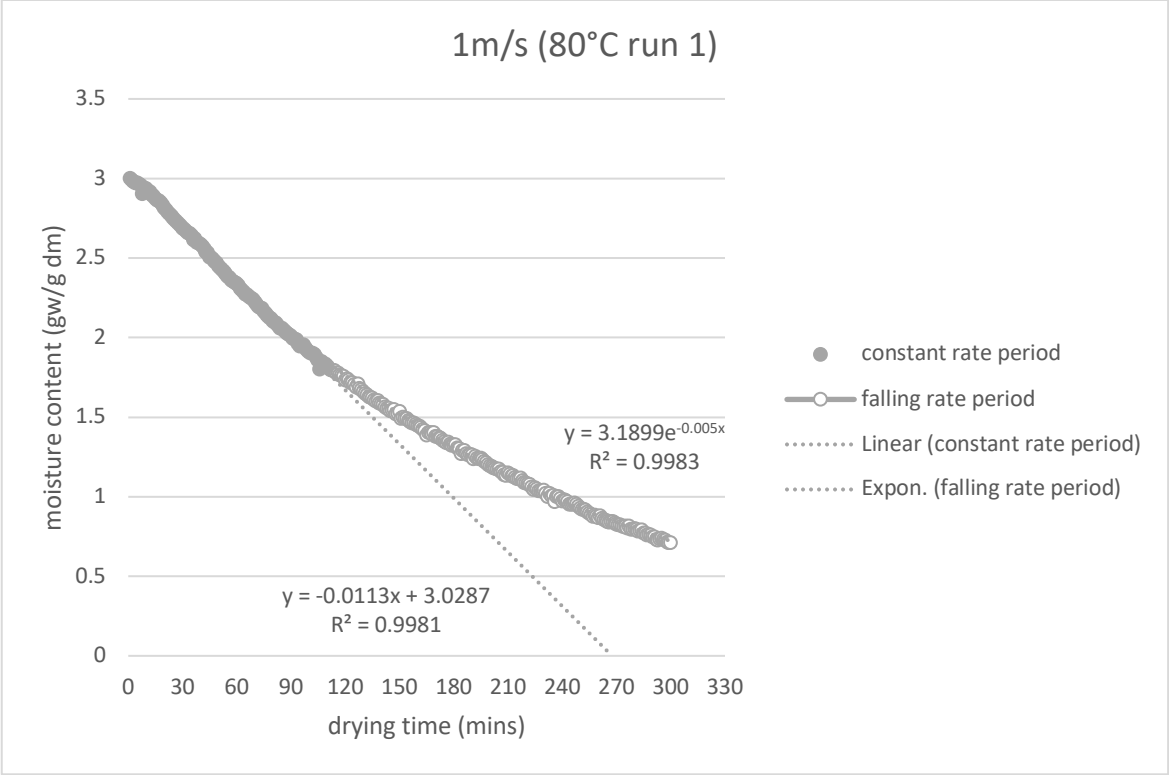

Figure D-0-11: Interpolation drying curve for VIP sludge during sunny weather, 1m/s air velocity, 80°C air temperature (run1)

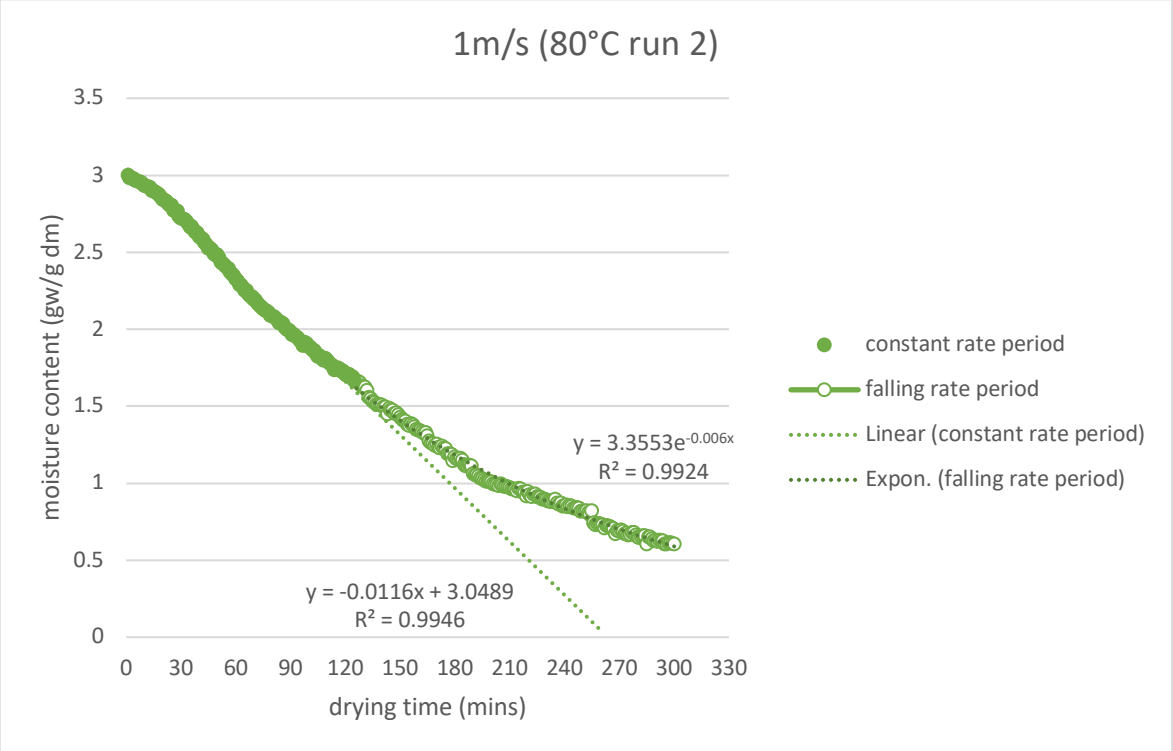

Figure D-0-12: Interpolation of drying curve for VIP sludge during sunny weather, 1m/s air velocity, 80°C air temperature (run2)

Appendix E: Drying rate curves as a function of time

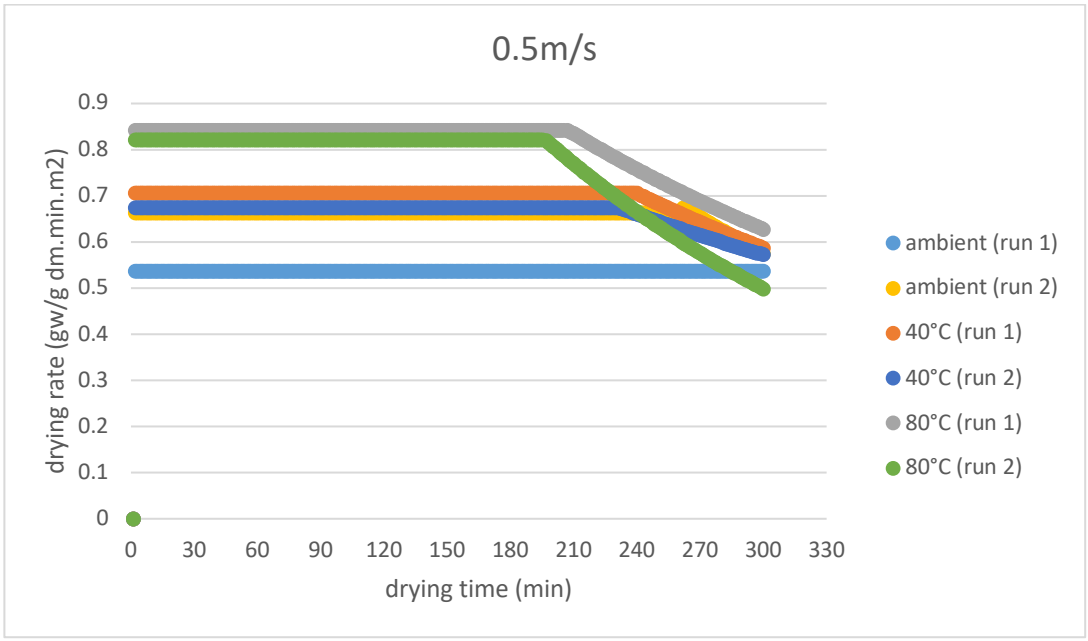

Figure E-1: Drying rate curves as a function of time during the VIP sludge solar drying in sunny weather conditions, at an air velocity of 0.5 m/s for varying air temperature (ambient, 40°C and 80°C)

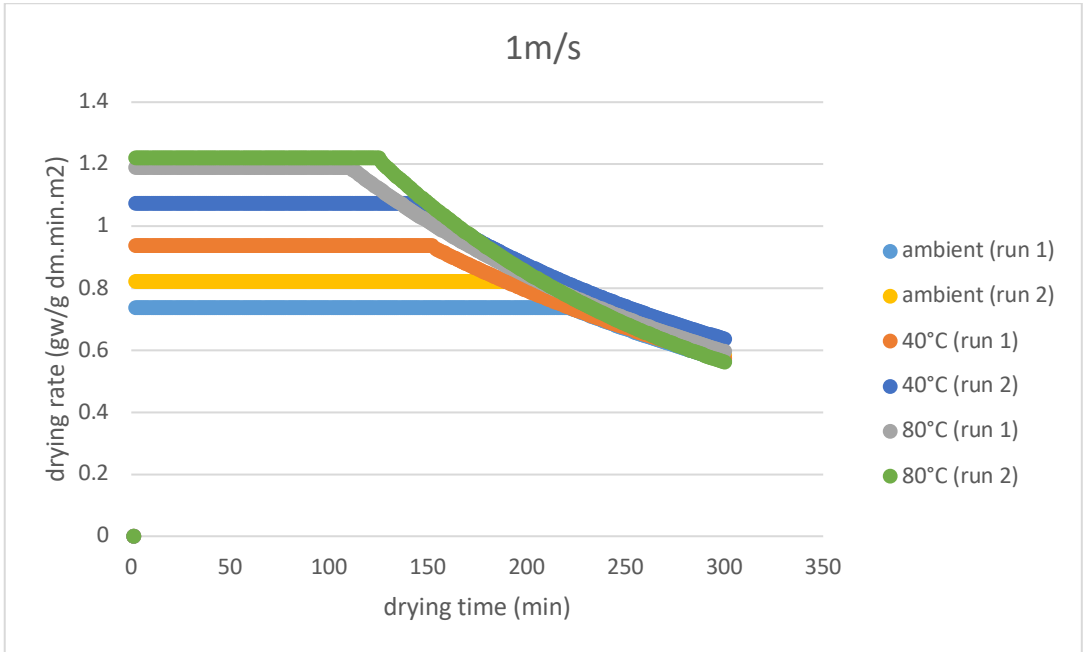

Figure E-2: Drying rate curves as a function of time during the VIP sludge solar drying in sunny weather, at an air velocity of 1m/s air velocity, for varying air temperature (ambient, 40°C and 80°C)

Appendix F: Comparison between the predicted drying curves from the tested models and the experimental data

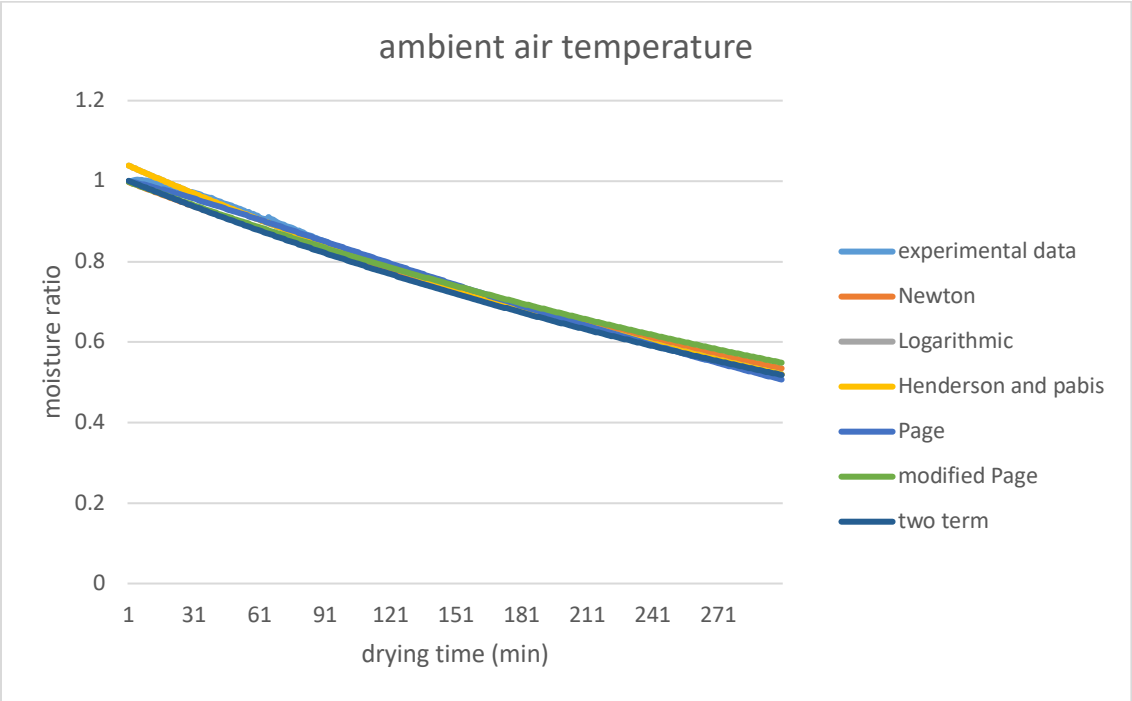

Figure F-1: Modelled and experimental drying curves during VIP sludge solar drying in sunny weather, at ambient temperature and air velocity of 0.5 m/s

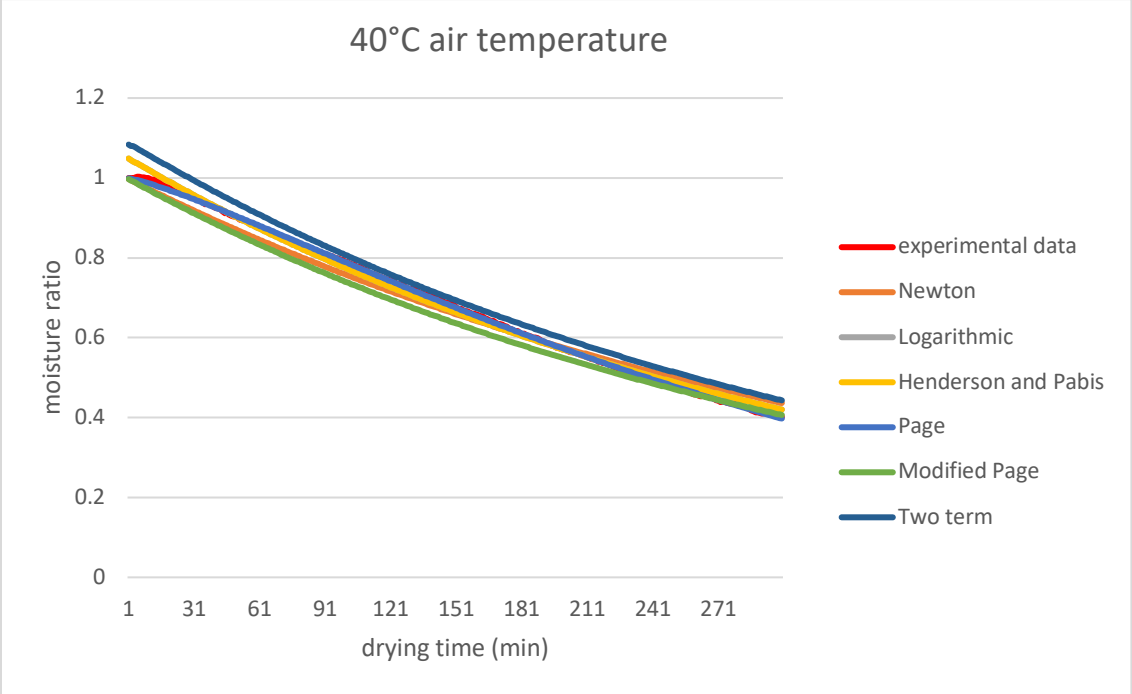

Figure F-2: Modelled and experimental drying curves during VIP sludge solar drying in a sunny weather, at 40°C and air velocity of 0.5 m/s

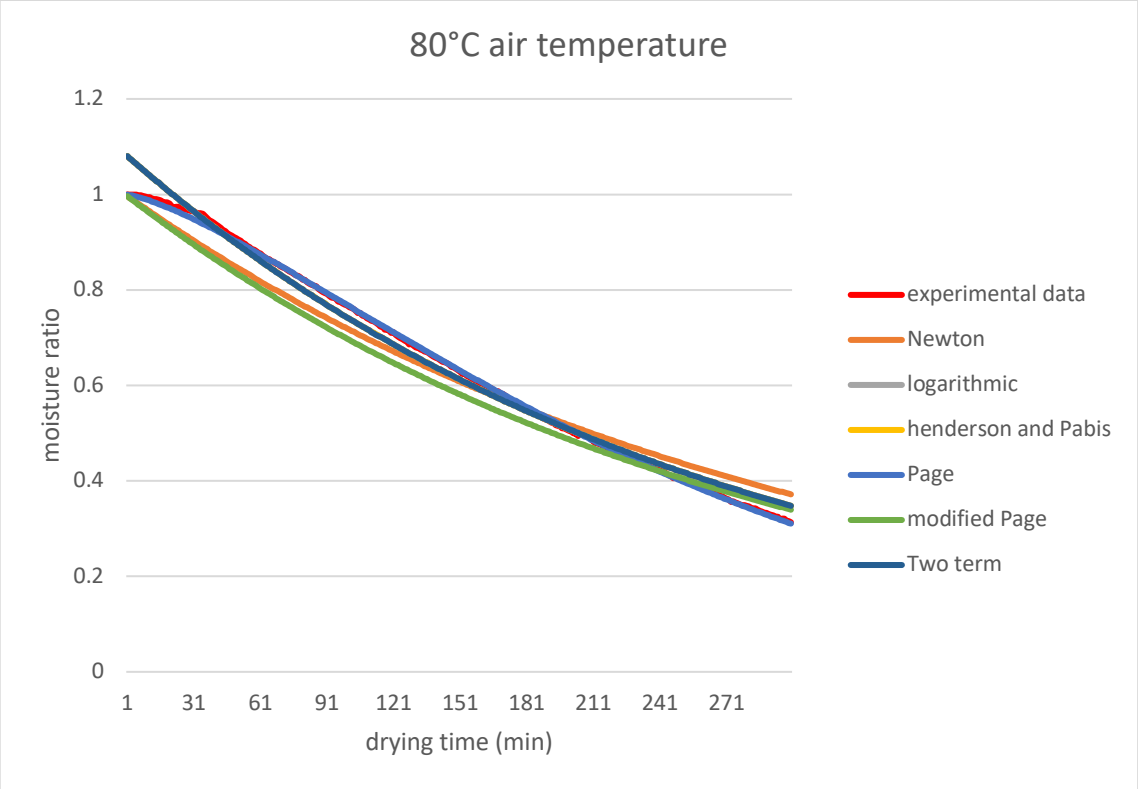

Figure F-3: Modelled and experimental drying curves during VIP sludge solar drying in sunny weather, at a temperature of 80°C and air velocity of 0.5m/s

Appendix G: Evolution of the temperature of the sludge and surrounding air within the drying chamber

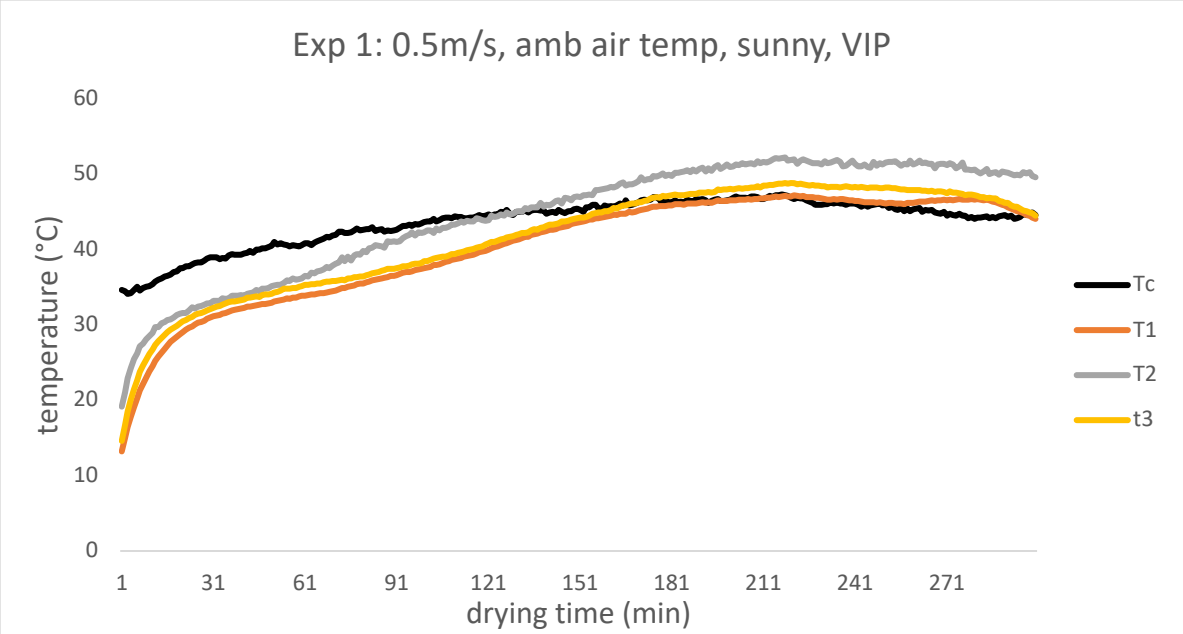

Figure G-1: Evolution of sludge temperature (T1, T2, T3) and air chamber temperature (Tc) as a function of time during the VIP sludge solar drying in a sunny weather, at ambient temperature and air velocity of 0.5m/s

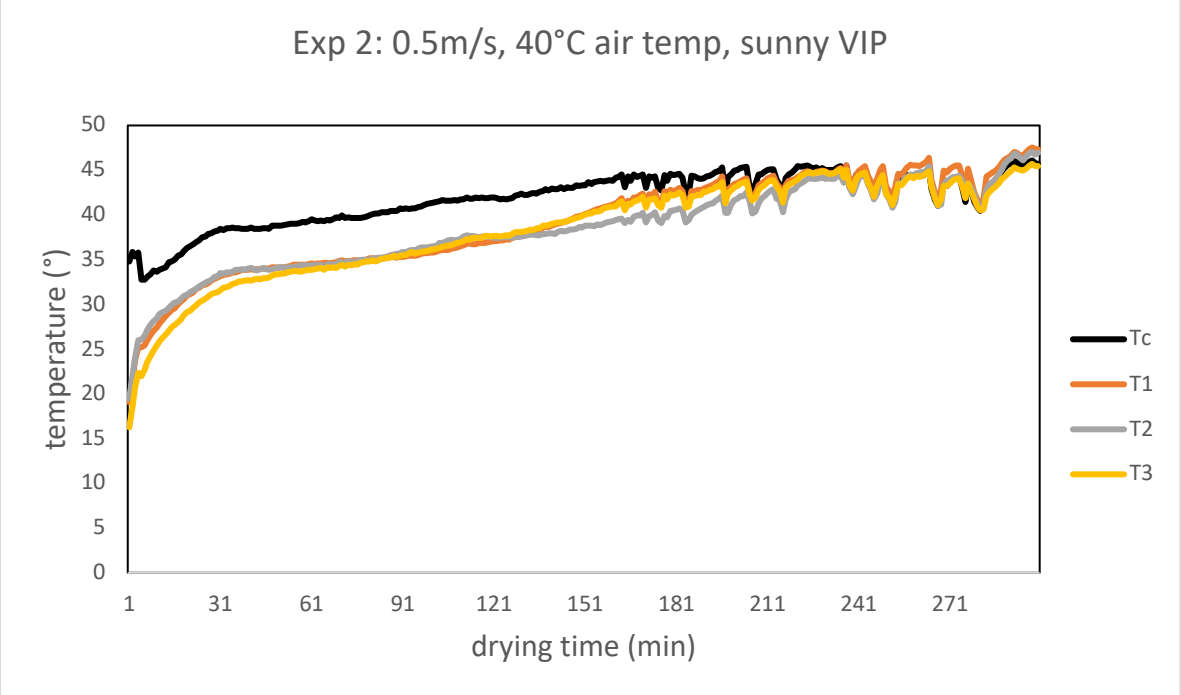

Figure G-2: Evolution of sludge temperature (T1, T2, T3) and air chamber temperature (Tc) as a function of drying time for VIP sludge solar drying in sunny weather at 0.5m/s air flow and 40°C air temperature

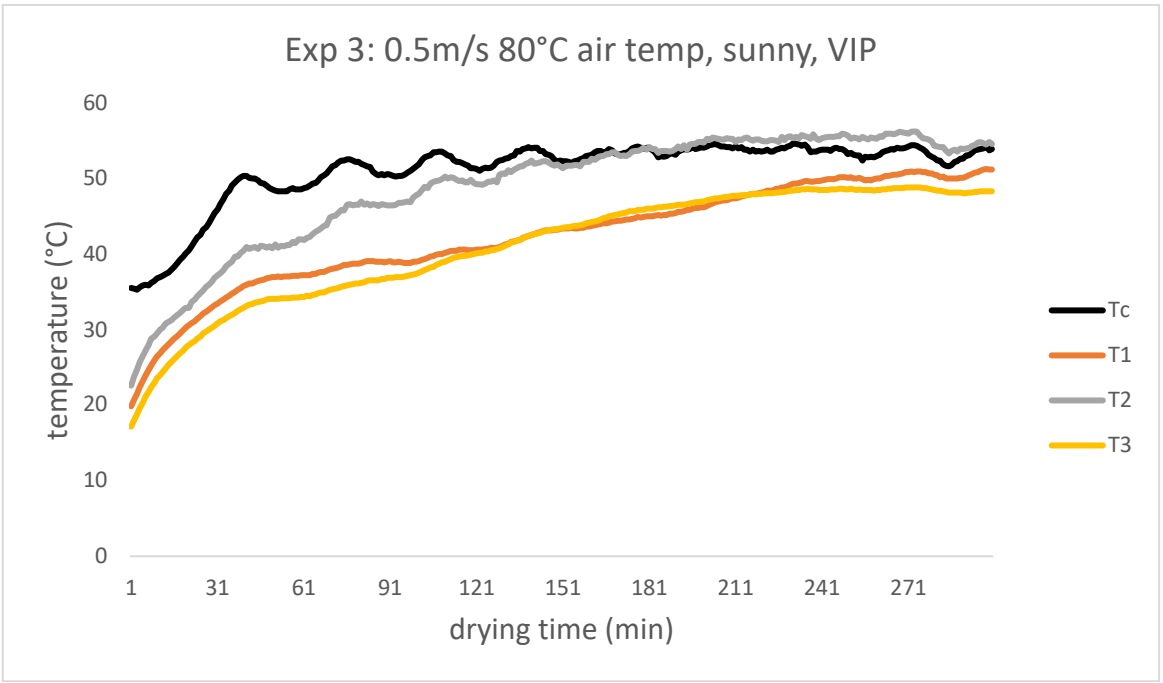

Figure G-3: Evolution of sludge temperature (T1, T2, T3) and air chamber temperature (Tc) as a function of drying time for VIP sludge solar drying in sunny weather, at 0.5m/s air flow and 80°C air temperature

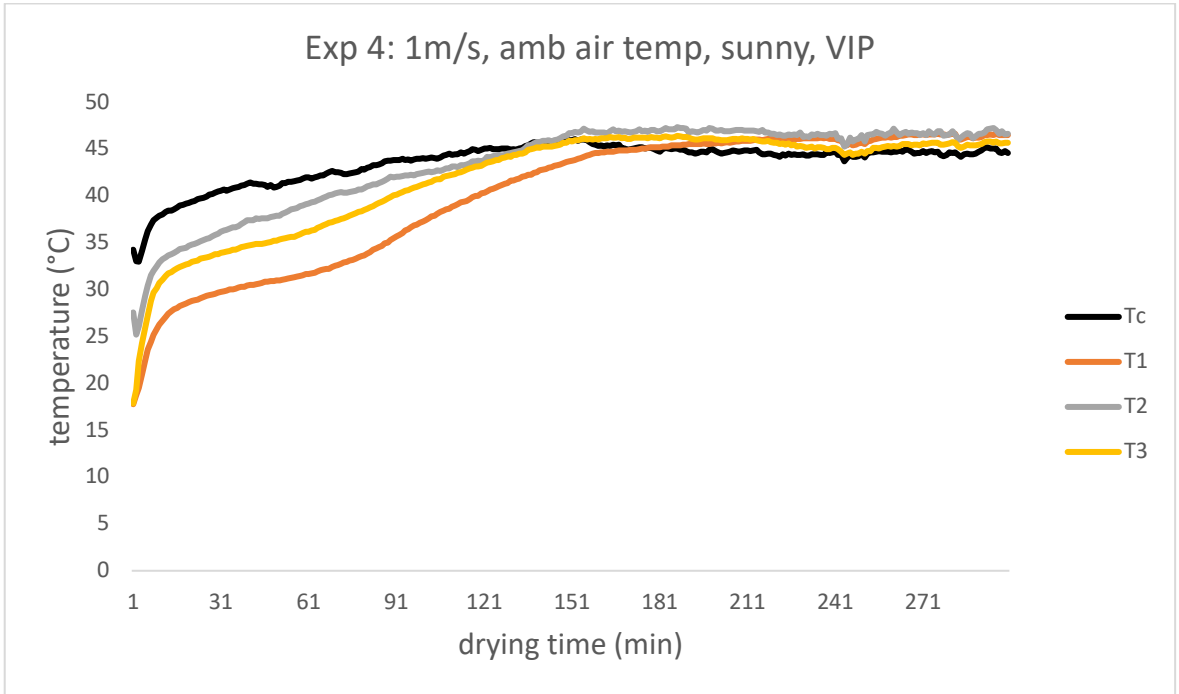

Figure G-4: Evolution of sludge temperature (T1, T2, T3) and air chamber temperature (Tc) as a function of drying time for VIP sludge solar drying in sunny weather, at 1m/s air flow and ambient air temperature

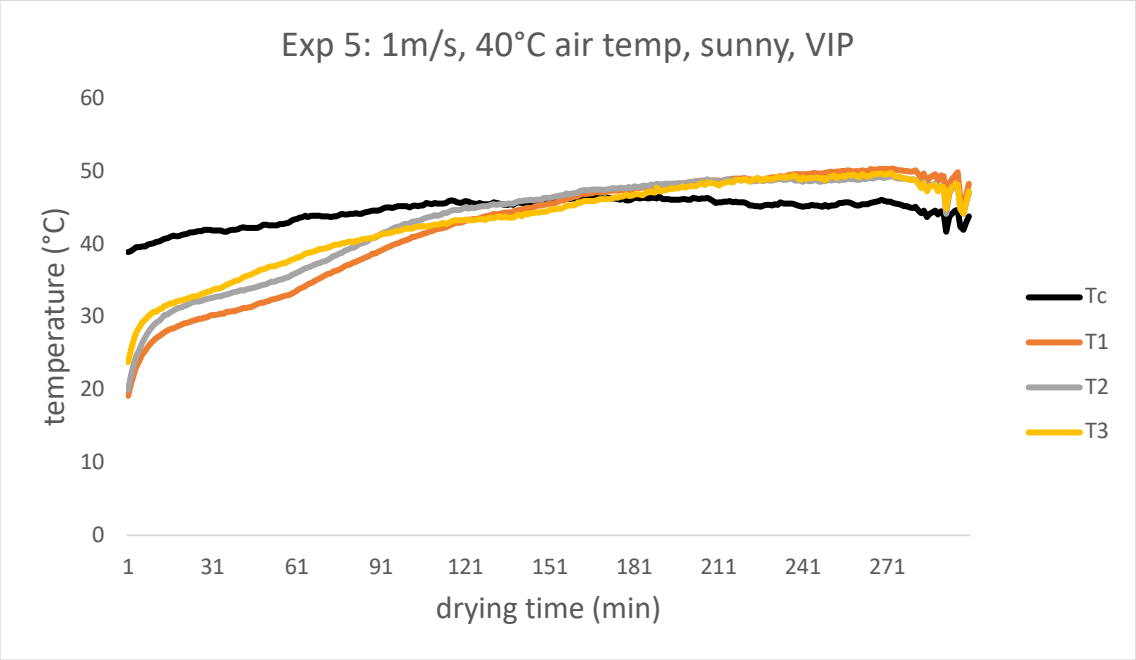

Figure G-5: Evolution of sludge temperature (T1, T2, T3) and air chamber temperature (Tc) as a function of drying time for VIP sludge solar drying in sunny weather, at 1m/s air flow and 40°C air temperature

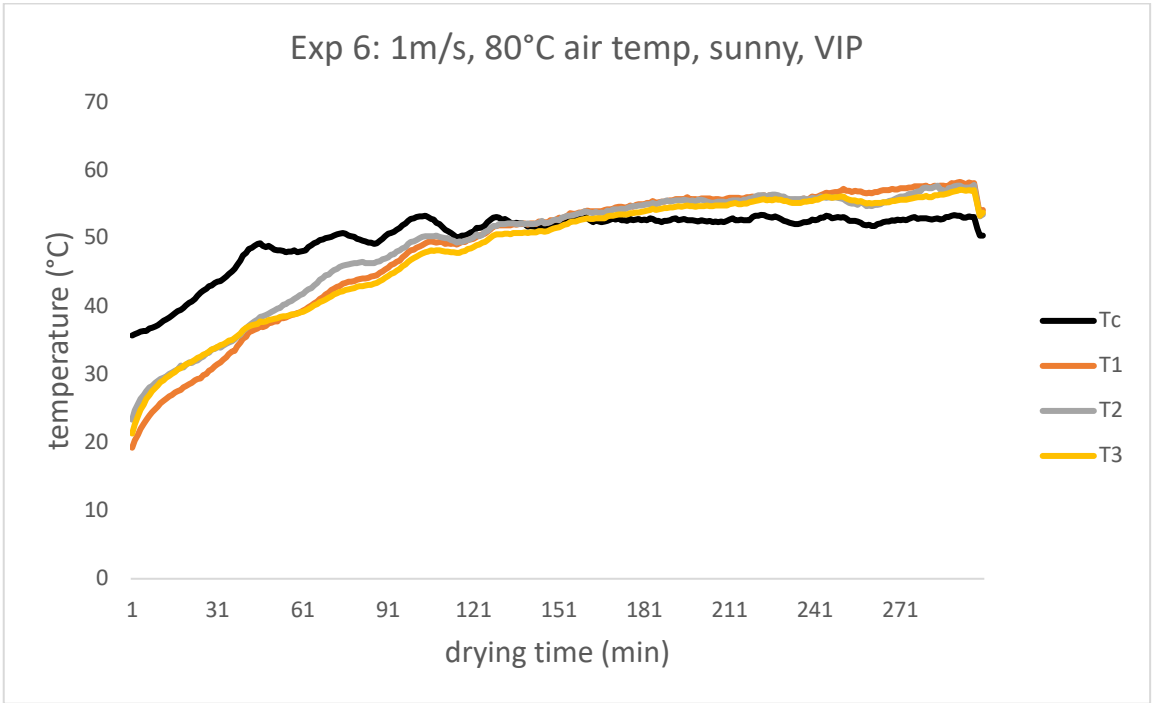

Figure G-6: Evolution of sludge temperature (T1, T2, T3) and air chamber temperatures (Tc) as a function of drying time for VIP sludge solar drying in sunny weather, at 1m/s air flow and 80°C air temperature

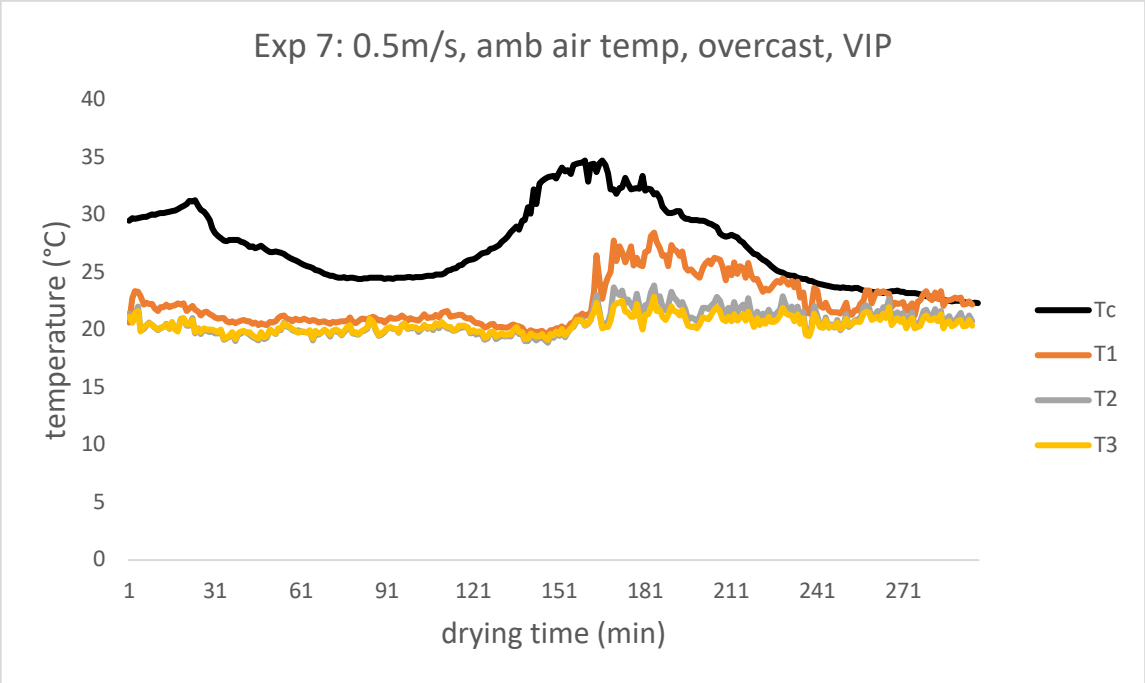

Figure G-7: Evolution of sludge temperature (T1, T2, T3) and air chamber temperatures (Tc) as a function of drying time for VIP sludge solar drying in overcast weather, at 0.5m/s air flow and 80°C air temperature

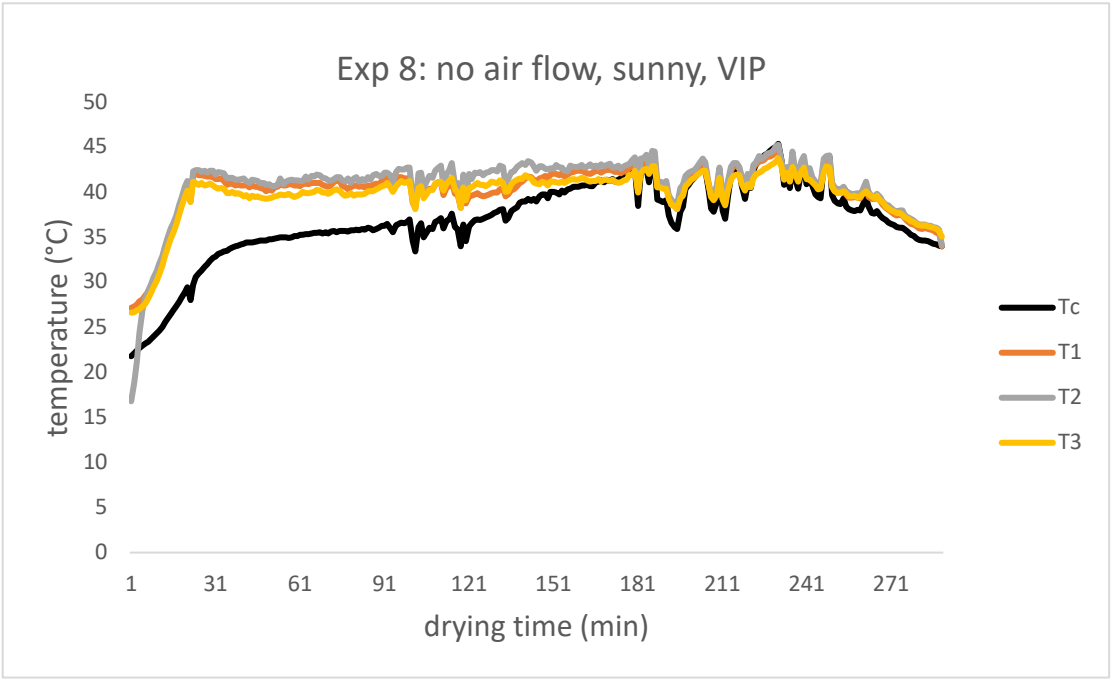

Figure G-8: Evolution of sludge temperature (T1, T2, T3) and air chamber temperatures (Tc) as a function of drying time for VIP sludge solar drying in sunny weather with no convection air flow

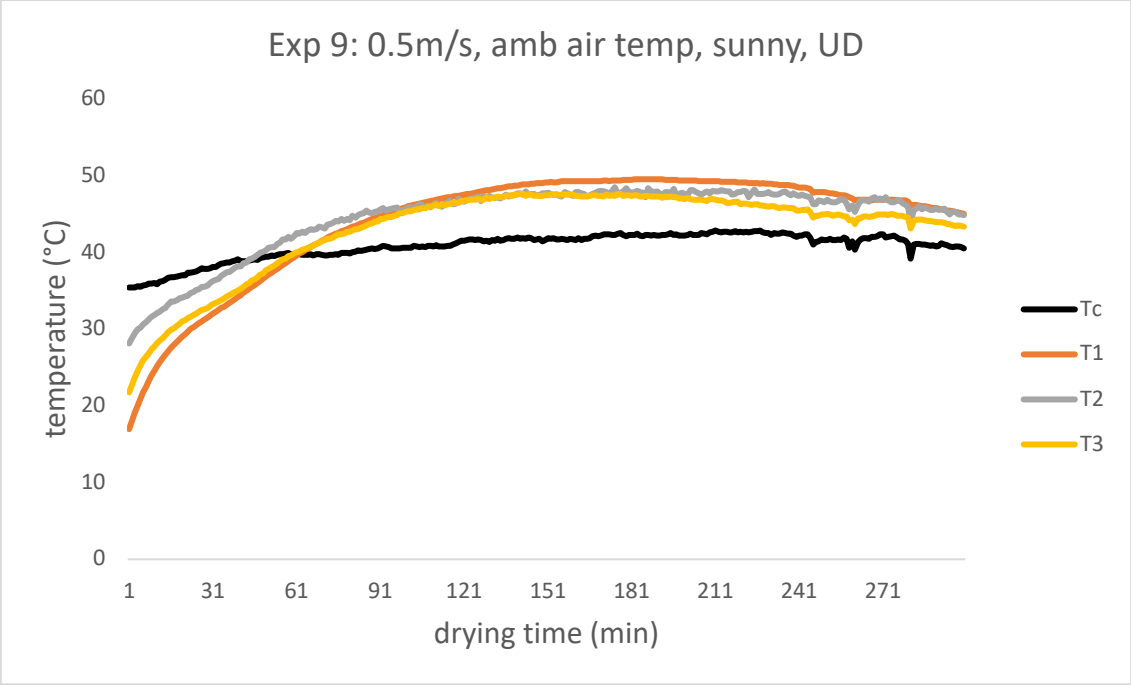

Figure G-9: Evolution of sludge temperature (T1, T2, T3) and air chamber temperatures (Tc) as a function of drying time for UD sludge solar drying in sunny weather, at 0.5m/s air flow and ambient air temperature

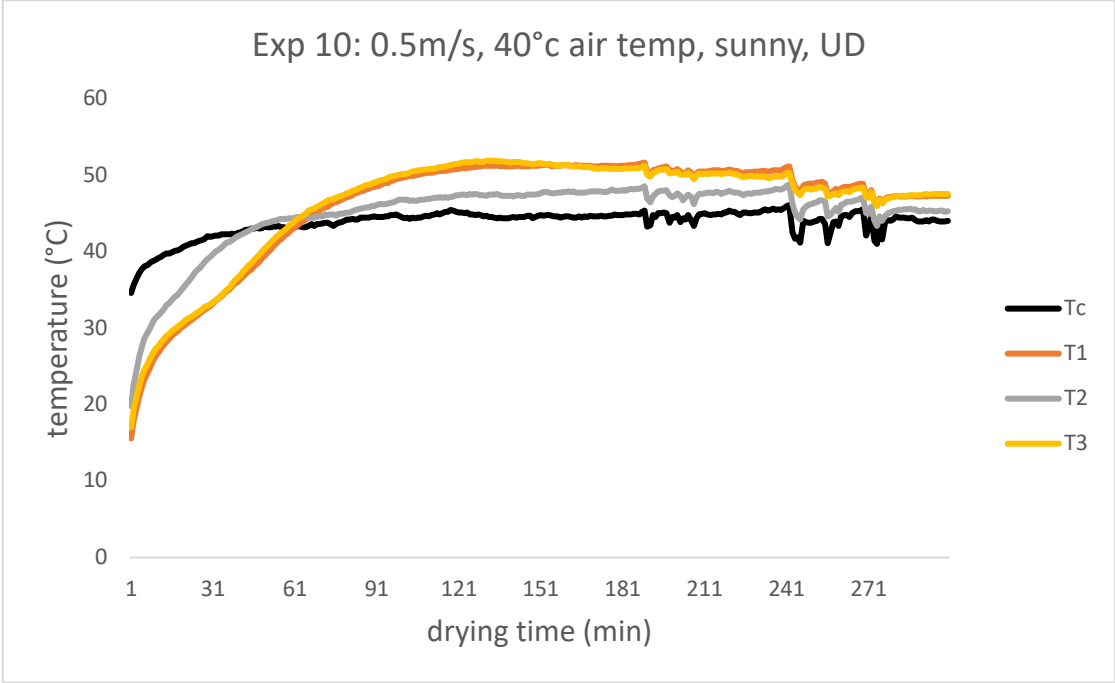

Figure G-10: Evolution of sludge temperature (T1, T2, T3) and air chamber temperatures (Tc) as a function of drying time for UD sludge solar drying in sunny weather, at 0.5m/s air flow and 40°C air temperature

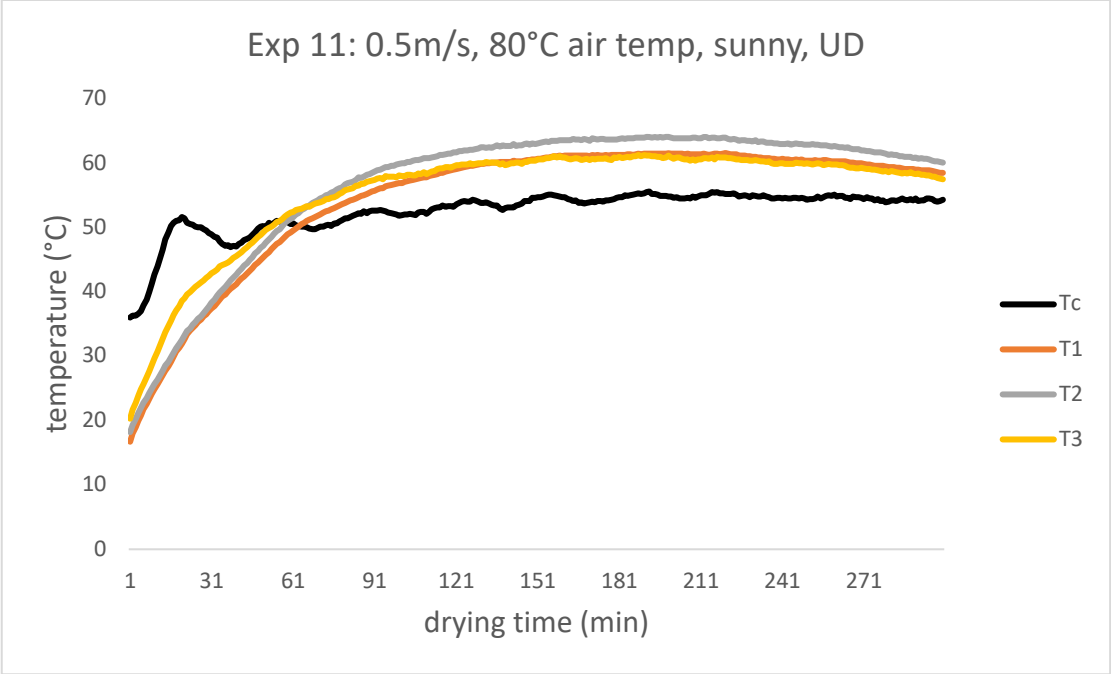

Figure G-11: Evolution of sludge temperature (T1, T2, T3) and air chamber temperatures (Tc) as a function of drying time for UD sludge solar drying in sunny weather, at 0.5m/s air flow and 80°C air temperature

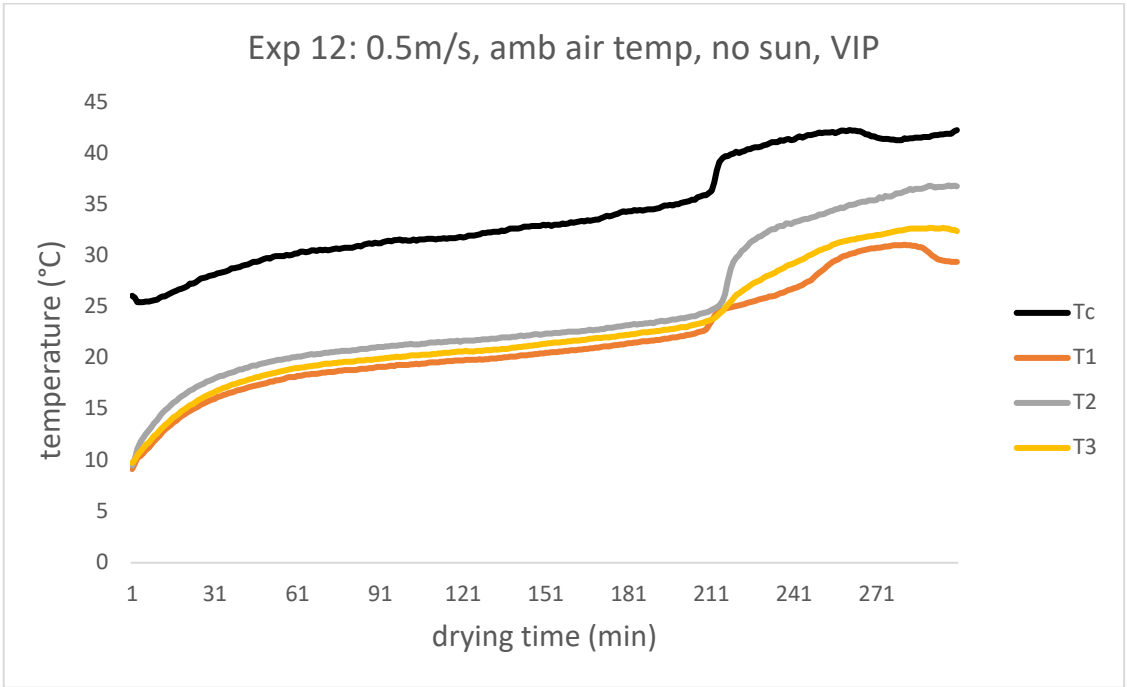

Figure G-12: Evolution of sludge temperature (T1, T2, T3) and air chamber temperatures (Tc) as a function of drying time for VIP sludge solar drying at 0.5m/s air flow, ambient air temperature and no solar irradiation